UNIVERSITY OF PISA

Department of Chemistry and Industrial Chemistry

PhD Thesis in Chemical Science

XXIV cycle, 2009-2011

SSD: CHIM/01 – Analytical Chemistry

Chemical information from human fluids for therapy monitoring and clinical diagnosis

Silvia Ghimenti

Supervisors: *Prof. Roger Fuoco*

Dott. Fabio Di Francesco

External advisor: *Prof. Joachim Dieter Pleil*

Table of Contents

CHAPTER 3 Materials and Methods

CHAPTER 4 Experimental section

ABSTRACT

In this study several analytical procedures have been developed and optimized to obtain chemical information of diagnostic or therapeutic relevance on non-traditional biological fluids, such as oral fluid, exhaled breath, and spent dialysate.

An analytical method to identify warfarin in oral fluid samples by HPLC with fluorimetric detection was developed in order to investigate the possibility of the minimal invasive monitoring of oral anticoagulant therapy. The method was used to highlight the presence of the drug in oral fluid with a concentration of 1 - 10 ng/mL. The results demonstrated the key role played by the salivary pH in regulating the drug transfer from the blood. In addition, a high correlation ($r = 0.84$, $p = 0.004$) between warfarin concentration in oral fluid and INR values was found for patients with an oral fluid pH ≥ 7.2.

An analytical methodology based on two-stage thermal desorption capillary gas chromatography and mass spectrometry was optimized for the analysis of exhaled breath samples. This procedure was applied to the non-invasive monitoring in breath samples of both volatile compounds during an oral glucose tolerance test and sevoflurane anaesthetic and its metabolite hexafluoroisopropanol (HFIP) after surgery. A three-compartment pharmacokinetic model was developed and fitted to the post-operative sevoflurane and HFIP breath data. Sevoflurane elimination kinetics after surgery were consistent in all subjects with a rapid wash-out of sevoflurane within 24 hours, whereas the production and elimination of HFIP were more varied.

Photometric and fluorimetric measurements of spent dialysate samples were proposed as possible tools to assess the removal of uremic toxins with the potential for non-invasive real time monitoring of the efficiency of hemodialysis treatment. Excellent correlations were obtained between UV absorption at λ_{abs} = 292 nm and uric acid concentration in spent dialysate (r = 0.90), and between uric acid concentration in spent dialysate and in plasma (r = 0.92). Furthermore, it was demonstrated that uric acid provides the most important contribution to UV absorption at λ_{abs} = 292 nm in spent dialysate (C_{UA} % = 75 %). A linear model capable of predicting concentration values of uric acid in blood from the UV absorption data at λ_{abs} = 292 nm was developed.

INTRODUCTION

Over the last few decades, alternative or non conventional matrices such as breath, oral fluid, sweat and other biological fluids have become more and more important in diagnostic medicine and therapeutic drug monitoring, as well as in toxicology, and occupational and environmental exposure. Analysis of these alternative fluids provides useful information due to the rapid diffusion equilibrium between the dissolved substances in the blood capillaries and these fluids through thin membranes. These membranes may be biological, such as the alveolar membrane (in the case of breath) and the glandular epithelial cell membrane (in the case of oral fluid and sweat), or artificial, such as those used in hemodialysis treatment.

In general these types of samples have the advantage that collection is almost non-invasive and easy to perform, thus minimally affecting the patient. Furthermore, they represent much simpler matrices from a chemical point of view, and the analysis can be carried out in a shorter time frame and be possibly used in outpatient scenarios. These fluids can also provide physiological information in real time, which is a useful and can be used alongside traditional methods. The main disadvantage of these kinds of samples is that compounds of interest are present at very low concentrations, and therefore high-sensitivity techniques are required to accomplish the analysis. Recent advances in analytical techniques have led to the detection of analytes at very low concentrations that were unthinkable a few years ago. Currently, mass spectrometry, combined with gas or liquid chromatography is the most widely used analytical tool because of its high sensitivity and specificity, and the ability to handle complex matrices.

The primary goal of this work is to present novel strategies for exploiting non-traditional biomarker media such as oral fluid and sweat, exhaled breath and hemodialysis fluid for clinical diagnostic applications.

Four specific projects are described to demonstrate the value of these biomarker fluids. They are: the monitoring of oral anticoagulant therapy in oral fluid, the measurement of diabetes biomarkers to assess glucose metabolism, the measurement of sevoflurane anesthetic and its primary metabolite hexafluoroisopropanol in exhaled breath in order to assess post-operative liver function, and monitoring the progression and effectiveness of hemodialysis.

CHAPTER 1

Non conventional human fluids

1.1 Oral fluid and sweat

Oral fluid in humans is a colourless mouth fluid possessing several functions involved in oral health and homeostasis, with an active protective role in maintaining oral healthiness [1, 2]. Oral fluid helps bolus formation by moistening food, protects the oral mucosa against mechanical damage and plays a role in the preliminary digestion of food through the presence of α-amylase and other enzymes. It also facilitates taste perception, allowing soluble food-derived molecules to reach the gustative papillae and buffer the acid components of food with the bicarbonates (originating from salivary gland carbonic anhydrase). Oral fluid also has a role in maintaining teeth enamel mineralization: several proteins (statherin, proline rich proteins – (PRPs) and mucins) allow Ca^{++} sovrasaturation in oral fluid to be maintained [3]. Oral fluid has defence functions against pathogen microorganisms, in the presence of defence proteins that react in specific (immunoglobulins) or non-specific (lysozyme, peroxydase, cystatins, lactoferrin, hystatins and others) ways, inhibiting microorganisms growth [4, 5].

Sweat is a clear, salty liquid produced by sweat glands in the skin. In humans, the main function of sweat is to help regulate body temperature by cooling the skin surface. This decrease in temperature is caused by the evaporation of water, main constituent of sweat at a rate of 0.6 calories per mL of sweat

evaporated [6]. The amount of sweat secreted from a person in a day depends on the needs of thermoregulation itself. Moisture may be lost from the skin by either insensible sweat (sweat not visible), likely caused by diffusion through the skin, and sensible sweat, which is actively excreted during stress and exercise.

1.1.1 Composition and physiology of oral fluid secretion

Oral fluid is a complex mix of fluids excreted into the oral cavity mainly from three pairs of major salivary glands (parotid, sublingual and submandibular) and from a large number of minor salivary glands (Figure 1.1).

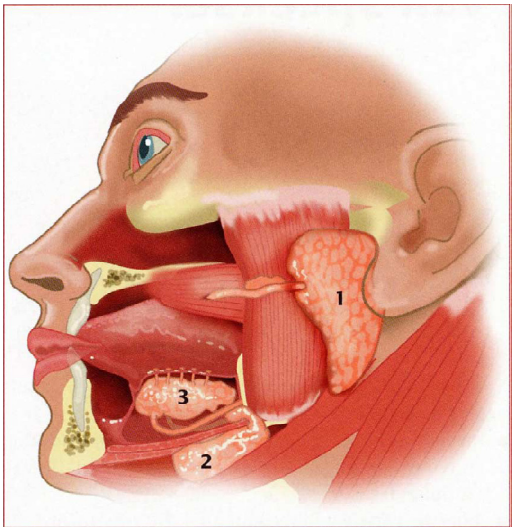

Figure 1.1 *The anatomical positioning of the three pairs of large salivary glands; the glandula parotis (1), the glandula submandibularis (2) and the glandula sublingualis (3).*

The parotid gland, located opposite the maxillary first molars at the top of the mouth, secretes oral fluid derived mainly from blood (serous fluid), whereas the sublingual glands, located at the sides of the mouth and the submandibular glands, located at the base of the tongue excrete both serous fluid and mucin. Minor salivary

glands are mainly Von Ebner glands (entirely serous organs situated in the connective tissue below the circumvallatae papillae) and Blandin-Nühm mucous glands [7].

Salivary composition varies in relation to the serous or mucous component of the glands [8]; the relative contribution of each type of gland to total unstimulated oral fluid secretion varies from 65 %, 23 %, 8 % to 4 % for submandibular, parotid, Von Ebner and sublingual glands respectively [9, 10].

Water is the greatest component of oral fluid, representing 99% of its composition, and other components such as inorganic electrolytes and organic molecules are also present [11].

The inorganic part is composed of weak and strong ions including Na^+, K^+, Ca^{2+}, Mg^{2+}, Cl^-, HCO_3^-, HPO_3^{2-} which can generate buffer capacity.The organic part contains components such as body secretion products (urea, uric acid and creatinine), putrefaction products (putrescine, cadaverine; lipids such as cholesterol and fatty acids), and more than 400 types of protein. The most relevant proteins have a glandular origin (α-amylase, histatins, cystatins, lactoferrins, lysozymes, mucins, and proline-rich proteins (PRPs)) or are plasma derived (albumin, secretory immunoglobulin A (sIgA), transferrin). The mucin gives oral fluid its sticky character. The low protein concentration in oral fluid makes drug binding minimal compared to that observed in plasma.

Oral fluid components have also a non-glandular origin, so oral fluid cannot be considered as the only production of salivary glands, because it also contains fluids originating from oropharingeal mucosae (oral mucosal transudate cells, bacteria, fungi, virus, upper airways secretions, gastrointestinal reflux) [12, 13]. Oral fluid contains also crevicular fluid, an extracellular fluid derived from the epithelia of the gingival crevice. Crevicular fluid is produced at approximately 2–3 μL/h per tooth and it can be considered as a plasma transudate [14]. Oral fluid may also

contain food debris and blood-derived compounds (actively or passively transferred), such as plasmatic proteins, erythrocytes and leucocytes in case of oral inflammation or mucosal lesions [12].

According to Thaysen and his colleagues theory [15], oral fluid secretion occurs in two stages: in the first phase a primary oral fluid isotonic to blood is released by the acinus cells; in the second phase, as this initial fluid moves down the ductal system of the salivary gland, an energy-dependent transport process reabsorbs sodium and chloride resulting in a hypotonic fluid secretion, with a lower ion concentration compared to plasma. In salivary gland ducts mineralocorticoid receptors are present, so salivary glands are mineralocorticoid-responsive [16]: for this reason salivary K^+ concentration is higher than the plasma concentration (22 vs 4 mmol/L) and Na^+ concentration is lower in oral fluid compared with that in plasma (5 vs 145 mmol/L) [12].
Several factors may modify the salivary ionic concentration, furthermore, the composition of unstimulated oral fluid is different from stimulated oral fluid, which is more similar in composition to plasma (Table 1.1).

Table 1.1 *Comparison of inorganic compounds between oral fluid and plasma.*

Inorganic compounds	**Unstimulated oral fluid (mmol/L)**	**Stimulated oral fluid (mmol/L)**	**Plasma (mmol/L)**
Na^+	5	20 - 80	145
K^+	22	20	4
Cl^-	15	30 - 100	120
Ca^{2+}	1 - 4	1 - 4	2.2
HCO_3^-	5	15 - 80	25
Mg^{2+}	0.2	0.2	1.2
NH_3	6	3	0.05

For example, an increase in the salivary flow rate, obtained by stimulation with acidic food, increases the concentrations of sodium, chloride and bicarbonate and decreases the concentrations of salivary potassium and phosphate, compared with unstimulated oral fluid [17] (Figure 1.2).

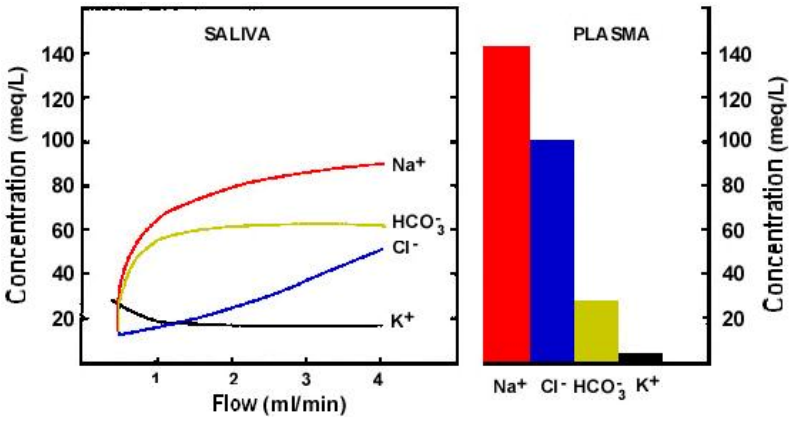

Figure 1.2 *Relation between the concentration of sodium, potassium, chloride and bicarbonate in the oral fluid and the rate of salivary flow.*

Healthy adult subjects normally produce 500 – 1500 mL of oral fluid per day [11], with typical flows of 0.05 mL/min while sleeping, 0.5 mL/min while spitting, and 1 mL/min to 3 mL/min or more while chewing but several physiological and pathological conditions can modify oral fluid production quantitatively and qualitatively, e.g., smell and taste stimulation, chewing, psychological and hormonal status, drugs, age, hereditary influences, oral hygiene [12] and physical exercise [10, 18].

Unstimulated oral fluid pH is in the range of 5.6 – 7 and increases with stimulation (to more approximate the pH of blood, i.e. 7.4) to a maximum of 8.0 [11].

1.1.2 Composition and physiology of sweat secretion

Sweat is a clear, hypotonic solution produced by two types of glands: eccrine and apocrine located in epidermis [19]. The apocrine glands are larger than the eccrine glands and secrete a more viscous substance. The apocrine glands are primarily located in the axillae, pubic and mammary areas. Besides opening directly onto the skin, sweat glands also develop in close association with hair and sometimes open inside hair follicles; as such, sweat is thought to be a major contributor to drugs appearing in hair.

The sweat produced by eccrine glands is a liquid basically colorless and odourless, slightly salty, whose composition may vary according to different physiological conditions. It consists of a dilute (water (99%) is its main constituent) electrolyte solution containing high concentrations of sodium, chloride as well as low levels of potassium, bicarbonate, glucose, lactic and pyruvic acids and urea and ammonium. A substantial individual variability in the composition of sweat was found depending on the mode of stimulation and age.

The apocrine sweat, however, is secreted intermittently and appears as a viscous liquid, milky, acrid smell, rich in organic cellular material, proteins, glycogen and fatty acids. Its pH is alkaline due to the presence of ammonia. It is produced in much less than the eccrine sweat but, being more easily attacked by bacteria, the greater responsibility of the production of body odours is attributed to it.

Sweat acts physiologically by regulating body temperature, since its evaporation from the skin surface reduces the excess heat. Sweating is increased by nervousness, exercise, stress and nausea and decreased by cold. Sweat excretion is also affected by other factors, such as ambient temperature, relative humidity, body

location (in general, sweat glands are distributed over the entire body, except for the lips, nipples and external genital organs), hormonal imbalances, overactive thyroid gland and the sympathetic nervous system, and certain foods and medications.
Between 300 and 700 mL/day of insensible sweat is produced over the whole body, whereas 2–4 L/h of sensible sweat may be produced by extensive exercise [11].

1.1.3 Mechanism of drug transport into oral fluid and sweat

Nearly identical considerations are thought to apply to the excretion of drugs in sweat as apply to excretion of drugs in oral fluid.
A thin layer of epithelial cells separates the oral fluid ducts from the systemic circulation. The lipid membrane of these cells determines which molecules may be transferred from the plasma into the oral fluid [20]. The clearance of compounds from plasma into oral fluid may involve several processes [21]:

1) ultrafiltration through gap junctions between cells of secretory units (intercellular nexus). Only molecules with MW<1900 Da are involved (water, ions, hormones such as catecholamines and steroids) and their salivary concentration is 300–3000 times lower in oral fluid than in plasma.
2) transudation of plasma compounds into oral cavity, from crevicular fluid or directly from oral mucosa. The presence in the oral fluid of some typical plasmatic molecules, like albumin, depends on this mechanism.

3) selective transport through cellular membranes: by passive diffusion of lipophilic molecules (steroid hormones) or by active transport through protein channels.

Salivary substances that so far play the dominant role in clinical chemistry diffuse from the blood compartment into oral fluid. At least five factors are known which influence the diffusion of the drugs into oral fluid [22, 23]:

1. *Molecular mass*

   The molecular weight appears to play a minor role, although the diffusion coefficient is inversely proportional to the molecular radius. As a general rule of thumb that smaller molecules diffuse more easily than larger ones.

2. *Lipid solubility*

   The major determinant for free diffusibility is the solubility in water and/or lipids, especially in the phospholipid layer of cell membranes. Lipophilic substances more easily diffuse than lipophobic molecules. Abundant evidence has been published that the lipophilic character of organic compounds as operationally defined by oil/water or octanol/water partition coefficients play an important role on drug action at all levels of organization (enzyme, membrane and cell) [24, 25, 26].

3. *Degree of ionization*

   The degree of ionization plays an important role because of the partition theory, which states that only the unionized fraction is able to pass the lipoid barrier between the three compartments: plasma, intracellular space and salivary fluid.

Because the pH value differs between the extra- and intracellular space, the total concentration as the sum of the ionized and unionized fraction varies on both sides. For neutral or weakly acidic drugs with a pK_a greater than 8.5 and weakly basic drugs with a pK_a less than 5.5, the variability of oral fluid pH has little effect on the oral fluid/plasma ratio. For acidic, largely ionized drugs the oral fluid/plasma ratio increases with rising pH-value, while for basic drugs the reverse situation occurs. In man, oral fluid is usually more acidic than plasma. Therefore, the oral fluid/plasma ratio is equal to or less than unity for all acidic drugs and equal to or greater than unity for all basic drugs. If the drug is protein-bound, this statement is only true for the free fraction.

The theoretical oral fluid/plasma ratio can be estimated from the equation of Rasmussen (Eq. (1.5 – 1.6)) derived from the Henderson–Hasselbalch equation (Eq. (1.1)) and the equation for mass balance (Eq. (1.2)), as demonstrated by many examples [27, 28, 29].

$$pH = pK_a + \log\frac{[A^-]}{[HA]} \tag{1.1}$$

$$[A] = [HA] + [A^-] \tag{1.2}$$

where [HA] is the concentration of the non-ionized form of the acidic drug, $[A^-]$ is the concentration of the anionic form, and [A] is the total concentration of drug in both forms.

Solving both equations for the total amount of drug in either form gives:

$$\frac{[A]}{[HA]} = 1 + 10^{(pH-pK_a)} \tag{1.3}$$

Because Eq. (1.3) applies to both oral fluid and plasma, the oral fluid/plasma ratio may be calculated by:

$$\frac{Oral\ Fluid}{Plasma} = \frac{[A_{oral\ fluid}][HA_{plasma}]}{[A_{plasma}][HA_{oral\ fluid}]} = \frac{1+10^{(pH_{oral\ fluid}-pK_a)}}{1+10^{(pH_{plasma}-pK_a)}} \quad (1.4)$$

A modification must be made to Eq. (1.4) to take into account the binding of drugs to plasma and oral fluid proteins because only the free neutral drug can cross the cellular membranes. Because of protein binding, the concentration of drugs in plasma (which drives the diffusion process) is reduced. Assuming that the [HA] must be the same in both oral fluid and plasma, because of equilibrium (HA is the species thought to be responsible for transport across the cellular membranes), Eq. (1.4) may be reduced to the standard equation, Eq. (1.5). A similar equation (Eq. (1.6)) can be derived for basic drugs if it is remembered that the un-ionized form of the drug is responsible for the transport across the oral fluid–plasma membrane:

$$\frac{Oral\ Fluid_{acidic\ drug}}{Plasma_{acidic\ drug}} = \frac{1+10^{(pH_{oral\ fluid}-pK_a)}}{1+10^{(pH_{plasma}-pK_a)}} \cdot \frac{f_p}{f_{of}} \quad (1.5)$$

$$\frac{Oral\ Fluid_{basic\ drug}}{Plasma_{basic\ drug}} = \frac{1+10^{(pH_a-pK_{oral\ fluid})}}{1+10^{(pK_a-pH_{plasma})}} \cdot \frac{f_p}{f_{of}} \quad (1.6)$$

where f_p is the free (unbound) fraction of drug in plasma and f_{of} is the free (unbound) fraction of drug in oral fluid.

The fraction of free drug (not bound to proteins) in oral fluid is assumed to be one, because of the much lower concentrations of protein in oral fluid compared to plasma.

Eqs. (1.5) and (1.6) predict that the concentrations of drugs in oral fluid will vary with the free fraction of drug in plasma rather than with the total level of drug [30].

Since it is only the free form of the drug in plasma that is available to produce a pharmacological effect, oral fluid concentrations may be of greater therapeutic value than plasma levels.

4. *Salivary pH*

   On the basis of the above-mentioned partition theory, the salivary pH value influences the secretion of ionized drugs. The pH-value depends on the flow rate. Stimulation leads to an increase of bicarbonate secretion with a concomitant rise of the pH-value from 5.8 to 7.8 [11]. Therefore, basic drugs are concentrated in oral fluid under resting conditions when the salivary pH is below that in blood. On the other hand, under maximal stimulation, basic drugs become concentrated on the intracellular side of the membrane.

   The salivary pH-value depends on psychological factors; it decreases, e. g., under anxiety situations [31].

5. *Protein binding*

   The fraction of a drug bound to protein cannot pass the cell membrane. Therefore, the salivary drug concentration directly reflects the free plasma fraction of a unionized drug.

Other factors that can influence the oral fluid/plasma ratio are the salivary flow rate, the phenomenon of fluctuating arterial-venous differences, the elimination kinetics, and the concentration-dependent protein binding.

1.1.4 Oral fluid and sweat sampling techniques

Oral fluid can be collected under unstimulated (resting) or stimulated conditions [32]. Salivary flow can be stimulated by a variety of agents: gustatory and masticatory stimuli have been used most frequently to increase salivary flow rate. The most commonly used stimulants are paraffin wax, Parafilm, rubber bands, gum base, and citric acid.

Common methods of oral fluid collection are spitting, draining, suction and collection on various types of absorbent swabs [33].

A variety of commercial collection devices that promote easy, quick and reproducible collection as well as a cleaner specimen which is more suitable for analysis are available [33, 34, 35, 36]. In general, these devices consist of an absorbent material that becomes saturated in the mouth of the donor, and after removal the oral fluid is recovered by centrifugation or by applying pressure to the material.

Examples of commercially available devices include Omni-SAL® (Cozart Biosciences Ltd, UK), Salivette® (Sarstedt, Germany), Drugwipe® (Securetec, Germany), Quantisal™ (Immunalysis Corp., USA), Intercept® (OraSure Technologies, USA), Saliva-Collection-System® (Greiner-BioOne, USA), ORALscreen™ and Finger Collector® (Avitar Technologies, Inc., USA).

Many sweat collection techniques such as wiping, blotting, occlusive patches, iontophoresis with pilocarpine stimulated secretions, and the use of capillary tubes have been developed.

Initially, sweat collection devices consisted of an occlusive bandage formed by one to three layers of filter paper or pieces of cotton, gauze or towel [37]. Heat or chemicals (e.g. pilocarpine) were used to increase sweat production.

However, this kind of patch was time-consuming to apply, uncomfortably large, prone to detachment and yielded a small volume of sweat for analysis.

To overcome these difficulties, non-occlusive sweat collection devices have been developed to wear for extended periods of time, consisting of an adhesive layer on a thin transparent film of surgical dressing to which a rectangular absorbent pad is attached. The non-occlusive, semipermeable membrane allows oxygen, carbon dioxide, and water vapor to escape. The adsorbent pad retains the nonvolatile components of sweat, such as salts, proteins, and drugs and metabolites. This device is being marketed as the PharmChek sweat patch [38]. A potential problem with the PharmChek patch is the absence of a layer between the skin and the absorptive pad, to prevent bacterial transfer into the pad and, therefore, the possibility of bacterial growth and drug degradation. Careful preparation of the skin prior to application of the patch should kill or remove bacteria and prevent these problems.

1.1.5 Oral fluid and sweat analysis

Oral fluid and sweat are used mainly in the field of toxicology for the detection of drug of abuse using immunochemical and chromatographic methods [39, 40, 41].

Immunochemical tests, mainly EIA (Enzyme Immuno Assay), are used for qualitative analysis of screening to verify the presence or absence of substances in the body but not the amount taken or still in circulation at the time of the investigation. Such tests require small amounts of sample without pre-treatment and have a good specificity.

The screening tests should be subject to confirmation using a method that provides structural information on the substances

under consideration. In this regard, analytical techniques such as mass spectrometry coupled with gas or liquid chromatographic separation (GC-MS or LC-MS) are used.

The quantitative determination by these instrumental techniques requires, unlike immunochemical tests, a stage of sample pre-treatment. Oral fluid and sweat specimens can be treated in a similar manner to other biological fluids, by deproteinization, ultracentrifugation, using liquid-liquid extraction (LLE) [42, 43, 44], solid-phase extraction (SPE) [45, 46, 47, 48, 49, 50] and solid-phase microextraction (SPME) [51, 52] techniques.

However, because of the simplicity of the matrix, in some cases the samples can be analyzed directly by liquid chromatography without preparation or following a simple filtration.

In the recent literature there are many works in which some drugs and drugs of abuse (chlorpropamide, propanolol, phenytoin, cocaine, amphetamines, cannabinoids and methdone), are determined by the analysis of oral fluid or sweat.

1.2 Physiology of respiration

The physiologic purpose of respiration is to carry oxygen from ambient air to mitochondria within the cells of peripheral tissues, where it is consumed for the oxidation of carbon-containing compounds (internal respiration), and to transport carbon dioxide away from the cells and the body. The most important mechanism for this to happen is diffusion, which is driven by a concentration gradient. However, a purely diffusive system can only establish a relatively small pressure gradient across the gas exchange barrier of the organism. This is acceptable for small organisms (diameter < 1 mm), however, convection is also needed for larger creatures in order to guarantee the high oxygen flow rate needed for their

metabolism. In mammals, an air pump consisting of the lungs, the airways and the respiratory muscles guarantees that respiratory gases are continuously renewed on one side of the alveolar membranes, while the heart and the circulatory system accomplish the same task on the other side. In this way, a very efficient gas exchange system is obtained: diffusion is optimized by having the maximum possible gradient across the alveolar capillary membranes and across the surface of mitochondria, while a minimum oxygen pressure difference exists between blood just come out of the lungs and blood reaching the peripheral tissues. The availability of a large surface across which gas exchange takes place further contributes to the high efficiency of the system. In humans, lung surface is so large and so thin that oxygen and carbon dioxide transport across the alveolar walls is three-fold faster than needed when cardiac output is normal [53]. In most cases, the gas-liquid equilibrium between alveolar air and blood can be considered almost instantaneous, and the ratio of concentrations in pulmonary blood and alveolar air is close to the in vitro blood/air partition coefficient. Even so, the O_2-carrying capacity of the blood would be largely insufficient to meet the demand of the systemic tissues if the body had to rely just on dissolved oxygen, without a remarkable increase of cardiac output. To increase the carrying capacity of the blood, the large majority of the oxygen and carbon dioxide is transported bound to proteins or in other chemical forms.

The respiratory system can be divided into two sections (Figure 1.3): a section, named dead space, which mainly acts as a conducting airway (nose, pharynx, larynx, trachea and other airways without alveoli), and a section whose main function is gas exchange (alveoli and alveolar sacs).

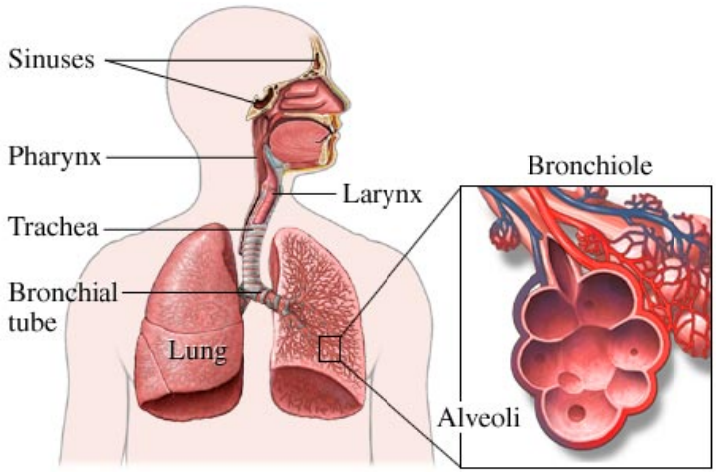

Figure 1.3 *Respiratory system.*

Upon inhalation, gas exchange occurs in the alveoli, the tiny sacs that are the basic functional component of the lungs. The alveolar walls are extremely thin (approx. 0.2 μm). These walls consist of single layers of epithelial cells in close proximity to the pulmonary capillaries that consist of single layers of endothelial cells. The close proximity of these two cell types allows permeability to gases and, hence, a gas exchange.

The blood supplying the alveoli is pumped to the lung from the right ventricle of the heart and then flows into the entire body. Thus it is poor in oxygen (used from the cells) and rich in carbon dioxide (produced from cells) (Figure 1.4).

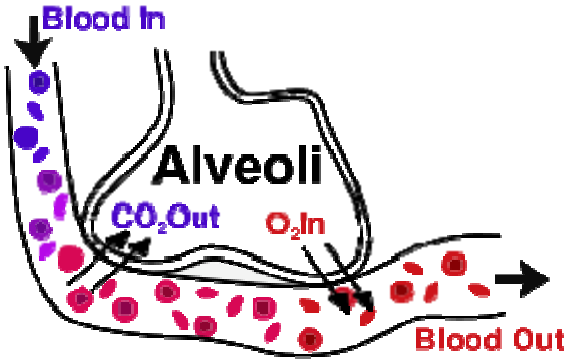

Figure 1.4 *Gas exchange in the alveoli.*

The chemical process of gas exchange is diffusion: a substance always diffuses from A to B if the concentration or pressure is higher in A rather in B. Thus in the alveoli the oxygen pressure (100-110 mmHg) is lower than in the inspired air and higher than in blood capillaries (40 mmHg). Carbon dioxide pressure in the alveoli, on the other hand, is lower (40 mmHg) than in capillary blood (46 mmHg) and the CO_2 moves in the opposite direction of the O_2. For the CO_2 the difference in pressure is small, but it is enough to eliminate the carbon dioxide produced by the organism as a result a good diffusivity of this gas. It is also important to consider that gas exchanges are also regulated by gas solubility in the liquid solution [54].

A typical respiratory cycle involves, in a time span of about 5 seconds, the exchange of half a liter of air in the lungs (tidal volume), so that the total ventilation, i.e. the volume of air moved in and out of the lungs per unit of time, is about 6 L/min. Not all the air we breathe is useful for the renewal of respiratory gases. The typical ventilation volume per respiratory cycle of the sections is 150 mL and 350 mL, respectively. Before inspiration, dead space is filled with end-tidal air remaining from the previous respiratory cycle. End-tidal air is the last fraction of expired air, whose composition resembles alveolar air. During inspiration, half a litre of fresh ambient air is then inhaled into the body, but only the first 350 mL reach the alveoli together with 150 mL of end-tidal air contained in the dead space, where they are diluted and mixed with alveolar air. During expiration, 150 mL of fresh ambient air, which filled the dead space, and 350 mL of air coming from the alveolar region are exhaled through the nose and/or mouth in sequence. By analyzing a respiration cycle, it can be noted that dead space is alternately filled with ambient and end-tidal air, and that only 350 mL of ambient air actually ventilates the lungs. Since

the volume of air contained in the lungs during normal breathing is approximately 3 L, it follows that the composition of alveolar air is pretty stable during respiration (the cyclic variations of oxygen and carbon dioxide are about 2% and 5%, respectively).

During expiration the breath composition changes in order to empty the airways and the lungs. Such a process can be monitored by tracking the CO_2 content in breath, Figure 1.5 [55].

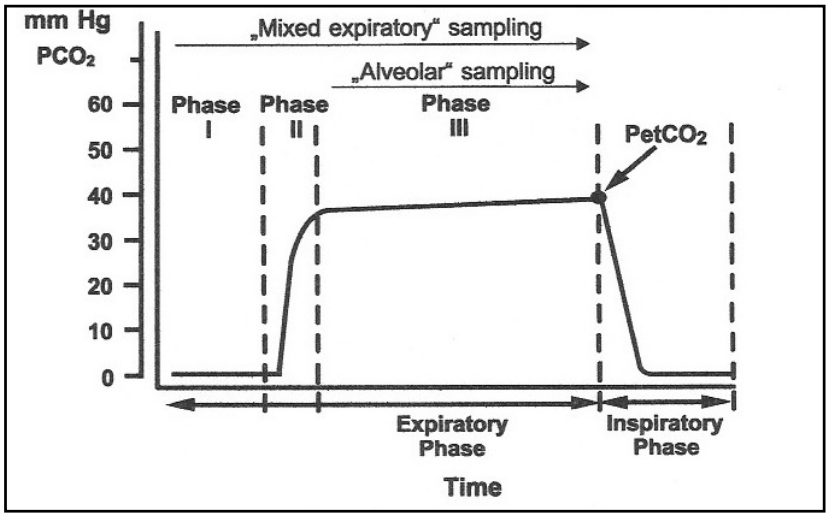

Figure 1.5 *CO_2 breath profile during a single respiratory cycle.*

Three phases can be identified: during Phase I the air in dead space is eliminated and the composition of this fraction is low in CO_2, being similar to inspired air; during Phase II, when mixed dead volume and alveolar air are emitted, the partial pressure of CO_2 quickly increases until a maximum value (35 mmHg) is reached and then during Phase III a plateau level that asymptotically approaches the alveolar concentration is reached; only in Phase III is the alveolar air eliminated, containing the volatile compounds released from blood.

Ambient air is the main source of xenobiotic contaminants and oxygen. Its content of oxygen and carbon dioxide is fairly constant, while the concentrations of xenobiotics may be highly variable.

Dead space air has a composition close to ambient air (but a higher water content). Differences may arise due to the chemicals originating and/or released in the conducting airways or to gas exchanges with the mucus layer (mainly for water soluble compounds).

The composition of alveolar air is due to the interaction of ambient air with blood through the alveolar membrane. There are considerable non-homogeneities in the composition of alveolar air in different lung regions even in healthy subjects, since posture and gravity alter both local ventilation (exchange of the air in the lungs) and perfusion (blood circulation). Pulmonary ventilation and perfusion are mainly regulated by respiratory and cardiac frequency [55, 56].

When the composition of ambient air changes, the time needed for each breath fraction to reach a new equilibrium ranges from a few seconds for dead space air to minutes or hours for alveolar air.

In fact, after exogenous compounds have reached pulmonary alveoli dissolved in blood on the basis of their blood/air partition coefficients, the compounds are then transferred through the body and released in the different tissues depend on the chemical affinity. The concentration of each compound in alveolar air is the result of a dynamic equilibrium that involves several compartments, each with its specific time constant.

In most cases, blood is the main source of markers and for this reason alveolar air should be considered the most representative of an individual's condition. If markers are released from conducting airways, dead space air should be sampled.

1.2.1 Breath sampling techniques

The inter- and intra-individual variability of physiology, the presence of circadian rhythms in the production and emission of some compounds, and the existence of confounding factors due to food consumption or ambient air make the collection of representative samples particularly difficult in many cases. There are no general rules to follow and this lack of standardization in the sampling procedures has been proposed as a possible explanation for the contradictory results obtained by different authors along with the intrinsic difficulties of accurate and precise quantitative analysis of gas sample [57].

Exhaled air can be sampled in two ways, i.e., by mixed expiratory sampling and end-tidal sampling, respectively. Mixed expiratory sampling entails collecting total breath, including the air contained in the upper airways (dead space) which experiences no gas exchange with blood. End-tidal sampling involves the collection of only end-tidal air, which contains most of the chemical information on blood composition. Separate sampling during expiration of dead volume air and end-tidal air may be advantageous in breath research in terms of providing an insight into the origin of chemicals identified in breath samples. The presence of exogenous compounds in breath is one of the main sources of noise affecting breath analysis; how to discriminate between compounds with endogenous (i.e., produced inside the body by the physiological or pathological metabolism) or exogenous origin is an age-old question. The debate on the best solution to this problem still divides the scientific community. Some authors propose that each compound should be weighed on the basis of its concentration gradient between breath and ambient air [58], while others suggest that compounds whose concentration in ambient air is comparable

with or higher than that in breath should not be taken into account in the characterization of subjects [59] and finally there are those who provide the subjects with purified air in order to circumvent the problem [60, 61].

Several types of breath sampling devices have been reported in the literature or are commercially available. Most are simple combinations of valves and tubing which the study subject uses to fill a sampling bag or a syringe [62, 63, 64], or a pre-evacuated stainless steel canister [65, 66 67]. In all these cases, the subject is breathing ambient air, thus the mixed expiratory sampling is accomplished.

In the latter case, the subjects themselves control the sampling by opening a manual valve through which their breath is sucked into the canister. The canisters afford optimum stability of the sample and absorption on the canister walls for specific class of compounds can be minimized by a suitable treatment of the surfaces. Nevertheless, they are relatively heavy and bulky if a large number of samples have to be collected. Due to cost, they are not disposable and so an effective cleaning procedure is needed [68, 69, 70]. The use of plastic bags has been investigated by many authors as a possible alternative [71, 72, 73]. The stability of samples can be affected by the absorption on, or permeation through the bag walls, the possible contamination due to the release of bag materials, and the cleaning procedures in the case of multiple use. Tedlar and Nalophan bags are largely used thanks to low cost and handiness.

Other authors have suggested more complex devices to deliver purified air to their subjects [74, 75]. Two passive devices are commercially available that allow the sampling of end-tidal air. The first sampler, QuinTron, is produced by Campro Scientific GmbH (Germany) and consists of a tee-shaped connector housing two one-way valves in its two outlets. The core of each valve is a thin

silicon disc that seals the outlet until threshold pressure is exerted. The two valves are regulated to open at different pressures; a 250 mL bag is connected to the valve opening at the lower pressure, while a 750 mL bag is connected to the other valve. A mouthpiece is fitted to the inlet of the tee-shaped connector. When the subject blows air into the device, the pressure rises in the connector until the first valve opens and the corresponding bag is filled with dead space air. The pressure then starts increasing again until the second valve opens, allowing the remaining breath to be released into the other bag. Another sampler, BioVOC™, is produced by Markes International (UK). The subject is asked to blow through a mouthpiece into a cylinder with an open end. Only the last portion of end-tidal air (150 mL) remains in the cylinder after expiration. The mouthpiece is then replaced with a piston used to push the sample through an absorbing tube which has been connected to the previously open end of the cylinder. Although these systems do not provide the optimum solution, they are attractive for their simplicity and low cost. Their main limitations are the poor control of the sampling conditions and the limited volume that can be sampled in a single breath. A more sophisticated Breath Collecting Apparatus (BCA) was developed by Phillips and produced by Menssana Research [58]. In this system, the subject breathes through a mouthpiece assembly consisting of an inlet valve for the inspiration of ambient air and an outlet valve connected to an open-ended stainless steel cylindrical reservoir, which is thermostated at 40 °C to avoid the condensation of water. The sampling port, located at the end of the reservoir near the mouthpiece, is connected in sequence to an absorption tube, a flow meter and a computer-controlled pump. The end-tidal air sampling is accomplished by activating the pump at appropriate times after expiration, since no measurements of expiratory gas concentration and flow are taken. The total volume sampled in the absorbing

tube during multiple breaths can be selected by the user. A CO_2-controlled breath sampling device was proposed by Schubert *et al* for mechanically ventilated patients [76]. A fast responding infrared absorption mainstream CO_2 analyzer supplies data to an electronic processing unit, which actuates a two-way valve diverting breath flow to an absorbing trap when the percentage volume of carbon dioxide exceeds the set-up point.

Alternatively, the breath sample can be collected into a bag and then pre-concentrated off-line into an absorption tube [77]. The system enabled the sampling of large volumes on multiple breaths and the separation of breath fractions by real time monitoring of CO_2 concentration.

Loccioni humancare with Professor T. Risby had developed novel sampling devices:

1) *Single Breath Sampler* developed to characterize a single breathing act. Mouth pressure and carbon dioxide concentration in real time are displayed and allow the breathing subject to apply a biofeedback technique on pressure and stabilize the expiration flow to a standard value making sampling repeatable and reliable. It is designed for connection with real time monitors (mass spectrometry, tunable diode laser analysers, photo-acoustic laser spectrometers, etc.) allowing to capture the signal from an external sensor for easy and fast data collection.
2) *Multiple Breath Sampler* developed to allow the subject breathing in a regular way and sample multiple breathing acts. Parameters can be set and changed to select the portion of interest in breath, according to the study performed. Breath can be then sample in desorption tubes or bags and analyzed with standard methods. It is designed for off-line gas analysis (gas cromatography, mass spectrometry, etc.).

1.2.2 Analytical techniques used for chemical breath characterization

Several techniques have been applied to breath analysis that can be differentiated with respect to detection power, types of analyte to which they can be applied, capability of providing unambiguous identification, or possibility of providing real-time data [78, 79].

The high separation efficiency of capillary gas chromatography (GC) and the high identification capability of mass spectrometry (MS) make GC-MS the most common method used to measure low concentrations of more than one thousand VOCs present in human breath [80, 81].

Due to the extremely low level of most substances in exhaled breath, a pre-concentration step is required in most cases to enhance detection power. Generally, there are three approaches to achieve pre-concentration, namely, the chemical, cryogenic, and adsorptive approach [82, 83, 84, 85].

The adsorptive trapping is currently the most convenient and widely used method. It retains volatile compounds by binding them to specific sorbents. There are two types of pre-concentration techniques that use solid phase adsorption, i.e., Solid Phase Micro-Extraction (SPME) and Solid Phase Extraction (SPE).

The SPME technique, developed by Pawliszyn in 1989, combines in one step analyte collection and extraction [86]. The SPME [87] does not use any solvent and may be easily coupled with the most diffused chromatographic techniques. This method utilizes a fused silica fiber (typical diameter, 50-200 μm) coated with a thin layer of stationary phase (typical thickness 10-100 μm) mounted in a holder. During extraction, the fibre is exposed to the sample for a pre-established time during which the analytes reach the distribution equilibrium between the sample and the fiber coating.

The extraction efficiency depends on the value of the analyte partition coefficient and the mass ratio between the sample and the stationary phase. Afterwards, the fiber is withdrawn in the holder which in turn is inserted, for a pre-established time, in a modified split/splitless injector of the GC with a small diameter liner (0.75 mm ID) heated at a suitable temperature so that the analytes are thermally desorbed and transferred into the column by the carrier gas [88]. The optimum time and temperature of desorption and the carrier gas flow influence recovery have to be found experimentally.
Several types of coatings with different thicknesses and polarities are commercially available and have an affinity with different classes of compounds [89, 90]. This extraction technique does not require any particular pre-treatment and is fast and easy use. The main disadvantages of this technique are the low pre-concentration factor, due to the limited capacity, and the difficulty in performing quantitative analysis, especially at trace level, due to the competition for absorption sites among minor constituents and more abundant compounds [91, 92].
In the SPE technique, a known volume of the sample passes through a desorption tube, packed with a suitable stationary phase, and the analytes are then retained on the basis of their chemical-physical properties. Analytes are released from the sorbent by applying a sharp temperature increase (Thermal Desorption (TD)) and transferred to the chromatographic column using a flow of an inert gas. Broadening of the chromatographic signal may happen and can be reduced by a two stage desorption system. In fact, the analytes desorbed from the tube are focused in a cryogenic capillary trap, which has a reduced internal volume. The trap is then rapidly heated. In this case the desorption process is faster and the transfer to the chromatographic column is performed with a smaller volume of carrier gas.

In order to have better analyte recovery and more reproducible results the packing material, desorption temperatures, timing, and gas flows need to be optimized both for the desorption tube and the focusing trap [93]. Sorbents should have high value of Breakthrough Volume (BTV), low affinity for water, and high thermal stability [92]. Carbon-based materials such as Carbon Molecular Sieves (CMS) and Carbon Blacks (CB) are frequently used, although they present some drawbacks [94]. Graphitized Carbon Black (GCB) is a very hydrophobic adsorbent with excellent thermal stability, low affinity to water, and high affinity to very volatile compounds [95]. Therefore, GCB could be used for the sampling of VOCs in exhaled breath, which has a high humidity content, without additional treatment.

Many of the porous organic polymers derive from the stationary phase used in a packed GC column. Tenax is one of the most frequently used trapping materials. This polymer is hydrophobic and does not retain water. Due to its low surface area (30 m^2/g), very volatile compounds are not trapped. The co-precipitated GCB with Tenax was introduced on the market as a Tenax GR which combines advantages of both materials [96]. If the sample contains compounds with different chemical-physical properties, the use of a multi-bed tube should be preferred.

Information on breath composition can also be obtained from direct breath measurements performed by different mass spectrometric techniques: Selected Ion Flow Tube Mass Spectrometry (SIFT-MS) or Proton Transfer Reaction Mass Spectrometry (PTR-MS). These techniques enable to eliminate the collection and pre-concentration phases and give real time responses.

SIFT-MS is a technique originally developed for the determination of rate coefficients for gas phase reactions. Recently SIFT has been

applied to the detection of trace gases in air and breath [97, 98, 99].

In short, the analysis occurs through a process of chemical ionization in a reaction tube (or flow tube). To analyze VOCs, a sample is introduced into the flow tube at a precisely controlled rate. Inside the flow tube, precursor ions, usually $H3O^+$, NO^+, or O_2^+, react with VOCs present in the sample. This reaction results in the formation of product ions, which are analyzed by a quadrupole mass spectrometer to identify and quantify VOCs.

SIFT-MS has been used for the monitoring of ammonia, acetone, isoprene, and ethanol in breath of healthy volunteers [100, 101], for the investigation of ethanol metabolism [102], the control of ovulatory cycle [103], the analysis of smokers' and passive smokers' breath [104], the assessment of exposure to volatile solvents [105], and the detection of bacterial infections, renal failure and diabetes [99].

PTR-MS is a relatively new technique allowing the quantification of gaseous VOCs at low concentration in real time [106]. This technique is different from SIFT due to some expedients adopted to increase detection power. The system works with an empty cathode ion source, which produces a high density of primary ions travelling across the tube without a pre-selector. The sample is introduced inside the tube without a carrier gas, thus avoiding dilution and increasing detection power by two orders of magnitude compared to SIFT [107].

In brief, chemical ionization is applied based on proton-transfer reactions, with H_3O^+ as the primary reactant ion, which is most suitable when air samples containing a wide variety of trace volatile organic compounds are to be analyzed. Almost all VOCs have proton affinities larger than H_2O, and therefore proton transfer occurs on every collision ($H_3O^+ + VOC \rightarrow VOCH^+ + H_2O$). The

ionized VOCs by proton transfer from H_3O^+ are analyzed in mass types rather than concentration.
PTR-MS has been used for exhaled breath profiling [108] and real time monitoring of anaesthetic agents [109] and to study effects of hemodialysis [110] or smoking [111].

In recent years Ion Mobility Spectrometry (IMS) has developed in comparatively small and effective devices to determine trace quantities of VOCs down to the low ppbv range in air [112, 113, 114]. The fundamental principle of operation is to separate ions according to their gas phase mobility as they travel through a purified gas in an electric field at atmospheric pressure.
The major advantage of IMS is that no vacuum systems are required and the ambient air can be used as carrier gas. IMS is often coupled with a GC system because of the intrinsic limited detection power, especially in the case of the detection of complex mixtures [115]. IMS has been used to identify some metabolites [116] as well as bacteria in human breath [112] coupled with multi-dimension capillary GC.

Recent advances in laser spectroscopic techniques make it possible for breath analysis to be performed on-line without the need to collect breath in containers or traps, thus allowing information about concentration during different phases of exhalation to be obtained. Laser-assisted analytical measurements are specific, fast, and characterized by a great detection power, and trace gas at the picomolar level can be determined with sub-sec resolution [117, 118, 119]. The major laser spectroscopic techniques, which are characterized by their high sensitivities and are currently being applied at breath analysis for detection of CO, CO_2, NH_3, NO, C_2H_6, C_2H_4 and COS, include tunable diode laser absorption spectroscopy (TDLAS), cavity ring-down spectroscopy (CRDS),

cavity leak-out absorption spectroscopy (CALOS), photo-acoustic spectroscopy (PAS) [120, 121, 122, 123].

Breath analysis is also conducted by using electrical sensors, which are comparatively inexpensive and smaller in size, but they have low detection selectivity and require frequent calibrations [124, 125, 126].

1.3 Renal physiology

The urinary system consists of two kidneys that filter blood and deliver the produced urine into the two ureters. From the ureters the urine is passed to the urinary bladder, which is drained via the urethra during urination. The kidneys are bean-shaped organs of about 11 cm long, 4 to 5 cm wide and 2 to 3 cm thick, and lie bilaterally in the retroperitoneum in the abdominal cavity.

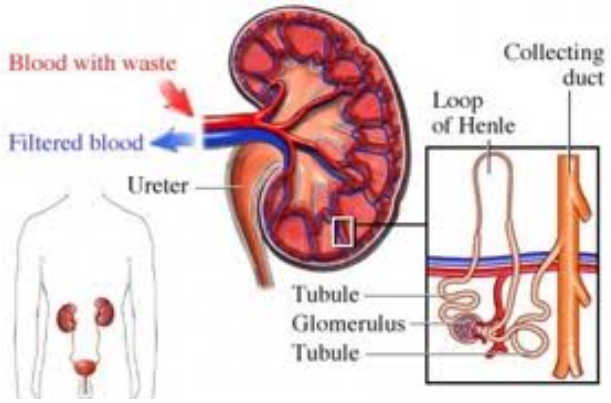

Figure 1.6 *Internal anatomy of the kidneys.*

The smallest functional unit of the kidney is the uriniferous tubule, each containing a nephron and a collecting tubule. There are approximately 1 to 1.3 million nephrons in each kidney. One nephron is composed of a vascular part (glomerulus), a drainage part (Bowman's capsule), a proximal tubule, Henle's loop and a distal tubule (Figure 1.6). Several nephrons are drained by one

collecting tubule, which enlarges downstream until it becomes a duct of Bellini and perforates the renal papilla.

The major function of the kidneys is removing toxic by-products of the metabolism and other molecules smaller than 69000 Da (i.e. smaller than albumin) by filtration of the blood flowing through the glomerulus. They also regulate body fluid composition and volume. Specifically resorption of salts (Na^+, K^+, Cl^-), glucose, creatine, proteins, and water takes place in the tubular parts. Because of these eliminating and conserving functions, the kidneys also contribute to the regulation of the blood pressure, hemodynamics, and the acid-base balance of the body. Additionally, kidneys have an endocrine function: they produce the hormone renin, erythropoietin and prostaglandines (derivatives of essential fatty acids to maintain homeostasis) and help in converting vitamin D to dihydroxycholecalciferol, a substance which controls calcium transport [53].

Renal insufficiency is a condition in which the kidneys lose their ability to purify the blood leading to the accumulation of toxins and waste products. According to the duration in which this occurs renal insufficiency can be divided into two main categories: acute (days to months) and chronic (years) renal failure.

As renal failure progresses, glomerular filtration rate as well as the amount of nephrons decreases. The main causes of end stage renal disease are diabetes and hypertension.

Dialysis is an artificial modality of renal replacement therapy used to manage renal insufficiency. It removes excess liquids and uremic toxins, assures the fluid balance and acid-base equilibrium, but partially replaces kidney functions: it can only replace a part of the excretory function, whereas the endocrine and metabolic function of the kidney cannot be restored.

The invention of dialysis dates back to the 19th century, when Thomas Graham discovered a method for separating gases by diffusion [127]. However, hemodialysis was not widely available till 1960, when the first patient was treated for chronic renal failure by intermittent hemodialysis.

1.3.1 Fundamentals of hemodialysis

Insufficient kidney function can lead to the accumulation of excess electrolytes, waste products and fluid. The concentrations of these compounds can reach toxic levels and need to be removed from the blood stream. Hemodialysis is a blood purifying therapy in which the blood of a patient is circulated through an artificial kidney, also called hemodialyzer. This is realized in an extracorporeal circuit (Figure 1.7) where one or two needles (or catheters) can be used as the patient's vascular access. A general hemodialysis therapy lasts about 9-15 hours a week, mostly spread over three sessions.

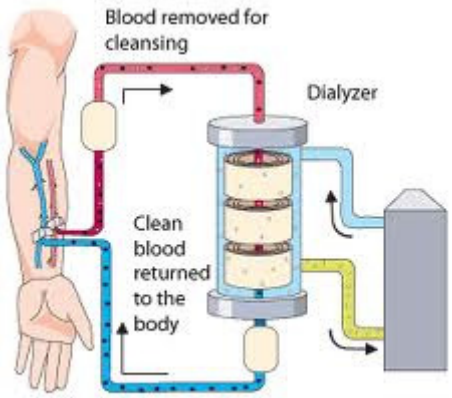

Figure 1.7 *The extracorporeal circuit in hemodialysis.*

Two types of hemodialyzers are in use: plate and hollow fiber dialyzers [128]. In a plate dialyzer, membrane sheets are packed together and blood and dialysate flow in subsequent layers. The

hollow fiber dialyzer consists of thousands of small capillaries (inner diameter in the range of 200 μm and wall thickness of 8-40 μm). Blood flows inside the capillaries whereas dialysate flows counter currently around them. Typical blood flow rates are in the range of 200 up to 350 mL/min, while dialysate flows are preferably twice the blood flow with a typical value of 500 mL/min. Membranes used in hemodialysis are of two basic types: organic cellulose derivatives (i.e. cuprophan, cellulose di-, tri- acetate and hemophan) and synthetic membranes (i.e. polyacrylonitrile, polysulfone, polyamide, polymethyl-methacrylate). With respect to the membrane characteristics, distinction can be made between low, medium, and high flux dialyzers on one hand (ultrafiltration coefficient lower than 15, between 15 and 40, and higher than 40 mL/h/mmHg, respectively), and low and high area dialyzers on the other (membrane surface lower and higher than 1.5 m^2, respectively).

In hemodialysis therapy, the dialyzer succeeds in purifying the blood and extracting the excess water due to basic transport phenomena, such as diffusion, ultrafiltration, and osmosis. As transport takes place between the blood and dialysate compartment over a semi-permeable membrane, fluid characteristics and membrane properties should also be considered.

Molecules in the blood, with a molecular size smaller than the pore size of the membrane, can diffuse across the semi-permeable membrane into the dialysate. The driving force for the diffusion is the concentration difference between the blood (high concentration) and the dialysate (low concentration). The diffusion is governed by Fick's law according to:

$$J = -D \cdot A \cdot \frac{dc}{dx} = -D \cdot A \cdot \frac{\Delta c}{\Delta x} \qquad (1.7)$$

where J is the flux [mmol·L^{-1}], D is the diffusity [cm^2·s^{-1}], A is the area of the membrane [m^2], and dc/dx is the concentration gradient [129].

The diffusity D is a unique property of the solute-solvent system at a specific temperature. The sign convention is adopted, which states that diffusion occurs in positive direction, i.e. from the region of higher activity (conc.) to that of lower so that the concentration will be decreasing in the direction of flux. Therefore, the right hand side of equation 1.7 must carry a negative sign [129]. The diffusity D is a constant at any particular temperature. Therefore, equation 1.7 can be written as:

$$J = -K_0 \cdot A \cdot \Delta C \tag{1.8}$$

where K_0 is the mass transfer coefficient [cm·min^{-1}] and ΔC is the concentration difference [mmol·L^{-1}] [129].

Equation 1.8 states that with a specific dialyzer (K_0·A is constant), the transfer of solutes from blood into dialysate will depend directly on the concentration difference (ΔC). This concentration difference is the driving force of dialysis. The concentration of solutes in blood and dialysate will linearly change, when solutes are transferred from one to the other. The solute concentration in blood decreases whilst in the dialyzer ($c_{Bi} \rightarrow c_{Bo}$). In contrast, the concentration in the dialysate increases ($c_{Di} \rightarrow c_{Do}$). The concentration difference at any point in the dialyzer determines the flux.

On the other hand, excessive body fluid has also to be removed from the body. However, the driving force for the removal of excessive body fluid is not same as for the solute removal (ΔC). The transfer of water from the patient to the dialysate is determined by a pressure difference (ΔP). The water flux can be calculated as follows:

$$Q_F = K_{UF} \cdot (P_B - P_D) \tag{1.9}$$

where Q_F is the ultrafiltration rate [ml·min^{-1}], and P_B-P_D is the pressure difference (driving force) between the pressure on the blood side and the dialysate side [129].

1.3.2 Dialysis fluid characteristics

The hemodialysis fluid should be considered as a temporary extension of the patient's extracellular fluid because of the bi-directional transport process when blood and dialysate are flowing through the dialyzer. Therefore, the composition of dialysis fluid is critical in achieving the desired blood purification and body fluid and electrolyte homeostasis. It contains (Table 1.2) reverse osmosis water, dextrose and different electrolytes like calcium-, magnesium-, potassium- and sodium chloride and sodium acetate or –bicarbonate [130]. The latter two fulfill the function of dialysate buffer, responsible for the correction of metabolic acidosis in the uremic patient. Hydrogen ions (H^+) are, soon after their production, buffered by plasma bicarbonate, and can only be removed by the diffusive flux of alkaline from the dialysate into the blood replacing the blood buffers [131].

Table 1.2 *Usual composition of dialysis fluid.*

Compound	**Concentration (mmol/L)**
Sodium	132 - 155
Potassium	0 - 4
Calcium	1.25 – 2
Magnesium	0.25 – 0.75
Chloride	90 - 120
Bicarbonate	27 - 40
Dextrose	0 – 5.5
pH	7.1 – 7.3

Besides the chemical composition, the physical and microbiological characteristics are also important. As the use of highly permeable membranes in hemodialysis is responsible for backfiltration and/or backdiffusion (filtration and/or diffusion from the dialysate compartment towards the blood compartment), toxic and pyrogenic substances can move from the dialysate towards the blood resulting in febrile reactions [132].

Nowadays, the composition of dialysis fluid is prescribed for each single patient to individualize the dialysis therapy according to the personal needs. The actual dialysis machines guarantee accurate proportioning of treated water and concentrated salts, continuous monitoring of the final composition and a constant maintenance of the required conductivity values.

The hemodialysis system is the end point of a hydraulic circuit where tap water is changed into reverse osmosis water through water supply, water pre-treatment, water purification [133], and dialysis fluid preparation. The pre-treatment consists of flowing tap water through filters, softener, carbon filter and microfilters. The subsequent treatment concerns flow through one or two reverse osmosis membranes and a deionizer, closing the purification chain with ultrafiltration and submicrofiltration.

1.3.3 Uremic toxins

The uremic syndrome results from the retention of solutes that are normally cleared by healthy kidneys and secreted into the urine. The gradual retention of a large number of organic metabolites of proteins, fatty acids, and carbohydrates characterizes the progression of renal failure.

Molecular weight is traditionally used as the parameter to classify uremic toxins, resulting in three groups of retention solutes: the

toxin class of low molecular weight (MW<500), middle molecular weight (500<MW<15000), and high molecular weight solutes (MW>15000). They can further be subdivided in protein-bound and nonprotein-bound solutes. Recently, an encyclopedic list of uremic retention solutes was composed by the European Uremic Toxin Work Group (EUTox), distinguishing between small molecules (MW<500), small protein-bound solutes (MW mostly <500), and middle molecules (MW>500) [134]. The main known uremic retention solutes are given in Table 1.3.

At present, about 90 uremic retention solutes have been identified. Forty-five of them are small molecules without known protein binding. Twenty-five compounds belong to the group of protein-bound solutes, with a molecular weight smaller than 500 Da, except two (i.e Leptin and Retinal-binding protein). From the 22 recognized middle molecules, 12 have a molecular weight exceeding 15000 Da [134].

Table 1.3 *Main known uremic retention solutes.*

Small water-soluble molecules	***Protein-bound solutes***	***Middle molecules***
Creatinine	Glyoxal	β2-Microglobulin
Guanidinosuccinic acid	Hippuric acid	β-Endorphin
Hypoxanthine	Homocysteine	Cystatin C
Methylguanidine	Indoxyl sulfate	Hyaluronic acid
Malondialdehyde	Kynurenic acid	Interleukin 1β
Oxalate	Methylglyoxal	Interleukin 6
Urea	p-cresol	Leptin
Uric acid	Pentosidine	Methionine-enkepahlin
Xanthine	Phenol	Retinal binding protein

Low molecular weight molecules are water-soluble and are relatively easy to remove using standard low flux dialysis membranes. Because the removal of small protein-bound solutes is hampered due to protein binding, their dialytic behaviour is comparable to that of larger molecules. The so-called middle molecules can only be removed using high flux dialysis membranes with large pores, unless they are adsorbed on the membrane.

CHAPTER 2

Clinical applications

2.1 Warfarin and Oral Anticoagulant Theraphy

Oral anticoagulant therapy (OAT) with coumarin derivatives such as warfarin, acenocoumarol and phenprocoumon, (also called vitamin K antagonists), extends the time it takes for the blood to clot, thereby reducing thromboembolic events in multiple clinical contexts [135]. These include atrial fibrillation, treatment of deep-vein thrombosis, pulmonary embolism, prosthetic heart valves, and acute myocardial infarction. In fact, oral anticoagulant treatment has been available for more than 60 years, and is prescribed for both prophylactic and therapeutic use to patients at increased risk of thromboembolism. The relation between blood clotting and coumarin derivates was established by Dam and Doisy who shared the Nobel Prize in 1943 for their work [136, 137]. Their main discoveries were the postulation and prove of the existence of vitamin K (K for German Koagulation) and the description of structure of the vitamin. The fundamental physiological mechanism of affecting synthesis of certain coagulation factors was known, however, the biochemical description and understanding was yet to be established in the mid 70's [138].

Both in Italy and around the world, patients receiving oral anticoagulant therapy are very numerous and tend to increase steadily in recent years. Reasons include improvements in clinical outcomes, increasing common disease indications for their use [139], and improvements in anticoagulant safety [140]. According

to an estimate of the Federazione Centri per la diagnosi della trombosi e la Sorveglianza delle terapie Antitrombotiche (FCSA), which takes into account the market data of drugs and the average daily doses, in Italy there are about one million patients being treated with an oral anticoagulant [141]. Being the mainstream therapy for such a large range of indications, it is not surprising that warfarin is a widely used drug with increasing prescriptions over time.

2.1.1 History of Warfarin

The history of the discovery and development of coumarin anticoagulants randomly started in the United States at the end of 1800 when farmers in North America experimented the sweet clover for the recovery of vast grasslands ravaged by herds of cattle. Shortly after, in 1921, a hemorrhagic epidemic spread, known as sweat clover disease, which decimated the cattle fed forage-rich clover.

The disease continued though the 1920s and early 1930s. In 1933, Karl Link embarked on a study of the cattle disease at the University of Wisconsin. The research performed by Karl Link identified that the cause of such bleeding was not a contagious disease, viral or bacterial infection, but a chemical produced by a chemical reaction catalyzed by fungi of the genus Aspergillus. In 1939 Link's team crystallized the anticoagulant material [142]. Almost a year later the structure was identified and the chemical was synthesized [143] and named "dicumarol". Soon, dicumarol was used throughout the world to prevent and to treat thromboembolic problems.

In parallel with dicumarol's introduction in clinical medicine, Link's group synthesized over 150 of related coumarins looking not

so much for a better anticoagulant for human patients but rather for a more effective rodenticide. In 1948, one of those substances, number 42, was selected as a candidate for use as rodenticide in a project sponsored by the Wisconsin Alumni Research Foundation (WARF). The initial letters of the sponsor combined with “arin” (from coumarin) gave the compound its official name “Warfarin”. Being a highly potent (ten times more potent than dicumarol), water soluble anticoagulant without discernable taste or odour, it was easily delivered via cereal grain in doses high enough to cause lethal internal bleedings in the exposed rodents.

Although the original oral anticoagulant dicumarol was an effective means of preventing thrombosis, researchers in the United States and Europe were continuously searching for more potent coumarins with faster onset of action, and a wider selection of administration routes. Since these properties were largely similar to those desired in a rodenticide, it is not entirely surprising that Link in 1950 proposed that warfarin should be tried as an antithrombotic. Equally unsurprising was the initial reluctance among clinicians to use warfarin in patients, given the fact that the substance was already a well-established rodenticide [144]. However, it’s reputation as a poisonous drug was somewhat mitigated in 1951, after a report of an army inductee failing to commit suicide by ingesting a packet of rat poison containing more than 500 mg of warfarin.

In 1955, the drug’s reputation was further improved as the President Dwight Eisenhower of the United States was treated with this drug at a dose of 35 mg/week after a myocardial infarction and so he became one of the first famous patients on warfarin [145]. He would stay on this treatment until his death and it was only suspended for an operation for a bowel obstruction and a cholecystectomy. The treatment would not protect him against further heart attacks and a stroke.

Warfarin has since then not only become used as a highly effective rodenticide but also as the major oral anticoagulant for human thromboembolic diseases throughout the world [146] with nearly 21.5 million prescriptions just in the USA in 2007 [147].

2.1.2 Physicochemical Properties of Warfarin

Warfarin, $C_{19}H_{16}O_4$, 3-(α-Acetonylbenzyl)-4-hydroxycoumarin (Figure 2.1) is a colourless crystalline material with a MW of 308.3 and melting point between 159°C to 160°C.

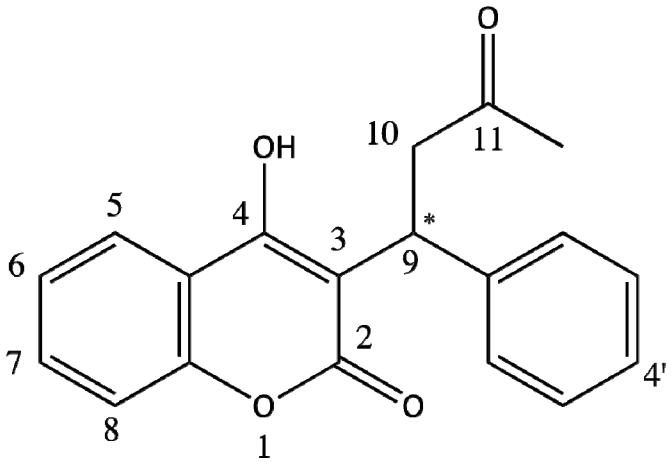

Figure 2.1 *Chemical structure of warfarin*

The rigid and aromatic structure gives to warfarin a strong native fluorescence; thus it make possible fluorescence detection [148]. Warfarin is practically insoluble in water, moderately soluble in ethanol and readily soluble in acetone.

Warfarin in the free acid form is not very soluble in water and is therefore always administered as the sodium salt. Warfarin sodium, $C_{19}H_{15}NaO_4$ (MW: 330.32), (3-(α-Acetonylbenzyl)-4-hydroxycoumarin sodium salt) is a white hygroscopic powder which is very soluble in water and in alcohols, soluble in acetone, very slightly soluble in ether and in methylene chloride. Warfarin

has an apparent dissociation constant (pKa) of 5.19 (at 25°C) and an octanol/water partition coefficient (log P_{ow}) of 0.7 at pH=7, 20°C [149, 150].

Table 2.1 *Physicochemical Properties of warfarin* [150].

Property	**Value**
Solubility in water at 20 °C	267 mg/L
Solubility in organic solvents at 20 °C	Acetone: 54600 mg/L n-Heptane: 6.4 mg/L Methanol: 22200 mg/L Ethyl acetate: 16900 mg/L
Melting point	165 °C
Log P at pH=7, 20°C	0.7
pKa at 25 °C	5.19
Vapour pressure at 25 °C	3.0 mPa
Henry's law constant at 25 °C	3.50 10^{-3} Pa m^3 mol^{-1}

Warfarin is a chiral molecule. The asymmetric carbon at position 9 of warfarin gives rise to two enantiomers, namely R-(+)-warfarin (R-warfarin) and its mirror image isomer S-(-)-warfarin (S-warfarin) (Figure 2.2). The main monohydroxylated metabolites of warfarin, such as 4'-, 6-, 7- and 8-hydroxywarfarin, also contain a single asymmetric centre (Table 2.2) [151].

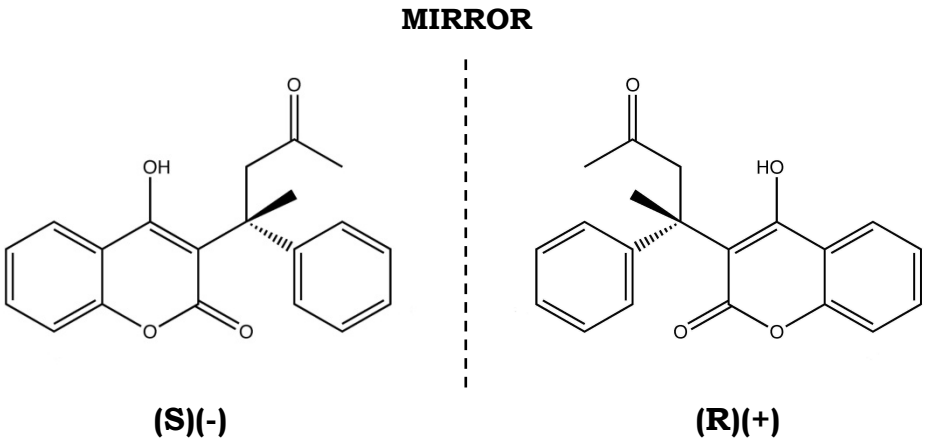

Figure 2.2 *Three dimensional structures of warfarin enantiomers.*

Table 2.2 *Structures of warfarin and its main metabolites. Adapted from* [152].

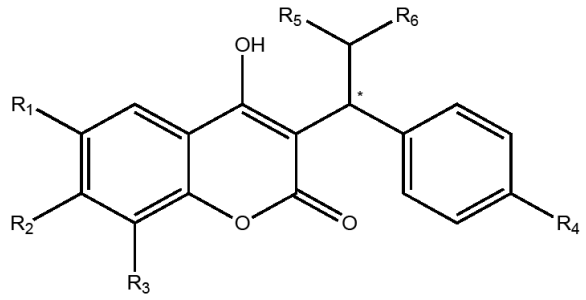

Compound	Functional groups structure					
	R_1	R_2	R_3	R_4	R_5	R_6
Warfarin	H	H	H	H	H	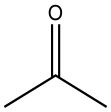
6-Hydroxywarfarin	OH	H	H	H	H	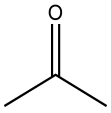
7-Hydroxywarfarin	H	OH	H	H	H	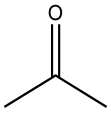
8-Hydroxywarfarin	H	H	OH	H	H	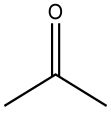
4'-Hydroxywarfarin	H	H	H	OH	H	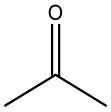
10-Hydroxywarfarin	H	H	H	H	OH a	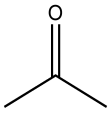
Warfarin alcohol	H	H	H	H	OH	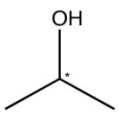

Note: *: Asymmetric centre; a: The second asymmetric centre generated at C-10 position.

2.1.3 Clinical Use of Warfarin

In the clinical setting, warfarin is administered for the prevention and treatment of venous thrombosis and pulmonary embolism [135]. It is also used for the prophylaxis and treatment of thromboembolic complications associated with atrial fibrillation, diabetes mellitus and hypertension associated with an otherwise normal heart. It is additionally used as an adjunct in the treatment of coronary occlusion. Warfarin does not affect established thrombi or reverse tissue ischemia but is instead used to prevent clot growth and secondary complications [135]. Thromboembolism remains a serious complication after heart valve replacement whether the prosthesis is a mechanical valve or a valve of bioprosthetic tissue. Relatively intensive anticoagulant treatment is recommended with mechanical valve replacement, and therapy is depending on valve type and position [153]. Bioprostheses do not always require OAT, but patients are often anticoagulated for a period of 3-6 months, and with less intensity compared to treatment of patients with mechanical heart valve replacement [154]. Atrial fibrillation is one of the relatively new major patient groups who receive OAT to prevent formation of clots due to abnormal blood flow caused by the fibrillation [155]. Acute myocardial infarction and treatment with anticoagulants have been discussed since introduction of the treatment for this clinical condition. The prophylaxis treatment of this is often combined with aspirin [156]. The optimum duration of oral anticoagulant therapy is influenced by whether thrombosis is unprovoked (idiopathic), associated with ongoing risk factors (such as malignancy), or is secondary to a reversible cause; a longer course of therapy should be given for idiopathic thrombosis [157] and when there is an ongoing risk factor. Treatment should also be longer in patients

with proximal vein thrombosis than in those with distal thrombosis and in patients with recurrent thrombosis vs those with a single episode. Other areas where OAT is applied are post-surgery, e.g. knee or hip replacement, and hereditary diseases such as thrombophilia.

The ranges of International Normalized Ratio (INR) recommended by the British Society of Haematology are shown in table 2.3.

Table 2.3 *Recommended Therapeutic Range for Oral Anticoagulant Therapy.*

Indications	**INR**
Prophylaxis of deep vein thrombosis (high risk surgery)	2.0 – 2.5
Treatment of deep vein thrombosis, pulmonary embolism, atrial fibrillation	2.0 – 3.0
Recurrent deep vein thrombosis and pulmonary embolism Arterial disease (myocardial infarction, arterial grafts) Cardiac prosthetic valves and grafts	3.0 – 4.5

2.1.4 Pharmacodynamics of Warfarin

Warfarin produces an anticoagulant effect by interfering with the cyclic interconversion of vitamin K and its 2,3 epoxide (vitamin K epoxide) (Figure 2.3) [158]. Vitamin K is reduced (to vitamin KH2) either by a NADH dependent reductase activity, reaction ‹1›, or a reductase reaction dependent on the conversion of dithiol into disulfide, ‹3› (shaded). The carboxylation reaction, ‹2›, which converts glutamate residues (Glu) into γ-carboxyglutamate residues (Gla) on the N-terminal regions of vitamin K–dependent

proteins, requires molecular oxygen and carbon dioxide, and is driven by a vitamin hydroquinone (KH2) dependent carboxylase activity. This activity simultaneously converts vitamin KH2 into vitamin K epoxide. The last step in the vitamin K cycle, reaction ‹3›, is a reductase of vitamin K epoxide dependent on conversion of dithiol into disulfide.

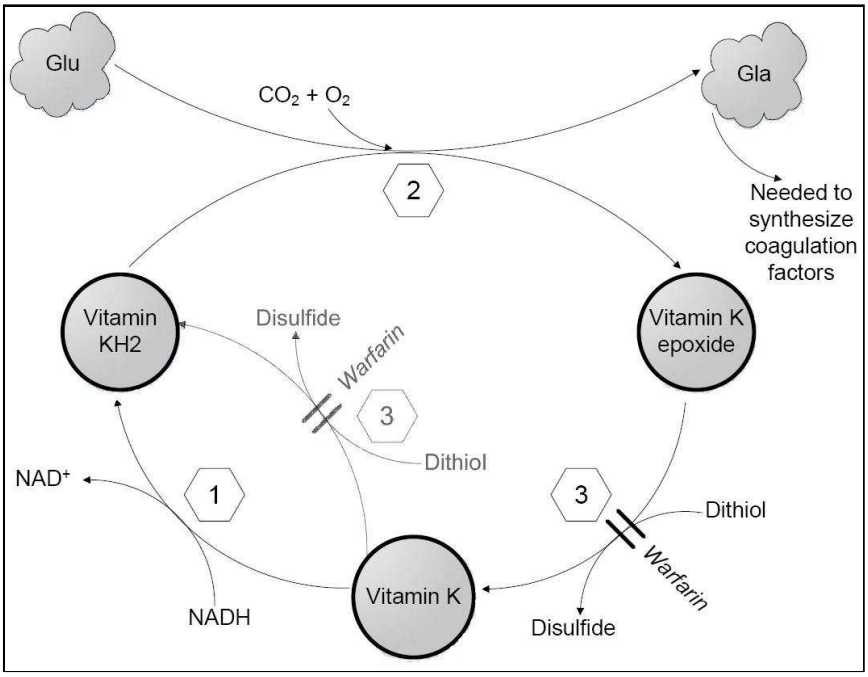

Figure 2.3 *A diagram of the actions involved in the vitamin K cycle and the site of action of oral anticoagulants.*

Warfarin acts by a partly or complete block of two different steps in the vitamin K cycle [159]: the two reactions indicated by ‹3› in Figure 2.3. When vitamin K hydroquinone (VKH2) availability is decreased, the vitamin K-dependent carboxylation of glutamic acids is reduced. If this reaction is halted, only a limited amount of vitamin K epoxide will be available for recycling of vitamin K by the enzyme Vitamin K epoxide reductase complex subunit 1 (VKORC1) [160].

This leads to synthesis of proteins induced by vitamin K absence, i.e. coagulation factors (II, VII, IX, and X) missing a carbon chain

and unable to function in the coagulation cascade [161]. In addition to their anticoagulant effect, the vitamin K antagonists inhibit carboxylation of the regulatory anticoagulant proteins C and S and therefore have the potential to exert a procoagulant effect. Synthesis of functional vitamin K dependent coagulation factors now becomes dependent on new sources of vitamin K.

Warfarin does not alter the degradation rate of clotting factors already in circulation; it only affects the synthesis rate of clotting factors. Therefore, the onset of anticoagulation induced by warfarin is delayed. The anticoagulation effect of warfarin takes about 8 hours to become apparent as a result of the time taken for degradation of carboxylated factors [162]. The onset of action of warfarin depends on the elimination half-lives of the relevant factors. Factor VII, with half-life of 6 hours, is affected first, then Factors IX, X and II with half-lives of 24, 40 and 60 hours, respectively [163]. The two enantiomers of warfarin display different anticoagulant potency in humans. S-warfarin is considerably more potent than R-warfarin in terms of the anticoagulant effect [162].

The anticoagulant effect of coumarins can be overcome by low doses of vitamin K1 (either ingested in food or administered therapeutically) because vitamin K1 bypasses vitamin K epoxide reductase (Figure 2.3). Patients treated with large doses of vitamin K1 (usually > 5 mg) can become resistant to warfarin for up to a week because vitamin K1 accumulating in the liver is available to bypass vitamin K epoxide reductase.

Warfarin also interferes with the carboxylation of γ-carboxyglutamate proteins synthesized in bone [164]. Although these effects contribute to fetal bone abnormalities when mothers are treated with warfarin during pregnancy [165], there is no

evidence that warfarin directly affects bone metabolism when administered to children or adults.

2.1.5 Pharmacokinetics of Warfarin

Warfarin is a racemic mixture of 2 optically active isomers, the R and S form, in roughly equal proportion. In studies that administered warfarin enantiomers separately, it was found that the S-enantiomer exhibits two to five times more anticoagulant activity than the R-enantiomer in humans but generally has a more rapid clearance [166]. Furthermore Chan *et al* [162] found that the anticoagulant effect of warfarin is predominantly contributed by S-enantiomer when warfarin was administered as *rac*-warfarin.

Warfarin is essentially completely absorbed from the gastrointestinal tract after oral administration and has a systemic bioavailability of more than 90% in humans [162]. The maximal blood concentration in healthy volunteers is generally achieved within 60–90 minutes after oral administration.

Once in the systemic circulation, warfarin's distribution to other tissues is very limited as indicated by a small volume of distribution (V_D), approximately 10 liters in an individual weighing 70 Kg [167].

Although this volume does not refer to any actual body fluid or space, it provides a measure of a drug's propensity to remain in the plasma, rather than being distributed to other parts of the body. This is of interest, since the body's systems for elimination of drugs usually only target drug residing in plasma. Hence, drugs with a smaller V_D tend to be cleared more rapidly, all other factors equal. Racemic warfarin has a half-life of 36 to 42 hours.

Approximately 99.5% of the warfarin is bound to human plasma serum proteins, primarily albumin, where it is pharmacologically

inactive and is protected from biotransformation and excretion [168].

Warfarin accumulates in the liver, where the 2 isomers are metabolically transformed by different pathways to inactive hydroxylated metabolites (predominant route) and also by reductases to reduced metabolites (warfarin alcohols). While S-warfarin is almost exclusively metabolized by the polymorphic cytochrome P450 2C9 (CYP2C9) enzyme, R-warfarin is metabolized by a wide range of cytochrome P450 enzymes, including CYP3A4, CYP2C19 and CYP1A2 (but not CYP2C9) [169].

Hepatic metabolism of warfarin is the major determinant of inter-subject variability in the warfarin dose-concentration-response relationship. Warfarin is metabolized in a complex manner involving: (1) keto reduction resulting in the formation of four diastereoisomeric metabolites designated as warfarin alcohols; (2) oxidation to yield regioisomeric 4'-, 6-, 7-, 8- and 10 hydroxywarfarin; (3) dehydration of warfarin alcohol to the cyclic metabolite and (4) various conjugation reactions [170]. The warfarin alcohols have minimal anticoagulant activity. Table 2.2 shows the structures of warfarin and its main metabolites.

Both reductive and oxidative metabolites of warfarin are principally excreted into the urine (≈ 80%) and, to a lesser extent (≈ 20%), into the faeces while enterohepatic circulation has been observed for the parent drug. Only 2-5% of the warfarin administered appears unchanged in human urine.

2.1.6 Monitoring of Warfarin effect

Coumarin anticoagulation needs to be strictly monitored because of the narrow therapeutic area between under- and over-anticoagulation. In case of under-anticoagulation the patient is at

risk for thromboembolic complications and in case of over-anticoagulation there is an increased risk of severe bleeding problems. Therefore, patients taking warfarin require frequent monitoring to adjust the dose in response to different interactions by food, drugs and illness [171, 172, 173]. This necessary monitoring represents an expensive investment for health care systems and an inconvenience for patients. Despite a close monitoring of therapy, thromboembolism and bleeding are common concerns and accounts for a large proportion of the morbidity and mortality in these patients: major bleedings have an incidence ranging from 0.3 – 13.4 % per year and that of major thromboembolism ranging from 0.4 – 3.5 % per year [174, 175], though highly dependent on selection of patients and definition of events.

A number of methods can be used to measure the effect of warfarin in individuals, including the measurements of vitamin K1 and vitamin K1 2,3 epoxide concentration [176], γ-carboxyglutamic acid concentration [177] and clotting factor concentrations. Of the various methods available, the PT test or INR test is the most common method for monitoring the effect of oral anticoagulants [135]. The PT is responsive to depression of three of the four vitamin K-dependent procoagulant clotting factors (II, VII and X), that are reduced by warfarin at a rate proportional to their respective half-lives. Thus, during the first few days of warfarin therapy, the PT reflects mainly reduction of factor VII, since this factor has the shortest half-life (≈ 6 hours) among the vitamin K-dependent factors. Subsequently, reduction of factors X and II contributes to prolongation of the PT. The PT assay is performed by adding calcium and thromboplastin to citrated plasma (Equation 2.1):

$$\text{Citrated plasma} + \text{Thromboplastin} + CaCl_2 \rightarrow \text{Fibrin Clot} \qquad (2.1)$$

The traditional term “thromboplastin” refers to a phospholipid-protein extract of tissue (usually lung, brain, or placenta) that contains both the tissue factor and phospholipid necessary to promote activation of factor X by factor VII. Thromboplastins vary in responsiveness to the anticoagulant effects of warfarin according to their source, phospholipid content, and preparation [178].

The responsiveness of thromboplastins can be measured by assessing their International Sensitivity Index (ISI). Difference in thromboplastin responsiveness was the main reason for clinically important differences in oral anticoagulant dosing. In 1983, the INR system proposed by Kirkwood was adopted by the World Health Organization (WHO) which then made international PT standardisation possible [179]. The calculation of INR is described in Equation 2.2.

$$INR = (\text{patient PT}/\text{mean normal PT})^{ISI} \qquad (2.2)$$

where ISI denotes the International Sensitivity Index of the thromboplastin used at the local laboratory to perform the PT measurement.

Warfarin dosing may be separated into initial and maintenance phases. An anticoagulant effect is observed within 2 to 7 days after beginning oral warfarin, according to the dose administered. When a rapid effect is required, heparin should be given concurrently with warfarin for ≥ 4 days. The common practice of administering a loading dose of warfarin is generally unnecessary, and there are theoretical reasons for beginning treatment with the average maintenance dose of ≈ 5 mg daily.

When treatment is initiated, there is a large uncertainty regarding the individual dose requirements and to avoid prolonged over- or underdosing, the INR is usually checked daily until the therapeutic range has been reached and sustained for 2 consecutive days, then 2 or 3 times weekly for 1 to 2 weeks, then less often, according to

the stability of the results. Once the INR becomes stable, the frequency of testing can be reduced to intervals as long as 4 weeks. The effectiveness and safety of warfarin therapy are critically dependent on maintaining the INR in the therapeutic range.

2.1.7 Factors influencing oral anticoagulant therapy

Drug interactions

The term *drug interaction* refers to a situation were the effect of a drug is altered by another drug, an herbal medicine or by food. The interaction can result in either increased or decreased pharmacologic effect of the drug, as well as an altered risk of specific side-effects. Clinically important drug interactions occur when either of the interacting drugs have a steep concentration-response curve and narrow safety margin such that a small change in plasma concentration leads to a substantial change in beneficial or adverse effect [180].

Drug interactions involving warfarin are exceedingly common. There have been more than 250 compounds proven to or suspected of having an interaction with warfarin [181]. One reason for this abundance is of course warfarin's narrow therapeutic range, where even minor changes in drug concentration or drug sensitivity can have major clinical consequences. Another factor that is likely to be of importance is the elimination of S-warfarin being heavily dependent on a single liver enzyme (CYP2C9), making it vulnerable to pharmacokinetic drug interactions targeting this phatway.

Understanding the mechanism of warfarin drug interactions provides an insight into the possible clinical significance of an interaction and can help elucidate strategies to avoid or minimise the impact in a given patient.

Drug interactions with warfarin can occur via two main mechanisms:

1. *Pharmacodynamic interactions*: modification of the pharmacological effect of warfarin without altering its concentration in the body;
2. *Pharmacokinetic interactions*: alteration of the concentration of warfarin reaching its site of action.

Pharmacodynamic warfarin interactions include drug and food containing vitamin K or altering the turnover of vitamin K, and antithrombotic drugs such as aspirin, that increases the risk of bleeding by inhibition of platelet aggregation in the blood [182, 183].

Pharmacokinetic mechanisms for drug interactions with warfarin comprise mainly of induction or inhibition of drug metabolising enzymes and to a lesser extent alteration of plasma protein binding.

Some drugs, e.g. the lipid-lowering agent cholestyramine, reduce the absorption of warfarin in the gut, thereby attenuating its anticoagulant effect. Drugs that bind extensively to albumin may displace warfarin from its binding sites on the plasma protein, thereby increasing the unbound concentration and the anticoagulant effect [184], but the effect is only transient and rarely of clinical importance. The most important pharmacokinetic interaction mechanism is altered hepatic metabolism of warfarin due to inhibition or induction of cytochrome P450 enzymes, CYP2C9 in particular. Important inhibitors of warfarin metabolism include e.g. the antiarrhythmic drug amiodarone and several azole-type antifungals, while inducers such as the anti-tubercolosis agent rifampicin and several anti-epileptic drugs may vastly increase the warfarin dose required for adequate anticoagulant effect.

Genetic variations

Mutations in the gene coding for warfarin metabolism enzymes have been shown to alter the response to warfarin treatment, thus increasing inter-individual INR variation. Some of the best documented wild types of CYP2C9*1 is CYP2C9*2 and CYP2C9*3 [185]. These mutations are associated with an impaired ability to metabolize warfarin, hence prolonging warfarin half-life and leading to reduced warfarin requirements. Screening for gene-mutations before initiating warfarin treatment is an ongoing discussion, but the relation between the mutations and higher risk of bleeding has been established [186, 187]. The VKORC1 enzyme is the target for warfarin's inhibitory effect on the vitamin K cycle. Mutations in this gene have shown to account for some of the difficulties to maintain INR at target level [188]. Whereas of three well-described wild types of CYP2C9, there is a higher degree of diversity in mutations on VKOR1C; some leads to warfarin resistance, while others lead to reduced VKOR activity [189]. Fifty percent of the inter-individual variation on warfarin response is believed to be directly accounted for by the pharmacokinetic variants (CYP2C9) and pharmacodynamic variants (VKORC1) [190]. A population based model of different types of genetic mutations and warfarin treatment showed the effect of different combination of wild type alleles. The model showed how equal dose of warfarin could potential lead to an INR value of 2 in one patient, and an INR value above 6 in another patient solely depending on gene mutations [191].

Dietary vitamin K

OAT can be affected by numerous environmental factors that can alter warfarin kinetics and dynamics [182]. Vitamin K dietary intake is one of these factors, which may alter the response to warfarin treatment. New external sources of vitamin K will increase the production of functional coagulation factors depending on vitamin K. The clinical relevance of changes in vitamin K has been discussed, and it has been shown how patients with poor dietary intake of vitamin K often has less stable control of anticoagulation [192]. It has been suggested to provide these unstable anticoagulated patients with oral vitamin K supplementation; however unrecognized intake of such can lead to warfarin resistance [193]. Other studies reported that steady-state warfarin treatment was not affected by dietary vitamin K intake [194, 195]. However, Khan and colleagues suggested that their findings, of vitamin K having no effect in their regression model, could be related to the fact that warfarin dosage had already been adjusted to control for individual vitamin K status. Further, they only involved patients whose dose of warfarin remained constant. Variations in vitamin K might be greater in patients who do not receive an optimized warfarin dose that remains constant. Although Loebstein and colleagues reported vitamin K as negligible; a recently published review by the same research group acknowledges that vitamin K plays an important role in maintaining therapeutic stability [196]. The magnitude of clinically relevant change in dietary vitamin K intake has been reported to be above 100 mg/day [197].

2.1.8 Approaches to counter challenges in OAT

Approaches to improve anticoagulant control include, among others, development of new antithrombotic drugs, use of different types of management of the treatment, and use of computer software that can aid in dose adjustment.

Development of new antithrombotic drugs

Through the last decade researchers have been working on development of a new type of antithrombotic drug, which could eliminate or minimize the difficulties in warfarin treatment: the relatively narrow therapeutic window, large inter-individual dose response, drug-to-drug interactions, and the need for close monitoring that is associated with the fear of adverse events of over-treatment. Direct thrombin inhibitors are a newly developed class of anticoagulants that acts by directly inhibiting activated clotting factor II. Another type of newly developed drug class is direct clotting factor X inhibitors [198, 199]. Both drug classes can be given in a fixed dose and does not require routine monitoring. Large-scale randomized controlled trials have been conducted with different types of commercially available analogues, and the usage has been explored in different clinical conditions [200, 201, 202].

Types of OAT management

The introduction of portable monitors (point-of-care devices) for the management of patients on oral anticoagulation allows the patient to self-test at home with a drop of whole blood. Portable monitors for monitoring long-term oral anticoagulation were introduced in the 1990s. POC monitors measure a thromboplastin-mediated

clotting time that is then converted to a plasma PT equivalent by a microprocessor and expressed as a PT or INR. Portable monitors have proved to be reliable with regard to analytical accuracy, although INR measurements tend to be lower with the portable coagulometers compared to laboratory analysers [203, 204].

Generally patients receive a structured educational programme given by the nurses or physicians responsible for their care. In addition, they receive training in self-testing, instructions to prevent bleeding and thromboembolic complications, and are made aware of the effects of diet and medications [205].

Patients who self-test can either adjust their therapy according to a pre-determined dose-INR schedule (self-management) or they can call a clinic to be told the appropriate dose adjustment (self-monitoring). Several trials of self-monitoring of oral anticoagulant therapy suggest this may be equal to or better than standard monitoring [206, 207].

There are several available point-of-care devices and the most well known is the CoaguChek® monitor. Other available monitors are the ProTime® Microcoagulation System, INRatio® Monitor, Hemochron Junior Signature, and the TAS near-patient test system. Potential advantages of self-monitoring and self-management include improved convenience for patients, better treatment adherence, more frequent monitoring, and fewer thromboembolic and haemorrhagic complications [208, 209].

Decision support systems

Computer programs with algorithms capable of predicting the next warfarin dose (or response to a future warfarin dose), can potentially aid poorly controlled dose management in OAT. Such systems are based on different approaches ranging from strict expert-based algorithms, population- based

pharmacokinetic/pharmacodynamic (PK/PD) models, and rigid mathematical methods such as regression modelling. Bayesian parameter optimization methods are common techniques in the latter two approaches, and are meant to account for inter- and intraindividual response to vitamin K antagonists [210].
Through the past 25 years computerized decision support systems (CDSS) have been available to assist clinicians in OAT. Some of the first studies have shown that such systems can be at least as effective as experienced physicians with regard to dose adjustment [211, 212, 213]. In a large scale multicenter randomized trial Poller and colleagues showed the effective use of the computer program DAWN AC [214]. The computer program gave significantly better INR control compared to physician management. Another approach by Manotti and colleagues using the software program PARMA (later PARMA 5) achieved similar results as the DAWN AC study; even though they obtained a slight higher Time (spent) in Therapeutic Range (TTR) [139, 215]. Poller and colleagues conducted yet another multicentre randomized study comparing the use of DAWN AC and PARMA 5 in different countries [216]. This proved that computer-assisted dosage could be both safe and effective. However, the American College of Chest Physicians Evidence-Based Clinical Practice Guidelines (8th Edition) do not directly recommend use of CDSS, and the guidelines state that it should be based on physician preferences [217].

Pending instrumental self-monitoring solutions easier to use and cheaper, or pharmacological solutions more effective and independent of external factors (lifestyle, diet, medication, etc.), a certain advantage for patients undergoing anticoagulant oral therapy with warfarin may be to carry out their monitoring in biological matrices alternatives to blood. In the case of oral fluid, an obvious advantage is the non-invasiveness of sampling resulting

in a direct and immediate relief of the patient. Contrary to the blood, the collection of biological fluids such as oral fluid can be performed without special equipment, even in the case of less cooperative patients such as children or elderly.

Furthermore, we believe it possible to find in the oral fluid useful information relevant to the coagulation level, with a potential clinical interest both for a deeper understanding of warfarin action and patient monitoring.

Since oral fluid is a matrix far less complex than blood, in case of success it is not unreasonable to imagine that the determination of warfarin concentration in oral fluid could become a non-invasive test enabling the efficacy and safety of warfarin therapy to be monitored by the patient itself in the time span between two conventional INR checks.

Thus, a non-invasive method providing information on the anticoagulation level, potentially implementable in low cost devices, could modify the present management of anticoagulation therapy and make warfarin more attractive in a moment when a new generation of drugs is appearing on the market.

2.2 Monitoring of volatile compounds in human breath

2.2.1 Diabetes mellitus

Diabetes mellitus is a group of metabolic diseases characterized by high glucose levels in blood (hyperglycaemia), that result from defects in insulin secretion, or action, or both [218]. Insulin is the hormone, produced by the pancreas, which permits glucose to enter into cells and to be used as source of energy. When this mechanism is altered, glucose accumulates in the blood circulation. Once the glucose haematic and renal threshold has

been exceeded, the effects of glycosuria (glucose in urine) and polyuria (loss of water and electrolytes) appear and give rise to polydipsia (increased thirst) and polyphagia (increased hunger).
The organism therefore tries to produce glucose through other metabolic pathways such as lipolysis (fat acids oxidation), which causes an increase in ketone bodies in blood (acetone, β-hydroxybutyric acid, acetoacetic acid).
There are two main types of diabetes:

1) Type 1 diabetes, formerly known as insulin-dependent diabetes mellitus (IDDM) or juvenile-onset diabetes, is caused by autoimmune destruction of the β-cells of the pancreas, rendering the pancreas unable to synthesize and secrete insulin [219].
2) Type 2 diabetes, formerly known as non-insulin-dependent diabetes mellitus (NIDDM) or adult-onset diabetes, results from insulin resistance, a condition in which cells fail to use insulin properly, sometimes combined with an absolute insulin deficiency [220, 221].

The diagnosis of diabetes is based on the results obtained by specific medical examinations besides on the clinical symptoms [218]. The oral glucose tolerance test (OGTT) is a diabetes diagnostic test which monitors glycaemia in the subsequent hours after dispensing a known amount of glucose (150 mL of a 50% glucose solution). After dispensing glucose, glycaemia rises. Within two hours, in subjects without diabetes, glycaemia reduces to 140 mg/dL; if this doesn't happen the OGT is considered positive and diabetes is diagnosed.

Chemical composition of exhaled air reflects the general metabolic conditions and it may give useful information on the state of health of a person. For these reasons we investigated the possibility of

diagnosing diabetes mellitus by non-invasive monitoring of volatile compounds in exhaled breath during the oral glucose tolerance test (OGTT).

2.2.2 Volatile anaesthetic agents: sevoflurane

Recently two new inhalant anaesthetic agents were commercialised in Europe, sevoflurane and desflurane. Both agents fit the mould of several other new anaesthetic agents and adjuvants. They permit greater control over the course of anaesthesia and more rapid recovery from anaesthesia than do their predecessors.
Sevoflurane was developed in the seventies [222] and since 1980 it is extensively examined in human and veterinary anaesthesia, especially on an experimental basis in the beginning. Since 1990 it can be used in clinical human anaesthesia.

2.2.2.1 Physicochemical Properties of Sevoflurane

The chemical structure of inhalation anaesthetics and their physical properties are important determinants of their actions and safety of administration.
Sevoflurane (1,1,1,3,3,3-hexafluoro-2-(fluoromethoxy)propane, $C_4H_3F_7O$) is a colourless, volatile, non-flammable liquid with a characteristic mild odour resembling ether. Chemically, sevoflurane is a polyfluorinated methyl isopropyl ether (Figure 2.4) with 7 fluorine atoms and a molecular weight of 200.05. The chemical structure of sevoflurane is responsible for its kinetic properties.

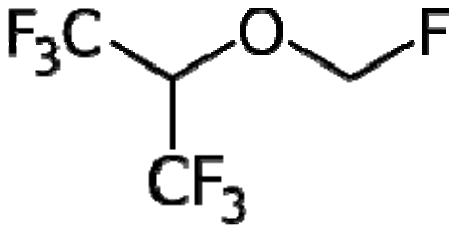

Figure 2.4 *Chemical structure of sevoflurane*

Fluorination of the carbon group resulted in a low blood-gas partition coefficient (0.69), which is considerably lower compared to halothane, enflurane and isoflurane [223].
The low blood-gas solubility produces the following properties:

1. more rapid increase in alveolar anaesthetic concentration during induction of anaesthesia;
2. more precise control of alveolar anaesthetic concentration during maintenance of anaesthesia;
3. more rapid decrease in alveolar anaesthetic concentration during elimination.

The human tissue-blood partition coefficients of sevoflurane in the brain (1.70), fat (48.0), kidneys (1.20), liver (1.80) and muscles (3.10) are intermediate between isoflurane en halothane. A low brain-blood partition coefficient is advantageous for a rapid control and adjustment of anaesthetic depth; whereas a low fat-blood partition coefficient is of primordial importance for a rapid recovery from anaesthesia [224].
The solubility characteristics of sevoflurane in rubber (14.0) and plastic are lower compared to isoflurane and halothane [225]. Consequently, the anaesthetic circuit extracts less agent during anaesthetic administration and redistributes less agent to rebreathed gases during elimination. This can be important since losses of volatile anaesthetic by circuit absorption may compromise measurements of anaesthetic uptake [226].

The boiling point (58.6 °C) and vapour pressure (157 mmHg at 20 °C) of sevoflurane are comparable with those from halothane, isoflurane and enflurane. Hence, conventional precision vaporisers without specific technical requirements can be used [227].
The most common measure of anaesthetic potency of an inhalation anaesthetic is the minimum alveolar concentration (MAC) of anaesthetic in volumes (percentage) which are necessary to prevent movement in 50% of patients during skin incision [228]. As is the case with other inhalational anaesthetics, the anaesthetic potency of sevoflurane is correlated with its lipid solubility. With an oil/gas partition coefficient of 47.2 its MAC has been reported to be 2.05% [229]. Thus its anaesthetic potency is about 50% less than that of isoflurane but 30% more than that of desflurane. Sevoflurane is readily degraded by carbon dioxide absorbents to haloalkene byproducts that are nephrotoxic in rats, but there is no evidence of such toxicity in humans. In contrast to some other inhalation anaesthetic agents, which are degraded by carbon dioxide absorbents with generation of carbon monoxide, sevoflurane degradation generates negligible quantities of carbon monoxide.

2.2.2.2 Pharmacokinetic Properties of Sevoflurane

The uptake of a volatile anaesthetic is described by the rate of increase of the F_A/F_I ratio; conversely, its elimination is described by the rate of decrease of the F_A/F_{A0} ratio, where F_A is the alveolar concentration of anaesthetic (measured at the end of expiration), F_I is the inspired anaesthetic concentration and F_{A0} is the alveolar concentration of the anaesthetic immediately before termination of its application [230].
In general, there is an inverse relationship between the blood/gas partition coefficient of a given volatile anaesthetic and the time

required until the alveolar and inspired concentrations are in equilibrium.

The alveolar equilibration of sevoflurane is rapid, 80% complete within 30 minutes, compared with that of isoflurane (73%) or halothane (58%) but not desflurane (90%) [231, 232]. The estimated tissue distribution of sevoflurane is similar to that of isoflurane.

Similar to uptake, the elimination of a given volatile anaesthetic is related to its solubility in blood and tissue. Between 95 and 98 % of the amount of sevoflurane taken up is eliminated through the lungs [230].

Sevoflurane is eliminated faster than isoflurane despite its greater blood/tissue partition coefficient. Thus, the wash-out of sevoflurane in the first 2 hours after discontinuation of anaesthesia is 1.6-fold more rapid than with isoflurane but slower than desflurane. Mean pulmonary elimination clearance of sevoflurane (3.58 L/min) is not significantly different from that of isoflurane (3.62 L/min), and total body clearance of both agents is identical (3.6 L/min).

Sevoflurane undergoes dose-independent hepatic biotransformation, principally by cytochrome P450 (CYP) 2E1, with 1 to 5% of the absorbed dose of sevoflurane undergoing metabolism to liberate inorganic fluoride ions (F^-) and hexafluoroisopropanol (HFIP) as the principal byproducts [233]. The latter compound accounts for 82% of the organic fluorinated metabolites. HFIP is rapidly glucuronidated and then undergoes rapid urinary excretion. Sevoflurane, unlike methoxyflurane, undergoes minimal renal defluorination.

Sevoflurane is eliminated directly via exhaled breath and indirectly by metabolic conversion at hepatic level to hexafluoroisopropanol (HFIP). Since this metabolite is also eliminated via the exhaled

breath, we hypothesized that the elimination kinetics of sevoflurane and HFIP could provide information on the liver function in a non-invasive way. Thanks to exhaled breath analysis, we studied the post-operative sevoflurane and HFIP elimination kinetics as a first step towards investigating the possibility of a non-invasive monitoring of the liver function in case of liver transplants.

2.3 Monitoring of uremic toxins in spent dialysate

2.3.1 Adequacy of hemodialysis

Dialysis dose can be defined as the amount of hemodialysis received per dialysis and the dialysis frequency per week [234]. It is a measure of how effective a dialysis treatment removes waste products from the body [235].

The concept of dialysis adequacy was developed in the early 1970s to assess the treatment efficiency of end-stage renal disease (ESRD) patients [236].

From the very beginning the removal of small molecules was considered important as they were directly linked to the symptoms and signs of renal failure [237, 238]. Therefore, urea has been suggested as a surrogate marker for small toxic solutes. In 1975 urea gained wide acceptance as a marker of solute removal in dialysed patients [239].

Two methods are generally used to assess dialysis adequacy: the Urea Reduction Ratio (URR) and the Kt/V.

Urea Reduction Ratio (URR)

The URR is a formula (equation 2.3), which expresses the reduction in blood urea during a dialysis session [234].

$$URR = [(BUN_{Pre\text{-}dialysis} - BUN_{Post\text{-}dialysis}) / BUN_{Pre\text{-}dialysis}] \cdot 100 \qquad (2.3)$$

where BUN is the blood urea nitrogen.

The URR is the simplest way to measure the delivered dialysis dose. It does not include the time of dialysis, the body size and effects of ultrafiltration [130]. Hence, the URR does not consider the residual renal function. The URR should be continuously higher than 65 % (with a three times per week HD schedule) to ensure an adequate treatment [240].

Normalised dose of dialysis (Kt/V)

In 1985 Gotch and Sargent [241] introduced the Kt/V ratio as a result of their "mechanistic" analysis of the National Cooperative Dialysis Study (NCDS). The study was performed between 1976 and 1981 in the USA with the aim to find a correlation between the dialysis dose and morbidity [237].

K represents the dialyser urea clearance (known from in-vitro studies), t is the dialysis time and V is the urea distribution volume [130]. The Kt/V value is the ratio between the volume of blood cleared of urea during a dialysis session (Kt) and the distribution volume of urea (V) which is equivalent to the total body water [242]. The gold standard for determining Kt/V in HD is by urea kinetic modelling (UKM) [242]. UKM is based on the principle of mass balance to describe urea nitrogen production and urea removal in the body [243].

The analysis of the NCDS by Gotch and Sargent revealed that a Kt/V < 0.8 (three times per week HD schedule) was associated with an increased morbidity. They concluded that a Kt/V of 1.0 was adequate [241]. Since then, there is a controversial discussion about the appropriate Kt/V value to ensure an adequate treatment [242]. The UK Renal Registry (2003) recommends a Kt/V value greater than 1.2 as an appropriate dialysis dose.

2.3.2 Monitoring of hemodialysis

As mention above, the Kt/V value and the URR value are the most commonly used parameter to judge the adequacy of hemodialysis treatment. For both values, the determinations of pre- and post-dialysis urea concentrations are necessary [130, 237]. The urea concentrations can be measured either on the blood side or on the dialysate side.

In the past few years, several devices have been developed that can measure urea continuously in blood or in spent dialysate [237]. The majority of urea measurements are based on an enzymatic reaction. The enzyme urease catalyses the following reaction [244]:

$$(NH_2)_2CO + 2H_2O \leftrightarrows NH_3 + NH_4^+ + HCO_3^- \qquad (2.4)$$

The amount of urea is measured indirectly by measuring the products of reaction in equation 2.4. This can be done by either measuring the breakdown products directly ($NH4^+$) or indirectly by measuring a secondary parameter (pH, conductivity) [237, 244]. It is important, that enough urease is present to convert all of the urea.

Current research is focused on the development of new urea kinetic models, in particular multi-compartment models to provide a more accurate estimate of the Kt/V value [236, 245, 246]. However, multi-compartment models require multiple blood tests to solve the complex equations. These difficulties preclude its use in routine clinical practice.

Another area of research is based on the spectroscopic determination of urea and other small molecules retained in ESRD patients. Recently, two research groups published their results. Fridolin et al. [247] applied UV spectroscopy to measure small waste products in spent dialysate. This group observed a good correlation between the UV absorbance (285 nm) and the removal

of small molecules such as urea, creatinine and uric acid. Similar results were found by Olesberg and co-workers [248], who used an FTIR (Fourier Transform Infrared) spectrometer. They found, that the absorption spectrum of urea in the range between 5000 – 4000 cm^{-1} (λ = 2.0 – 2.5 μm) is relative strong and distinct from other components. In both cases, the results need to be validated.

Desire for a simple, compact, inexpensive, mobile and reliable method for estimating the efficiency of the dialysis has arisen due to increasing number of dialysis patients and related treatment quality requirements. Inspired by a wish to improve quality estimation of the dialysis, we followed the same research line of Fridolin group with the idea of non-invasive real time monitoring of the efficiency of hemodialysis from the analysis of spent dialysate.
By optical monitoring of the spent dialysate it is possible to monitor the removal of several clinical important solutes associated with dialysis outcome. Therefore, there is a good possibility to develop an on-line monitoring system that can be a valid tool for clinicians to assess removal of uremic toxins and deliver personalized hemodialysis treatments. Furthermore, it can prevent serious pathological conditions, decrease mortality of patients and also alert immediately about any deviations in dialysis treatment.

CHAPTER 3

Materials and Methods

3.1 Chemical reagents

Warfarin, i.e. 3-(α-acetonylbenzyl)-4-hydroxycoumarin sodium salt (purity ≥ 98%), sodium phosphate monobasic (purity ≥ 99.0 %), potassium phosphate dibasic (purity ≥ 99.0 %), urea, uric acid, creatinine and β_2-microglobulin (purity ≥ 99.5 %) were purchased from Sigma-Aldrich (Milan, Italy). Pilocarpine hydrochloride and sodium nitrate were from Galeno (Comeana, Italy). Ethanol, 1-propanol, 2-propanol, 1-butanol, ethyl acetate, 2-pentanone and 4-heptanone were purchased from AccuStandard, Inc. Chemical Reference Standard (USA). Isoprene, acetone, acetonitrile, pentane, 2-methylpentane, hexane, 1,1,1,3,3,3-hexafluoro-2-propanol, dimethylsulphide, dimethyldisulphide, 2,3-butanedione, acetoin, benzene, toluene, chloroform, carbontetrachloride, trichloroethylene, tetrachloroethylene and m-cresol puriss p.a. standard for GC grade > 99% were purchased from Fluka, Sigma-Aldrich (Milan, Italy). Sevoflurane was from Abbott, Italy.

Labelled isopropanol-D8 and toluene-D8 (purity 99.8 %) were purchased from ARMAR Chemicals (Switzerland).

HPLC grade methanol, acetonitrile, hexane, and dichloromethane were purchased from ROMIL Super Purity Solvent (United Kingdom). Formic acid (purity 95-97 %) and sulphuric acid (purity 95-98 %) were purchased from Sigma-Aldrich (Milan, Italy). Ultra pure water was produced by a Milli-Q Reagent Water System (Millipore, USA).

The thromboplastin reagent (HemosIL RecombiPlasTin 2G), thromboplastin diluent (HemosIL RecombiPlasTin 2G Diluent), calibration plasma, normal control assay, low and high abnormal control assays used for INR measurements and quality control were supplied from the Instrumentation Laboratory (Milan, Italy).
All chemicals were used without any further purification.

3.2 Preparation of standards

1 L of phosphate buffer stock solution (1 M, pH 7.02) was prepared by dissolving 18.30 g of sodium phosphate monobasic and 49.21 g of potassium phosphate dibasic in water. The solution was filtered through a 0.45 µm membrane and after pH control was stored at 4 °C. This solution was then diluted to 25 mM to obtain the phosphate buffer solution (PBS) used for HPLC analyses.

A 1 mg/mL stock solution of warfarin was prepared by dissolving 0.11 g of pure compound in 100 mL of water and stored at 4 °C until used. This solution was diluted with PBS to prepare a 10 µg/mL standard solution that was further diluted with PBS to achieve 0.5, 1, 2, 5, 10, 20, 50 and 100 ng/mL standard working solutions.

Pooled patient oral fluid samples (POFSs) were obtained by pooling samples from 20 patients. Control oral fluid samples (COFSs) were obtained from 10 volunteers who stated that they were not taking warfarin. Aliquots of COFS were spiked with known amounts of warfarin to obtain standard oral fluid samples (SOFSs) at different concentration levels.

Pilocarpine hydrochloride and sodium nitrate solutions in water were prepared by dissolving the weighed reference compounds to achieve a concentration of 5 g/L and 10 g/L respectively.

Two mixtures were prepared by mixing 50 µL of twelve (MIX 12) and thirteen (MIX 13) pure liquid compounds respectively. Then a gaseous mixture (MIX 25) was obtained by introducing 10 µL of liquid MIX 12 and 10 µL of liquid MIX 13 into a 2 L glass flask equipped with a septum, pre-evacuated and held at 37 °C. The corresponding concentrations are reported in Table 3.1.

A gaseous sevoflurane sample was prepared by evaporating 10 µL of liquid sevoflurane in a 2 L glass flask equipped with a septum, pre-evacuated and held at 37°C. The corresponding concentration was 954 ppmv.

A gaseous mixture of labelled isopropanol-D8 and toluene-D8 (MIX 2D), to be used as an internal standard, was prepared by evaporation of 5 µL of both compounds in a 2 L glass flask equipped with a septum, pre-evacuated and held at 37°C. The corresponding concentrations were 830 ppmv for isopropanol-D8 and 600 ppmv for toluene-D8.

Table 3.1 *Concentration of compounds in MIX 25.*

Analytes	Glass flask concentration [ppmv]
Pentane	85
Ethanol	184
Isoprene	98
Acetone	133
Dimethylsulphide	133
2-propanol	128
Acetonitrile	203
2-methylpentane	74
Hexane	75
1-propanol	142
2,3-butanedione	135
Ethyl acetate	108
Chloroform	132
Carbontetrachloride	110
Benzene	119
1-butanol	116
Trichloroethylene	119
2-pentanone	92
Hexafluoroisopropanol	94
Dimethyldisulphide	109
3-hydroxy-2-butanone	118
Toluene	92
Tetrachloroethylene	102
4-heptanone	70
m-cresol	93

Stock solutions of uric acid, creatinine and β_2-microglobulin, at a concentration of 1, 6 and 0.1 mg/mL respectively, were prepared by dissolving the weighed amount in water. Such solutions were diluted to a concentration of 50, 20 and 2 µg/mL for uric acid, 60, 6 and 0.6 µg/mL for creatinine and 25, 10, 5 and 2 µg/mL for β_2-microglobulin to obtain standard working solutions.

A 10 mg/mL stock solution of urea was prepared by dissolving the weighed amount in water.

A pooled patient dialysate sample was obtained by pooling aliquots of each patient sample collected 240 minutes after the beginning of the dialysis treatment.

3.3 Instrumentation

A iontophoretic equipment (New Ionoderm, Roversi Elettromedicali, Fiorano (Mo), Italy) was used for sweat stimulation.

A centrifuge Centrifugette 4206 (ALC, Milan, Italy) and a centrifuge Allegra 21R equipped with a S4180 swinging bucket rotor (Beckman Coulter, USA) were used for samples centrifugation and ultrafiltration respectively.

High performance liquid chromatography was carried out by a Jasco HPLC system (Jasco Europe, Italy) equipped with an autosampler (AS 2055), a quaternary low pressure gradient pump (PU 2089) and a spectrofluorimetric detector (FP 2020). The column temperature was controlled by a thermostat (HT 3000, ClinLab, Italy). The HPLC system was controlled by ChromNAV™ software from Jasco.

To validate the analytical method for warfarin determination, few selected samples were also analyzed by a Micro HPLC system (Perkin Elmer Series 200) coupled with an autosampler (Series 200) and a triple quadrupole mass spectrometer (Applied Biosystems Sciex API 365) operating in the Selected Reaction Monitoring (SRM) mode. The mass spectrometer was equipped with an Atmospheric Pressure Photo-Ionization (APPI) interface operating in negative ion mode.

The INR measurements were carried out at the clinical chemical laboratory of the Azienda Ospedaliero Universitaria Pisana (AOUP) by an automatic system (ACL TOP700, Instrumentation Laboratory) equipped with an autosampler. Spectrometric INR measurements were performed at a wavelength of 671 nm to minimize optical interference (e.g. hemoglobin and bilirubin).

Absorption and fluorescence spectra were recorded by a spectrophotometer (Lamba 25, PerkinElmer, USA) and a spectrofluorimeter (LS 45, PerkinElmer, USA) respectively.

A low flow Pocket Pump (210-1002TX, SKC, Italy) was used to transfer breath samples into adsorption tubes.

Thermal desorption (TD) and GC-MS analysis were performed by an automated two-stage thermal desorption unit (STD 1000, DANI Instrument, Italy) equipped with an internal focusing trap packed with 70 mg of Tenax GR (DANI Instrument, Italy), a gas chromatograph (Trace GC Ultra, Thermo Electron Corporation, USA) and a quadrupole mass spectrometer (Trace DSQ, Thermo Electron Corporation, USA) operated in the positive electron impact (EI) ionization (70 eV) and Total Ion Current (TIC) and Selected Ion Monitoring (SIM) acquisition mode. The thermal desorption system was controlled by TD Manager™ software from DANI and the GC-MS system was controlled by Xcalibur™ software from Thermo.

3.4 Optimization of HPLC assay for warfarin determination

3.4.1 Absorption and fluorescence spectra of warfarin

Warfarin absorption and fluorescence spectra allowed to select the best wavelengths for the HPLC assay. Figures 3.1 and 3.2 show the

warfarin absorption spectrum in the range 220 – 440 nm and the warfarin fluorescence spectrum (excitation wavelength of 308 nm) in the range 330 – 590 nm, measured in a standard solution in PBS 25 mM at pH = 7 with a warfarin concentration of 10 µg/mL.

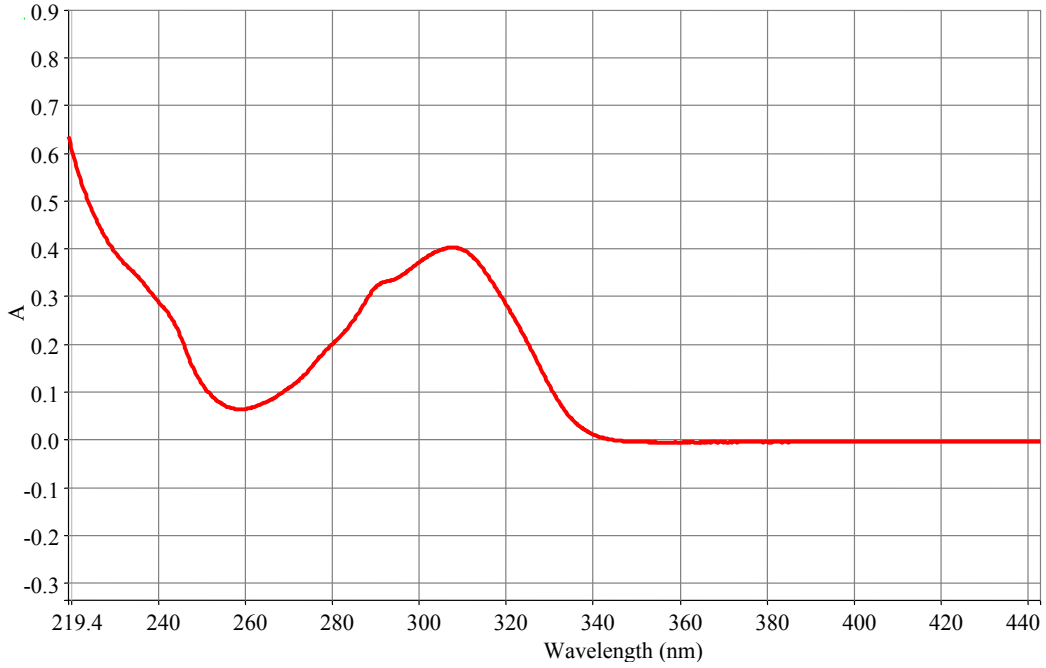

Figure 3.1 *Absorption spectrum of warfarin in PBS.*

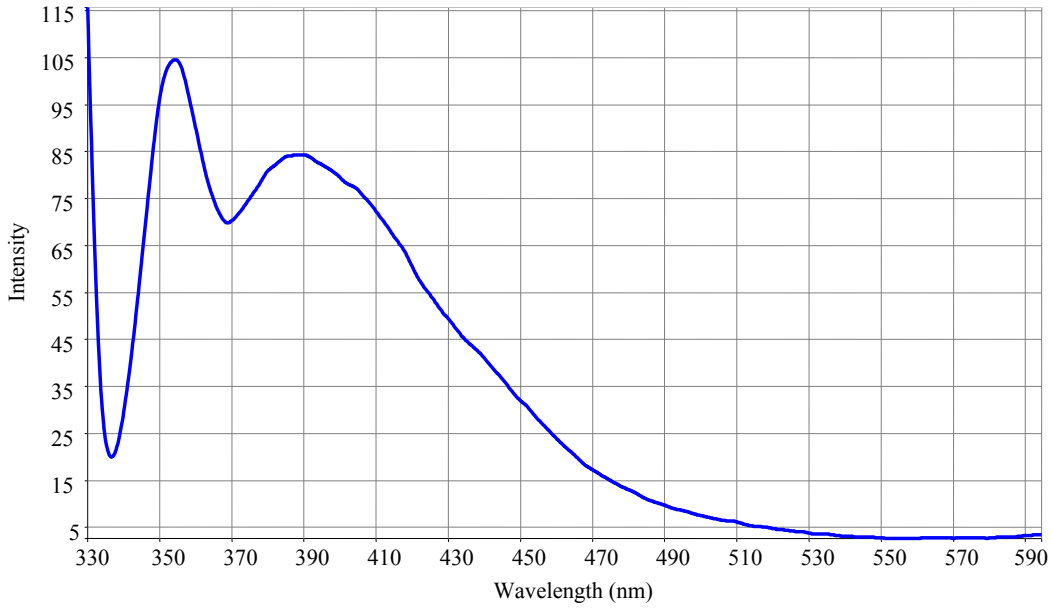

Figure 3.2 *Fluorescence spectrum of warfarin in PBS.*

The absorption spectrum exhibits a maximum at about 310 nm. Fluorescence emission measurements were made at 400 nm (where a broad peak is observed) after excitation at a wavelength of 310 nm.

3.4.2 Selection of the mobile phase

The optimization of the mobile phase was performed by using a standard working solution of warfarin and a SOFS with a warfarin concentration of 2.0 ng/mL.

Because of the weakly acidic nature of warfarin (pKa = 5.19), a neutral mobile phase consisting of 25 mM phosphate buffer at pH = 7 and methanol as organic modifier was selected to obtain warfarin in the dissociated form, which is more prone to interact with the stationary phase.

Standard working solutions of warfarin and SOFSs were analyzed by using mobile phases with different compositions.

Chromatographic separation was carried out in isocratic conditions with a C-18 reversed-phase column Chromspher 5 PAH (Varian, 150 × 4.6 mm, 5 µm), coupled with a guard column ChromSep SS (Varian, 10 × 2 mm), flow rate of 1.0 mL/min; injection volume of 25 µL, column temperature of 25 °C and fluorescence detection with an excitation and an emission wavelength of 310 and 400 nm respectively.

The best chromatographic separation was achieved by a mobile phase consisting of 28 % methanol and 72 % PBS (25 mM at pH = 7).

3.4.3 Selection of the injection volume

Increasing volumes (5, 10, 25 and 50 µL) of a standard working solution with a warfarin concentration of 20 ng/mL were analyzed to evaluate the effect of the injection volume on the peak shape. Chromatographic separation was carried out by the Chromspher 5 PAH column in isocratic conditions with a 28 % methanol and 72 % PBS (25 mM at pH = 7) mobile phase at a flow rate of 1.0 mL/min; column temperature of 25 °C and fluorescence detection with an excitation and an emission wavelength of 310 and 400 nm respectively.

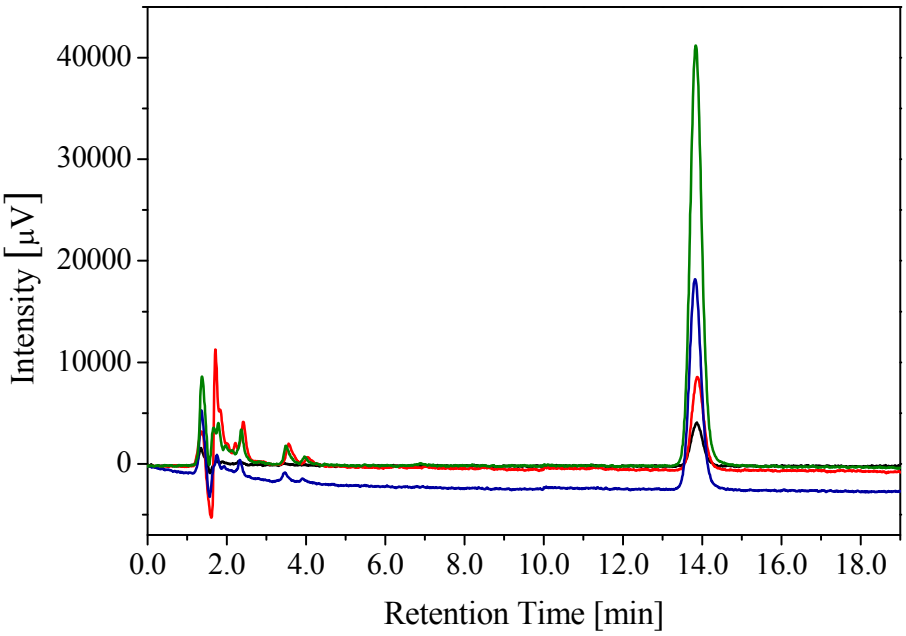

Figure 3.3 *HPLC chromatograms of a standard working solution of warfarin at different injection volumes:5 µL (black line), 10 µL (red line), 25 µL (blue line) and 50 µL (green line).*

The area of the warfarin fluorescence signal increased linearly (R^2 = 0.999) in the observed range of the injected volume (Figure 3.3). An injection volume of 25 µL was selected and used in all subsequent measurements.

3.4.4 Experimental conditions in method validation

HPLC-fluorimetry

A column Poroshell 120 EC-C18 (Agilent Technologies, 100 × 4.6 mm, 2.7 µm) connected to a guard column TC - C18 (12.5 x 4.6 mm, 5 µm, Agilent Technologies), was used to evaluate the presence of interfering substances. The mobile phase composition was optimized and resulted 35 % methanol and 65 % PBS (25 mM at pH = 7) at a flow rate of 0.7 mL/min and 25°C.

HPLC-MS/MS

Comparative measurements were performed on standard working solutions of warfarin and SOFSs by HPLC-MS/MS. Chromatographic separation by the Perkin Elmer HPLC system was carried out in isocratic conditions on a C-18 reversed-phase column Chromspher 5 PAH coupled with a guard column ChromSep SS. A 50 % acetonitrile, 50 % water containing 0.1 % formic acid mobile phase was used at a flow rate of 1 mL/min and 25 °C. Warfarin was quantified by the mass spectrometric detector observing the following two ion transitions (expressed by their mass number/charge number ratios): m/z 307 → 161 and m/z 307 → 250.

3.5 Thermal desorption gas chromatography mass spectrometry (TD-GC-MS) assay for breath analysis

Gas chromatographic separation was performed by a 6% cyanopropyl phenyl siloxane and 94% dimethylpolysiloxane capillary column (DB-624, 60 m l., 0.25 mm i.d., 1.4 µm film thickness, Agilent Technologies). Helium 5.6 IP (SOL Group, Italy) was used as carrier gas. The experimental conditions used for the

thermal desorption, gas chromatographic and mass spectrometric methods are given in Table 3.2.

Table 3.2 *Thermal desorption, gas chromatographic and mass spectrometric methods.*

MTD 1	
Thermal desorption method	
Valve and transfer line Temperature	170 °C
Tube desorption Temperature	250 °C
Tube desorption Time	5 min
Tube desorption Pressure	90 kPa
Trap focusing Temperature	5 °C
Trap desorption Temperature	250 °C
Trap desorption Time	30 min
Gas chromatographic method	
Inlet Temperature	200 °C
Oven temperature ramps	35 °C for 10 min; 4 °C/min until 130 °C for 2 min; 25 °C/min until 260 °C for 15 min
Column head Pressure	210 kPa
Inlet mode	split
Split flow	10 mL/min
Transfer line temperature	260 °C
Mass spectrometric method	
Ion source temperature	250 °C
Scan mode	Full Scan 18-200 amu and SIM
Scan rate	813.1 amu/sec Dwell Time 50 ms for each ion

In Table 3.3 are shown the ions of the compounds that were identified by MS operating in selected ion mode (SIM).

Table 3.3 *Characteristic ions in SIM mass spectra used in MTD 1.*

Segment	Compound	SIM Mass	Retention Time (min)
0 – 8.40	Pentane	43	6.89
	Ethanol	45	7.19
	Sevoflurane	131	7.35
	Isoprene	67	7.64
8.40 – 10.10	Acetone	58	8.48
	Dimethylsulphide	62	8.71
	2-propanol	45	9.14
	Acetonitrile	41	9.50
10.10 – 14.50	2-methylpentane	71	10.49
	Hexane	57	12.69
	1-propanol	31	13.75
14.50 – 20.00	2,3-butanedione	43	15.11
	Ethyl acetate	43	15.91
	Chloroform	83	16.72
	Carbontetrachloride	119	18.03
	Benzene	78	18.79
20.00 – 24.20	1-butanol	56	21.22
	Trichloroethylene	95	21.29
	2-pentanone	43	22.01
	Hexafluoroisopropanol	99	23.43
24.20 – 27.00	Dimethyldisulphide	94	25.07
	3-hydroxy-2-butanone	43	25.15
	Toluene-D8	98	25.87
	Toluene	91	26.12
27.00 – 35.00	Tetrachloroethylene	166	28.19
	4-heptanone	43	33.23
35.00 – 56.00	m-cresol	108	41.83

3.6 Optimization of HPLC assay for uremic toxins determination

The determination of the absorption spectra of urea, uric acid, creatinine and β_2-microglobulin and fluorescence spectrum of β_2-microglobulin allowed to select the best wavelengths for HPLC and flow injection analyses.

Figure 3.4 shows the absorption spectra of these four uremic toxins in the range 200 – 600 nm measured in standard solutions at a concentration of 8.3 mM, 11.9, 5.3 and 8.6 µM respectively. Figure 3.5, on the other hand, shows the fluorescence spectrum of β_2-microglobulin (excitation wavelength 220 nm) in the range 230 – 510 nm obtained by using a standard solution of β_2-microglobulin at a concentration of 0.17 µM.

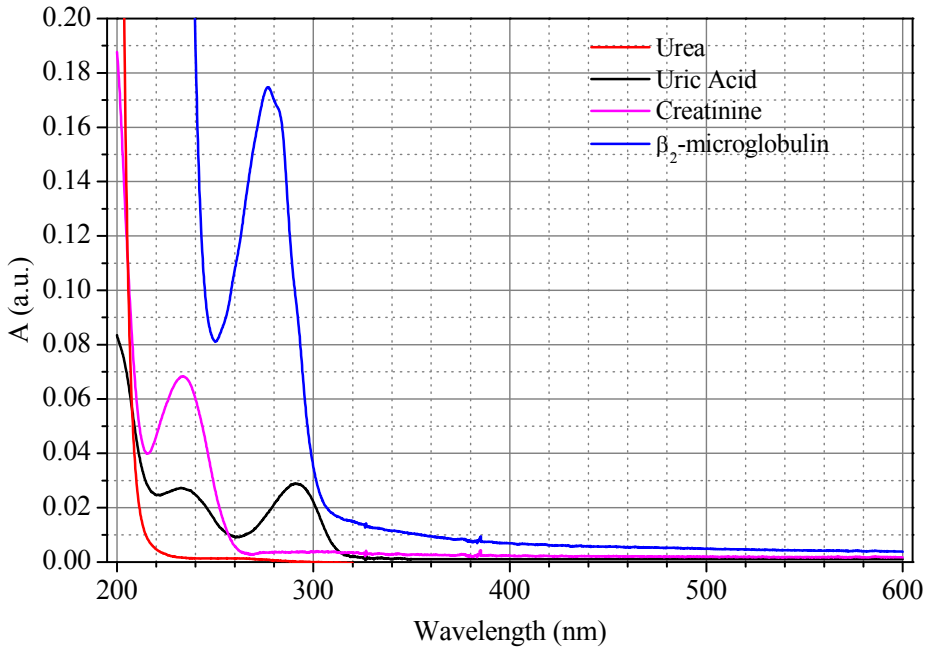

Figure 3.4 *Absorption spectra of urea (red line), uric acid (black line), creatinine (magenta line) and β_2-microglobulin (blue line).*

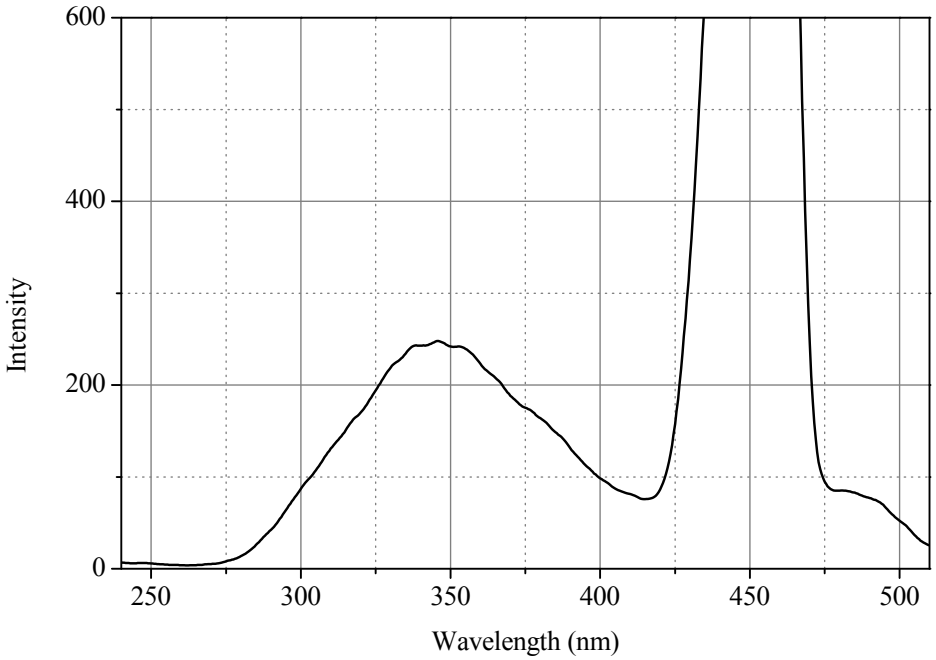

Figure 3.5 *Fluorescence spectrum of β_2-microglobulin.*

From these spectra, three wavelengths for UV absorption (235, 292 and 280 nm) and a pair of wavelengths for spectrofluorimetric measurements (excitation wavelength 220 nm, emission wavelength 340 nm) were selected.

As it can be seen in Figure 3.4, urea do not shown light absorption in the range 200 – 600 nm, so it does not contribute to the UV signal.

The flow-injection measurements were carried out by the Jasco HPLC system using milliQ water at a flow rate of 1 mL/min. The injection volume was 25 µL and the total run time was 2 minutes.

Chromatographic separations by the Jasco HPLC system were carried out in isocratic conditions with a XTerra MS-C18 column (Waters, 250 x 4.6 mm, 2.5 µm). A mobile phase containing 98% of a 1% formic acid solution in water and 2% acetonitrile and was used at a flow rate of 1 mL/min at 25 °C. The injection volume was 25 µL.

CHAPTER 4

Experimental section

4.1 Samples collection and preparation

The quality of information in any analytical investigation is closely linked to the ability to obtain representative and homogeneous samples and to ensure the minimum possible alteration of the chemical composition of the sample during storage, pre-treatment and analysis. The manipulations required by the analytical procedure and the contact with the various materials used are definitely the most important aspects. In view of this premise, particular attention was paid to issues regarding oral fluid, sweat, breath and spent dialysate sampling and sample treatment.

4.1.1 Oral fluid

4.1.1.1 Sample collection device

Three different devices from Salivette (Salivette®, Sarstedt, Germany), namely a cotton swab, a cotton swab impregnated with citric acid and a polyester swab, were compared to evaluate the release of interfering compounds from the swab materials and the sample recovery.

An aliquot (2 mL) of a standard working solution with a warfarin concentration of 10 ng/mL was absorbed into the three swabs and recovered by centrifugation at 3000 rpm for 5 min. An aliquot (25

µL) of each sample was then analyzed by HPLC with fluorescence detection.

The chromatographic separation was carried out in isocratic conditions by the Chromspher 5 PAH column with a 72% PBS and 28% methanol mobile phase at a flow rate of 1.0 mL/min, injection volume 25 µL, temperature 25°C.

The recovery percentage was calculated from the ratio between the average warfarin concentration in the samples recovered from the swab and the initial concentration.

The results summarized in Figure 4.1 and Table 4.1 show that the polyester swab was the device more suitable for oral fluid sampling for the lowest background contamination and the highest recovery percentage.

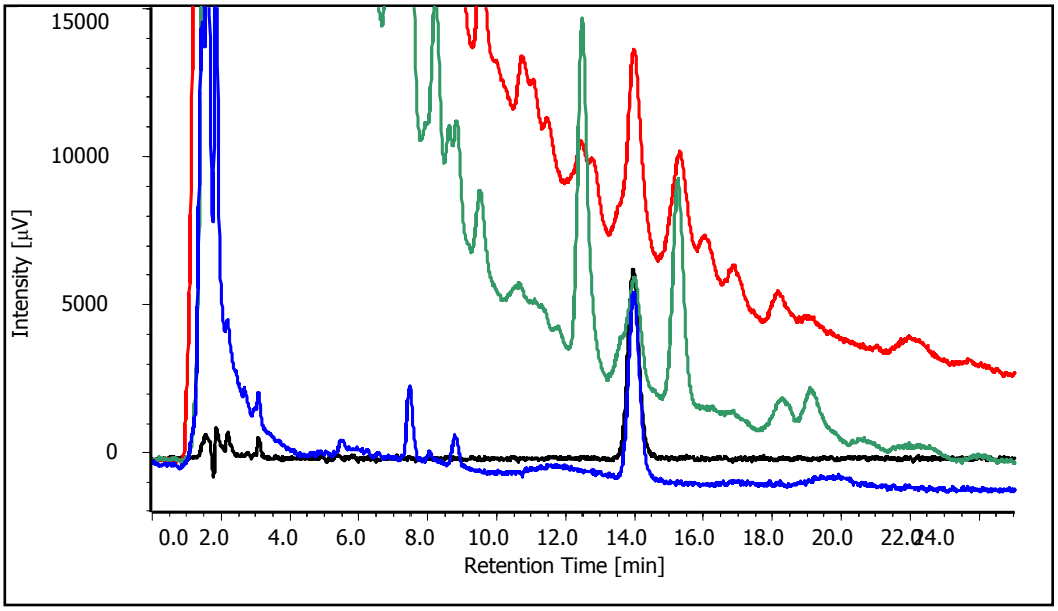

Figure 4.1 *HPLC chromatograms of a standard working solution containing 10 ng/mL of warfarin (black line) and of the solutions recovered by the three different swabs: cotton (red line), cotton + citric acid (green line) and polyester (blue line).*

Table 4.1 *Sample recovery percentages from the different swabs.*

Swab	Average recovery % (CV %)
Cotton	88 % (10 %)
Cotton + citric acid	62 % (3 %)
Polyester	98 % (1 %)

Therefore, the collection of oral fluid samples was carried out by roll-shaped biocompatible polyester swabs (Salivette®, Sarstedt) which were delivered to the study subjects to be kept in the mouth for 5 minutes. Oral fluid was then recovered by centrifugation of the swabs at 3000 rpm for 5 minutes.

All samples were collected at the same time (8.30 - 10.00 AM) to avoid any effects due to possible circadian variations. Patients generally take warfarin in the late afternoon, therefore it can be assumed that the last dose had been completely absorbed when samples were collected.

4.1.1.2 Sample storage

According to the medical literature, oral fluid specimens should preferably be kept refrigerated after collection to maintain sample integrity; this prevents the degradation of some molecules in oral fluid and the bacterial growth. In the present work, oral fluid samples were stored in 1.5 mL polypropylene tubes (Safe-Lock, Eppendorf) at room temperature when analysis was carried out within 90 minutes from collection, otherwise at 4 °C in the refrigerator.

The stability of the treated samples (i.e. centrifuged and filtrated) during a one and half month storage at 4 °C was assessed in

aliquots of a pooled patient oral fluid sample (POFS) obtained by pooling samples from 20 patients (Table 4.2 and Figure 4.2).

The accuracy of the initial warfarin concentration estimate in the POFS (2.9 ng/mL) was confirmed by calculating the average warfarin concentration in the 20 oral fluid samples composing the POFS (2.8 ng/mL). The difference between these two values was not statistically significant ($p < 0.05$).

Table 4.2 *Time stability of a POFS stored at 4 °C.*

Time (days)	0	7	14	21	28	42
Average warfarin concentration [ng/mL]	2.9	2.8	3.2	2.6	2.9	2.6
SD (n=3)	0.03	0.01	0.04	0.06	0.02	0.09
Relative error %	--	-1.3	10.3	-8.3	1.2	-10.3

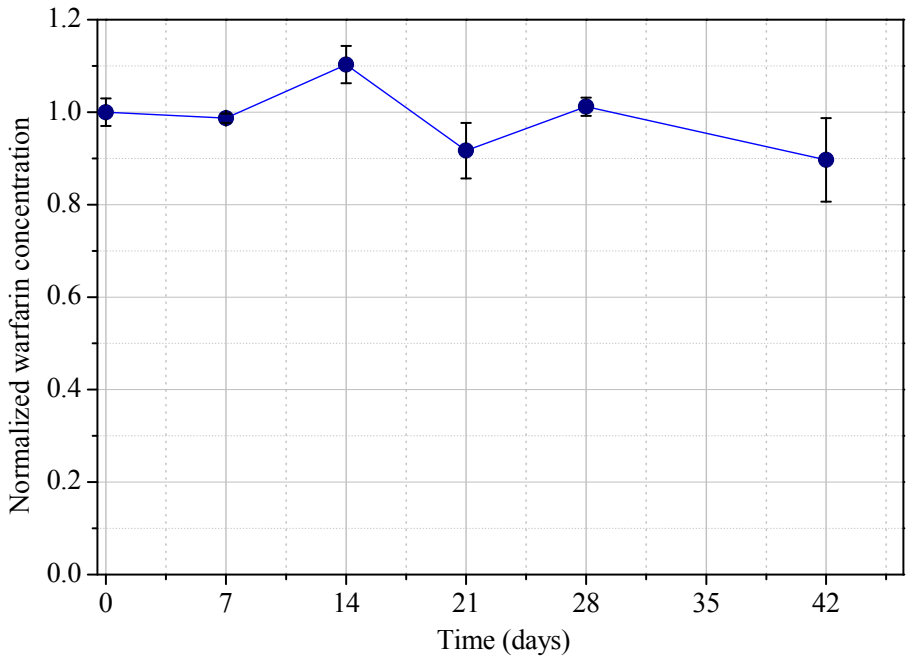

Figure 4.2 *Time stability of a POFS stored at 4 °C.*

These results allowed to state that no significant degradation occurred in oral fluid sample stored in 1.5 mL polypropylene tubes at 4 °C within the considered time span.

4.1.1.3 Sample preparation

The analysis of biological samples generally requires a preliminary stage to obtain the analyte in the appropriate form for the analytical determination. In oral fluid, for example, albumin and other proteins could potentially form stable complexes with warfarin, thereby reducing the free fraction of analyte. To exclude this possibility, two procedures were compared with the simple oral fluid filtration by 0.2 µm regenerated cellulose syringe filters (Spartan, Whatman). The first procedure (extraction of warfarin from oral fluid samples) consisted in the addition of sulphuric acid followed by a liquid/liquid extraction with organic solvents, the second (ultrafiltration of oral fluid samples) consisted in the ultrafiltration by centrifugal filters with a cutoff at a molecular weight of 3000 Da, which prevent any complex with albumin (60000 Da) to pass into solution.
The three procedures were compared in terms of percentage of recovery, time and costs. All measurement were performed in triplicate using aliquots of the same POFS.

4.1.1.3.1 Extraction of warfarin from oral fluid samples

Aliquots (1 mL) of POFS were spiked with 2 mL of 0.5 M sulphuric acid and 500 µL of ethanol. The addition of sulphuric acid dissociates any warfarin/protein complex, allowing to measure the total warfarin concentration, whereas ethanol prevents the

formation of emulsions. The resulting solution was added with 4 mL of a 1:5 dichloromethane/hexane mixture for the extraction of warfarin and then stirred for 15 minutes and centrifuged for 5 minutes at 3000 rpm. Freezing the solution at -80 °C facilitated the separation of the two phases. The upper organic phase was transferred into a clean vial and evaporated under vacuum. The residue was then reconstituted with 1 mL of PBS and analyzed by HPLC with fluorescence detection.

4.1.1.3.2 Ultrafiltration of oral fluid samples

Aliquots (1 mL) of POFS were transferred into Amicon tubes (Amicon® Ultra-4, Millipore) with a molecular weight cutoff of 3000 Da and ultrafiltered by centrifugation at 4000 rcf for 40 minutes at 20 °C. The ultrafiltrate was so ready for analysis.

Table 4.3 *Average percentage sample recovery (n = 3) for the different pre-treatment procedures.*

Sample pre-treatment	**Average recovery % (CV %)**	**Time and costs**
Extraction	89 % (4 %)	medium
Ultrafiltration	93 % (2 %)	high
Filtration	99 % (1 %)	low

The results obtained, summarized in Table 4.3, allowed to conclude that simple filtration was the best procedure in terms of quantitative recovery of the analyte, time and costs.

4.1.1.3.3 pH measurement of oral fluid samples

Before starting the clinical study, the possibility of measuring pH of the oral fluid samples was evaluated since warfarin is a weak

acid (pKa = 5.19 at 25 °C) and the drug transfer from plasma to oral fluid can be influenced by this parameter [27].

pH paper strips (Pehanon, Macherey Nagel) having a 0.3 (pH) unit resolution in the range 5.2 to 8.1 were used to measure the pH of patients' oral fluid samples during the clinical study.

Since about two hours elapsed between sample collection and the analysis, the stability of the pH value during this time span had to be tested. pH values of several patient oral fluid samples were measured in the same day immediately after collection (1), after centrifugation of the sampling device (2), after filtration of the sample (3) and at two hours from collection (4).

Table 4.4 shows a typical result highlighting that no significant changes occurred in the pH of oral fluid samples during sample recovery and treatment as well as at two hours from collection.

Table 4.4 *Oral fluid pH value during the various stages of the methodology.*

Stage	**Oral fluid pH**
1	6.6
2	6.7
3	6.6
4	6.7

4.1.2 Sweat

Sweat stimulation and collection was carried out according to methods reported in literature for the diagnosis of cystic fibrosis [249, 250]. Pilocarpine was delivered through the skin in the forearm region via iontophoresis (2 mA for 5 minutes), and then the skin was rinsed with water and dried with paper. A paper filter (Whatman n.42, 55 mm), previously put in a plastic canister and weighed, was applied onto the stimulated region and hold in place

by wrapping the forearm with a plastic film. After 30 minutes, paper was removed and weighed again, sweat was then eluted from the filter by adding 9 mL of PBS. An extraction procedure was set up to lower the level of sweat dilution; 200 µL of concentrated sulphuric acid and then 9 mL of 1:5 dichloromethane/hexane mixture were added to the sample. After centrifugation at 3000 rpm for 5 min, the upper organic phase was transferred into a clean vial and evaporated under vacuum. The residue was then reconstituted in 1 mL of PBS and stored at 4 °C until assay.

4.1.3 Breath

The analytical methodology used for collection and pretreatment of breath samples was developed in previous work [251, 252].

The sampling procedure was optimized by comparing three different bag materials such as Nalophan, Tedlar and Cali-5-bonds. The comparison between these materials was carried out by testing the release of interfering compounds and the chemical stability of accurately prepared gas mixtures containing many compounds of interest at known concentration. Nalophan, due to low background contamination and cost that enables the preparation of ready-to-use disposable bags, was the most suitable material for breath collection.

The breath sampling system consisted of a disposable mouthpiece, a non-return valve, a Nalophan bag and a Teflon tube (Figure 4.3). The Teflon tube allowed the connection of the bag to the adsorption tube for transferring the breath sample. The mouthpiece, the non-return valve and connections were sterilized by low-temperature, hydrogen peroxide gas plasma technology.

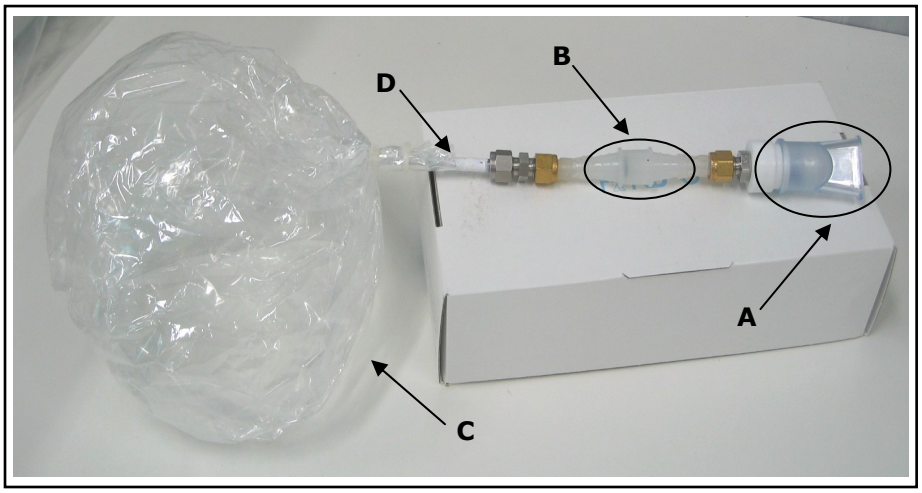

Figure 4.3 *Breath sampling system: A) disposable mouthpiece; B) non-return valve; C) Nalophan bag; D) Teflon tube.*

Nalophan bags were home made from a 20 µm thick roll of Nalophan tube, (Tillmanns S.p.a., Milan, Italy). To make a sampling bag, a 50 cm portion was cut from the roll. One end was wrapped, folded and tightened by nylon cable ties, the other one was wrapped and tightened around a Teflon tube (1/4 inch i.d.) connected to a valve.

Due to the low concentration in breath of most volatile organic compounds (VOCs), we pre-concentrated the collected sample before the analysis by flowing a fixed volume of sample into an adsorption tube filled with a suitable stationary phase (solid phase extraction, SPE).

The choice of the stationary phase was carried out by evaluating the performances of two different adsorption tubes, one packed with Tenax GR and the other (multi-bed adsorption tube) with Carbopack Y - Carbopack B – Carboxen 1003.

Due to the high content of water vapour in the breath, which could decrease the retention of analytes in the adsorption tube, the tests were carried out by introducing in the pre-concentration system a cartridge containing a drying agent. In particular, we tested the

effectiveness of anhydrous sodium sulphate, magnesium perchlorate and anhydrous calcium sulphate.
Tenax GR, characterized by a high breakthrough volume for most volatile organic compounds and a low affinity for water, and sodium sulphate were, respectively, the stationary phase and the drying agent most suitable for our purpose.

On the basis of previous studies, sampling bags were stabilized at 37 °C for half an hour to prevent water condensation on the bag walls, then a known volume of sample was sucked through a drying tube filled with 9 g of anhydrous sodium sulphate (SKC, Italy) for water removal and a glass thermal desorption tube pre-packed with 250 mg of 60/80 mesh Tenax GR phase (70% Tenax TA, 2,6-diphenyl-p-phenylene oxide and 30% graphite, Supelco, Sigma-Aldrich, Italy) by a pocket pump. The flow was set up on the pocket pump and controlled by a flow meter. During the sample transfer, the sampling bag and the drying tube were kept at 37 °C, whereas the adsorption tube was at ambient temperature (Figure 4.4).

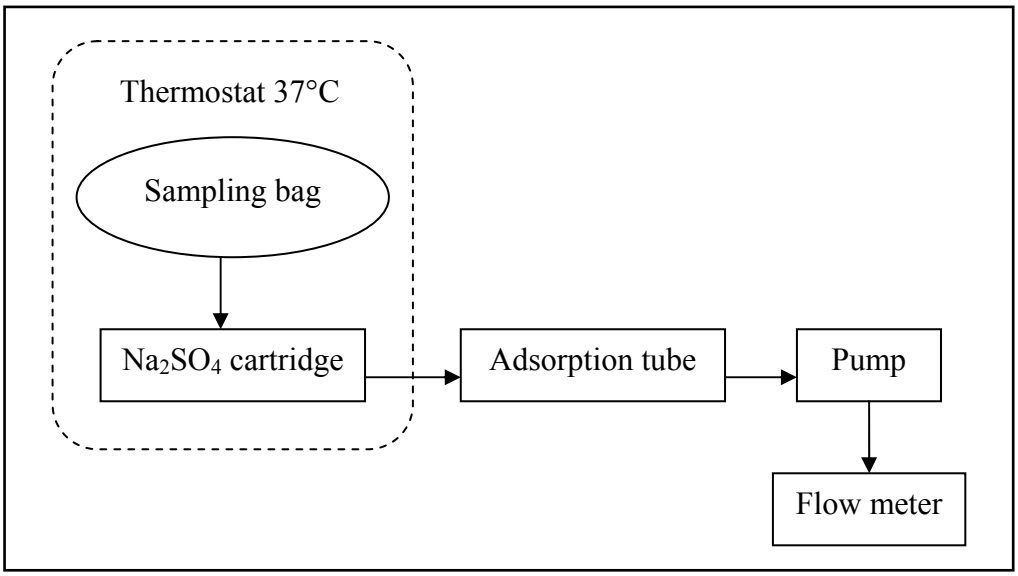

Figure 4.4 *Schematic diagram of sample transfer in the adsorption tube.*

4.1.4 Spent dialysate

Spent dialysate samples were collected 10, 30, 60, 120, 180 and 240 min respectively after the beginning of the dialysis session and analyzed by flow-injection. Aliquots of each sample were stored at -20 °C in polypropylene tubes (Safe-Lock, Eppendorf) for further analyses by HPLC. Blood samples were collected before the patient was connected to the dialysis machine and 60, 120 and 240 min after the beginning of the dialysis treatment.

4.2 Method validation for oral fluid samples analysis

The method validation included the evaluation of interferences, matrix effect, calibration curve, limit of detection and quantitation, intra-day and inter-day precision, stability and recovery.

4.2.1 Interferences

The possible presence of interfering endogenous substances was investigated by comparing the warfarin concentration determined in a standard working solution containing 5.0 ng/mL, a standard oral fluid sample (SOFS) with a spiked concentration of 5.0 ng/mL and two patient oral fluid samples (POFSs) with unknown concentrations. The samples were analyzed in triplicate, by HPLC-Fluorimetry with both columns (i.e. Chromspher 5 PAH and Poroshell 120 EC-C18) and by HPLC-MS/MS with the column Chromspher 5 PAH. Table 4.5 shows the warfarin mean concentration and the coefficient of variation for all the samples.

Table 4.5 *Comparative determination of warfarin in a standard solution, SOFS and POFS by HPLC-Fluorimetry with both columns (Chromspher 5 PAH and Poroshell 120 EC-C18) and by HPLC-MS/MS.*

Sample	Warfarin mean concentration [ng/mL], (n=3) (CV%)			
	Expected value	**HPLC-Fluo (Poroshell)**	**HPLC-Fluo (Chromspher)**	**HPLC-MS/MS**
Standard solution	5.0	4.6 (5%)	4.9 (3%)	5.2 (3%)
SOFS	5.0	5.3 (6%)	5.0 (4%)	4.9 (4%)
POFS-1	unknown	3.5 (6%)	4.5 (5%)	3.2 (7%)
POFS-2	unknown	7.1 (4%)	11.1 (4%)	6.3 (6%)

These results highlighted a very good agreement between the various methods in the case of the standard solution and the SOFS, both with an expected value of 5.0 ng/mL. The difference between the concentrations measured with HPLC-MS/MS and HPLC-Fluorimetry was about 10%.

The situation was quite different for the two samples collected from patients under oral anticoagulant therapy. The concentration values obtained by the HPLC-MS/MS, which were assumed as reference values, and by the HPLC-Fluorimetry with Poroshell 120 EC-C18 were in good agreement (+9% for POFS-1 and + 12% for POFS-2), whereas the values obtained by the HPLC-Fluorimetry with Chromspher 5 PAH column were much higher (+40% for POFS-1 and + 76% for POFS-2). The interference, which was only present in the patients' samples, may result from the presence of a warfarin metabolite [253]. On the basis of these results, the Poroshell 120 EC-C18 column was used in the subsequent evaluations of the performance of the method and in the clinical study.

Figure 4.5 shows the HPLC chromatograms of a warfarin standard solution, a COFS, a SOFS and a POFS. The standard solution, the

SOFS and the POFS had approximately the same warfarin concentrations.

Chromatographic separation was carried out in isocratic conditions by the Poroshell 120 EC-C18 column with a 65% PBS and 35% methanol mobile phase at a flow rate of 0.7 mL/min, injection volume 25 μL, temperature 25°C and fluorescence detection.

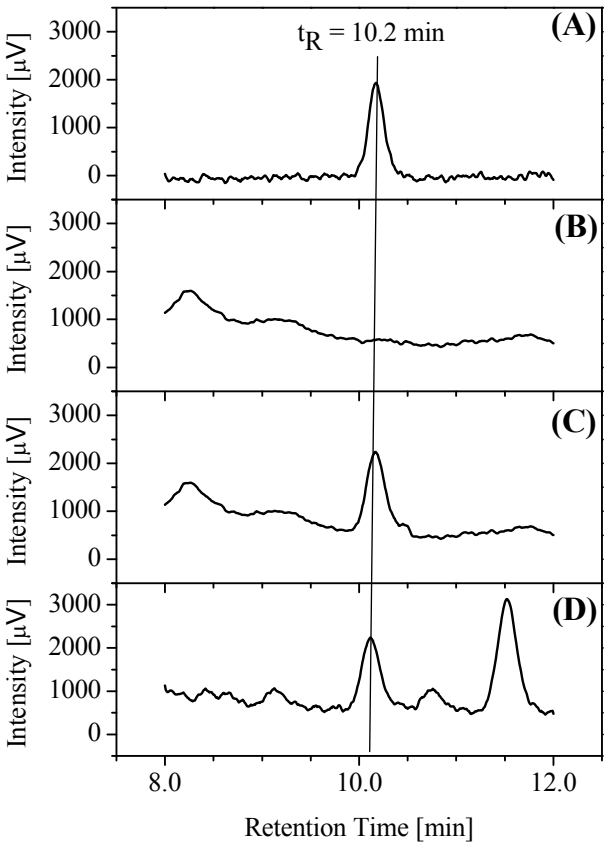

Figure 4.5 *HPLC chromatograms of: A) a standard working solution with a warfarin concentration of 1.5 ng/mL; B) a control oral fluid sample (COFS); C) a standard oral fluid sample (SOFS) with a warfarin concentration of 1.4 ng/mL; D) a patient oral fluid sample (POFS) with a warfarin concentration of 1.4 ng/mL.*

The warfarin peaks had a symmetric shape and were well separated from the other chromatographic signals. The retention time (t_R) was 10.2 min with a standard deviation of 0.1 min in five replicate measurements.

The same experimental conditions were used for the analysis of patients' sweat. These analyses proved problematic for the collection of an insufficient amount of sample in most cases, likely due to a diminished capability of sweating at older age [254]. Only qualitative information was obtained confirming the presence of the drug at concentration levels similar to oral fluid (Figure 4.6).

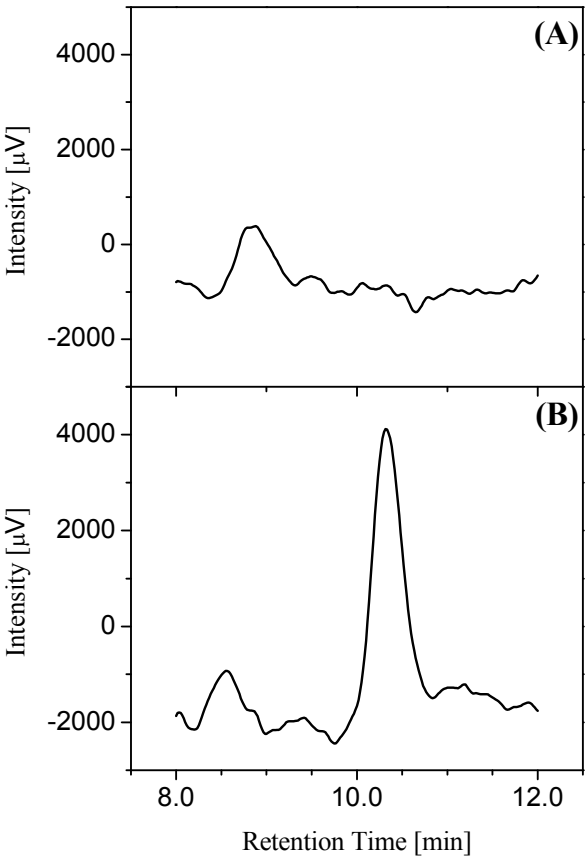

Figure 4.6 *HPLC chromatograms of representative sweat samples: A) a blank sweat sample from a volunteer not taking the drug; B) a patient sweat sample, a warfarin concentration of about 4 ng/mL was estimated (t_r = 10.2 min).*

4.2.2 Matrix effect

The evidence that the shape and position of the warfarin peaks were not affected by the presence of the oral fluid matrix (Fig. 4.5)

suggested the absence of any notable matrix effect. This hypothesis was confirmed by comparison of the slopes of the calibration curves obtained in the 1-10 ng/mL concentration range for a set of standard working solutions and a set of spiked POFSs. The two set were prepared as follows:

- calibration curve with standard working solutions: 20 µL of standard working solution with a warfarin concentration respectively of 10, 20, 40 and 100 ng/mL were added to 180 µL of 25 mM PBS (Figure 4.7 black line);
- calibration curve with spiked POFSs: 20 µL of standard working solution with a warfarin concentration respectively of 10, 20, 40 and 100 ng/mL were added to 180 µL of pooled patient oral fluid sample (Figure 4.7 blue line).

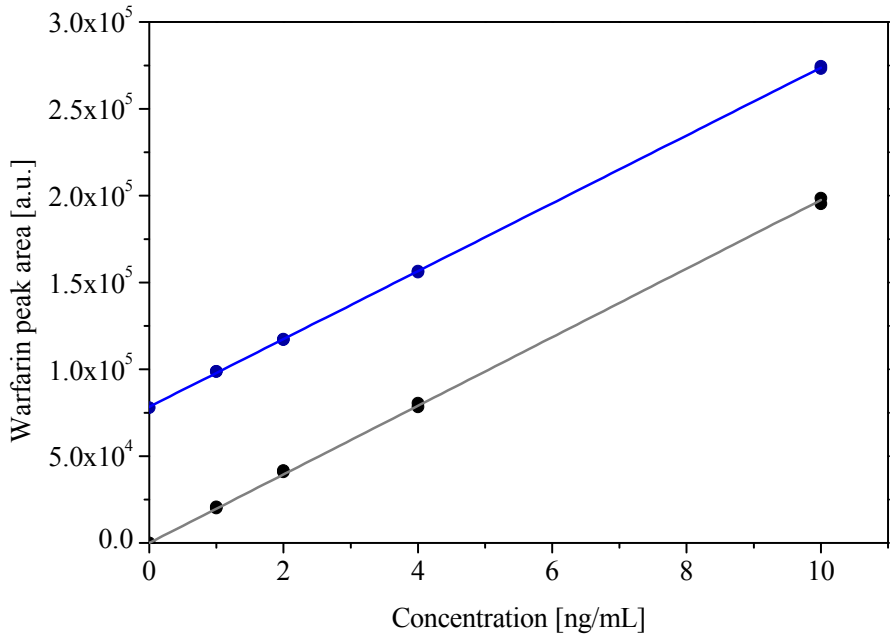

Figure 4.7 *Calibration curves obtained with standard working solutions (A, black line) and spiked POFSs (B, blue line).*

Table 4.6 shows a comparison of the parameters of the two calibration curves.

Table 4.6 *Statistical data of warfarin calibration curves.*

Parameter	**A**	**B**
Equation	Y = a X + b	Y = a X + b
Slope	19750	19540
Standard Error	90	60
Intercept	0	78390
Standard Error	--	270
Coefficient of determination	0.999	0.999

The limited difference of the slopes of the two calibration curves, which were 19750 ± 90 and 19540 ± 60 respectively, confirmed the hypothesis that oral fluid matrix does not affect results. The slopes values were compared by testing the null hypothesis and their difference resulted not significant (P = 1, two-tailed).

4.2.3 Calibration curve

In order to evaluate the working range, standard working solutions of warfarin in PBS at concentration levels ranging from 1 to 20 ng/mL were used as calibrators. These solutions were analyzed in triplicate and then fluorescence detector response (i.e. warfarin peak area) was plotted against corresponding warfarin concentration value (Figure 4.8).

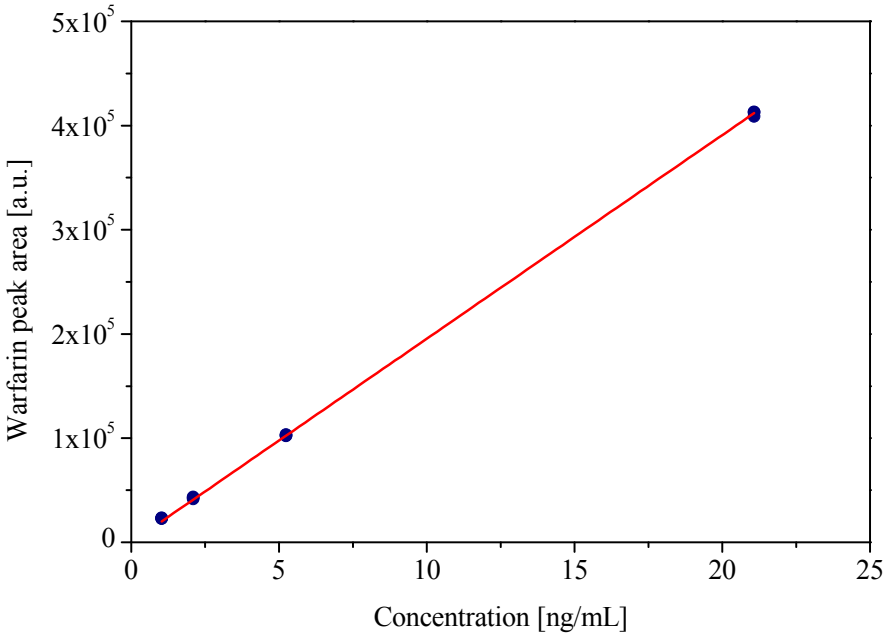

Figure 4.8 *Typical warfarin calibration curve.*

As it can be seen in Figure 4.8, the warfarin peak area linearly increased with the warfarin concentration of standard working solutions in the observed concentration range.

According to a linear regression analysis, the best fit model was: $y=(19550 \pm 60)\ x$, $R^2=0.999$ (Table 4.7).

Table 4.7 *Statistical data of warfarin calibration curve.*

Parameter	Value
Equation	Y = a X + b
Slope	19550
Standard Error	60
Intercept	0
Standard Error	--
Coefficient of determination	0.999

4.2.4 Limit of detection and quantitation

In order to assess limit of detection (LOD) and limit of quantitation (LOQ), a SOFS at about 0.5 ng/mL was prepared and assumed as "blank" or the closest concentration to the limit of detection. This sample was analyzed five times and the corresponding results are shown in Table 4.8. According to the IUPAC definition [255], the LOD was evaluated as three times the standard deviation s_b of the "blank", which corresponds to about 0.2 ng/mL, whereas the LOQ as ten times the standard deviation s_b of the "blank", which corresponds to about 0.8 ng/mL.

Table 4.8 *Statistical data of five replicate measurements of a SOFS sample.*

RUN	Warfarin concentration [ng/mL]
1	0.4
2	0.6
3	0.4
4	0.5
5	0.5
Average [ng/mL]	0.5
s_b [ng/mL]	0.1

4.2.5 Precision and accuracy

Intra-day and inter-day precision and accuracy assessment was conducted at three different concentration levels of standard working solutions, 1, 5 and 20 ng/mL, with three determinations per concentration and per day.

Table 4.9 *Precision and accuracy of standard working solutions (n=3).*

	Nominal concentration [ng/mL]					
	1.00		5.20		20.5	
Day	**Average**	**CV %**	**Average**	**CV %**	**Average**	**CV %**
1	1.00	0.6	5.01	1.6	19.8	0.8
2	1.03	4.7	5.12	0.4	20.1	1.2
3	0.92	2.4	5.20	0.8	20.6	0.8
Average	0.98		5.11		20.2	
CV %	5.8		1.9		2.0	
Relative Error %	-2.0		-1.7		-1.4	

Table 4.9 shows that the precision or within-run repeatability did not exceed 5 % at low concentration level and 2 % at medium and high concentration levels and that the inter-day accuracy was within 2 % of the actual value at each concentration.

The quality control procedure for INR measurements consisted in analysing three reference samples (normal, low and high INR levels) provided by the Instrumentation Laboratory at least once every eight hours. A coefficient of variation <1% for measurements performed on the same day and <3% for measurements performed on different days demonstrated the good repeatability of the method.

4.2.6 Quality control of analytical data

The quality control of data over time was assessed by systematically measuring a standard solution with known content of warfarin (5 ng/mL) and comparing the data obtained with the expected value. The use of a standard solution of warfarin was suggested by its stability, homogeneity and availability in sufficient quantity to repeat the analysis over time.

Therefore, multiple measurements of the standard solution were included within all the sequences of analyses of patients' samples. These data made it possible to draw a control chart (Figure 4.9) reporting the daily average values of the ratio between warfarin peak area and concentration (purple dots), the average of all the ratios obtained during the experimental campaign (purple dashed line), the attention limits (average ± SD, magenta line) and the control limits (average ± 2SD, blue line).

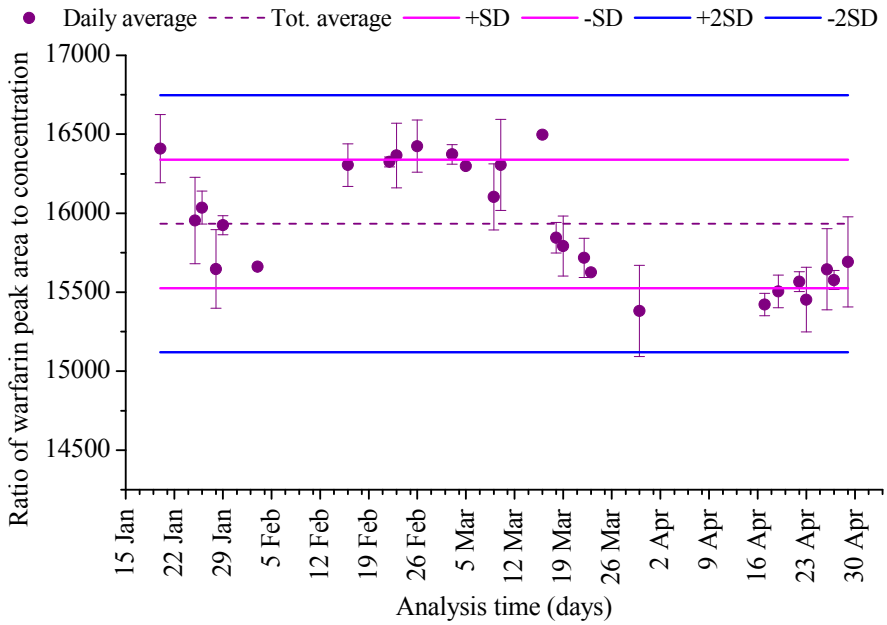

Figure 4.9 *Warfarin control chart.*

As it can be seen from the control chart, in about four months of experimental activity, the control limit was never exceeded, indicating very good control of experimental conditions.

4.2.7 Effect of pH on warfarin recovery

The recovery percentage of warfarin from the sampling swabs was estimated at three levels of pH (5.2, 6, 6.9 and 7.5) covering the range of variability observed in the oral fluid samples. Four SOFSs

with a warfarin concentration of about 5 ng/mL, a volume of 4mL and an initial pH value of 6.9 were used for the experiments. Two of them were acidified to pH 5.2 and 6 by adding 20 µL and 10 µL of phosphoric acid 1 M respectively, another was alkalinized to pH 7.5 by adding 8 µL of sodium hydroxide 1 M. Each of these four samples was divided into four aliquots. The first aliquot was analyzed without any further treatment, the other three were absorbed into the synthetic swabs and treated as normal samples. The recovery percentage was then calculated from the ratio between the average warfarin concentration in the samples recovered from the swab and the initial concentration.

The recovery of warfarin from the sampling swabs was generally satisfactory. A slight dependence on pH was found, with recovery percentages equal to 93 ± 0.2 % at pH 5.2, 99 ± 0.1 % at pH 6.0 and 100 ± 0.1 % at pH 6.9 and 7.5 (Table 4.10).

Table 4.10 *Sample recovery percentage from the swab at four levels of pH.*

pH	Average recovery % (CV %)
5.2	93 % (0.2 %)
6.0	99 % (0.1 %)
6.9	100 % (0.1 %)
7.5	100 % (0.1 %)

Only a very limited fraction of patients (4 %) showed a pH value of the oral fluid lower than 6.0, so the slightly different recovery percentage was considered negligible. In a few trials carried out with acidic oral fluid samples, the small fraction of warfarin remaining in the sampling swab was recovered by changing the sample pH to about 7.0 by the addition of 50 - 100 µL of PBS 1 M, reabsorbing the sample in the sampling swab and centrifuging the

swab a second time. Thus, recovery percentages obtained were almost quantitative.

4.3 Method validation for breath samples analysis

4.3.1 Determination of the response factors for the quantification of compounds

Instrumental responses may change over time, so quantification by the simple comparison of peak areas it is not always the best practice. Thus, the determination of the instrument response factor relative to an internal standard of each compounds becomes necessary to achieve a reasonable level of accuracy.

Since breath is a gaseous matrix, a gaseous standard mixture was prepared to calculate a response factor (K) and determine the concentration of the compounds of interest.

Adsorption tubes were loaded with MIX 25 and a labelled internal gaseous standard mixture, composed of Toluene-D8 and Isopropanol-D8 (MIX 2D). The response factor for each compound was calculated with reference to the labelled compounds according to the following relation:

$$K = \frac{A_i \cdot m_{D8}}{A_{D8} \cdot m_i} \qquad (4.1)$$

where A_i and m_i are the chromatographic peak areas (a.u.) and the theoretical amounts (ng loaded in the desorption tube) of the i^{th}-*compound,* A_{D8} and m_{D8} are the chromatographic peak areas (a.u.) and the theoretical amounts (ng loaded in the desorption tube) of the internal labelled standard (toluene-D8).

A_i and A_{D8} were obtained by injecting 250 µL of MIX 25 and 50 µL of MIX 2D through a septum into the aspiration flow, during pre-concentration of 250 mL of pure air in the adsorption tube.

The concentrations of compounds were calculated as follows:

$$C_i = \frac{A_i \cdot m_{D8}}{A_{D8} \cdot K} \cdot \frac{1}{V} \qquad (4.2)$$

where A_i is the chromatographic peak area of generic compound (a.u.), A_{D8} and m_{D8} are the chromatographic peak areas (a.u.) and the theoretical amount (ng loaded in the desorption tube) of internal standard (toluene-D8), K is the response factor and V is the sampled volume (L).

The average response factors for the components of MIX 25 and the corresponding coefficients of variation are reported in Table 4.11.

Table 4.11 *Response factors of the compounds in MIX 25.*

Analytes	Response factor (K)	CV %
Pentane	0.11	3%
Ethanol	0.09	6%
Isoprene	0.07	6%
Acetone	0.11	3%
Dimethylsulphide	0.05	5%
2-propanol	0.51	7%
Acetonitrile	0.34	3%
2-methylpentane	0.12	6%
Hexane	0.30	3%
1-propanol	0.17	5%
2,3-butanedione	0.34	5%
Ethyl acetate	0.43	4%
Chloroform	0.62	5%
Carbontetrachloride	0.71	6%
Benzene	1.54	1%
1-butanol	0.16	4%
Trichloroethylene	0.39	4%
2-pentanone	0.93	5%
Hexafluoroisopropanol	0.54	7%
Dimethyldisulphide	0.61	5%
3-hydroxy-2-butanone	0.03	6%
Toluene	1.26	2%
Tetrachloroethylene	0.68	6%
4-heptanone	1.06	6%
m-cresol	0.16	29%

4.3.2 Linearity of sevoflurane

The range of linearity for sevoflurane was assessed for the response of the mass spectrometer detector and for the breakthrough volume on Tenax GR adsorption tube. Two gaseous samples of sevoflurane were prepared. The first was prepared by injecting 5 µL of liquid sevoflurane in a pre-evacuated 2 L glass flask equipped with a septum, the second by injecting 5 µL of liquid sevoflurane in

the flow of pure air during the filling of a 10 L Nalophan bag. Glass flask and Nalophan bag were kept at 37 °C.

To evaluate linearity of mass spectrometry detector response, increasing volumes (10, 20 and 50 µL, triplicate samples) were drawn from the glass flask, directly injected into the GC-MS and analyzed according to the methods reported in Table 3.2.

Figure 4.10 shows the sevoflurane average peak area versus the injected volume.

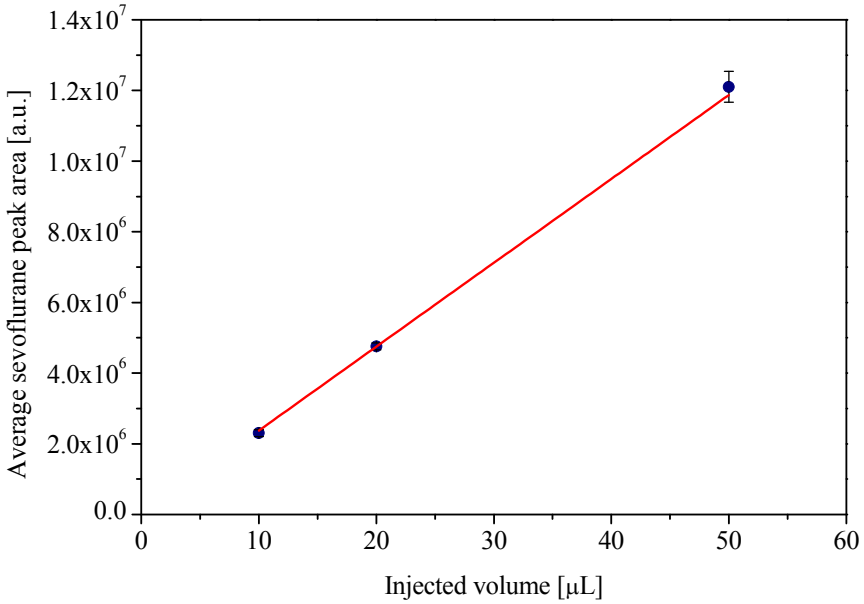

Figure 4.10 *Calibration curve of gaseous sevoflurane directly injected into the GC-MS.*

Increasing volumes (10, 20 and 50 mL) of sample drawn from the bag were transferred into the adsorption tubes by a pocket pump (flow 10 mL/min) to evaluate the sevoflurane breakthrough volume for Tenax GR adsorption tubes. The tubes were analyzed according to the methods reported in Table 3.2.

Figure 4.11 shows the sevoflurane average peak area versus the volume of sample pre-concentrated in the adsorption tube.

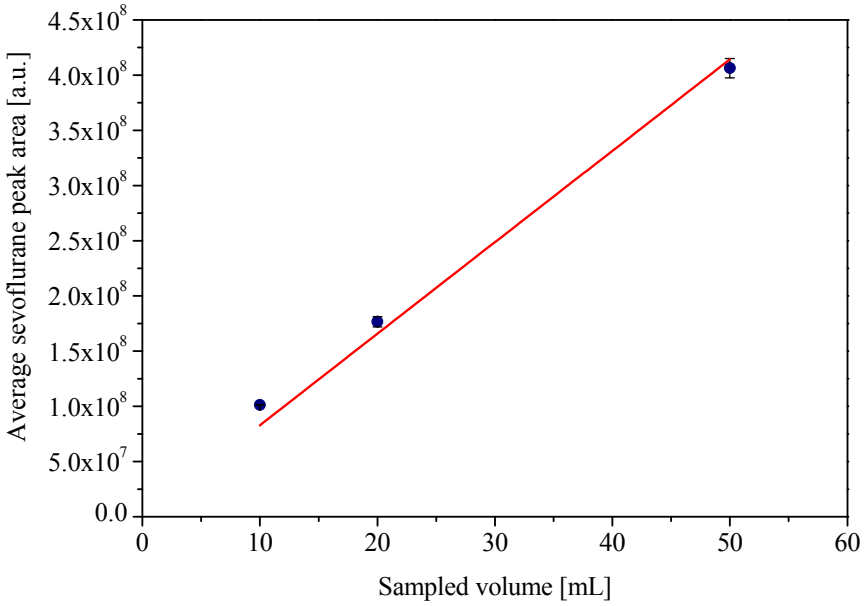

Figure 4.11 *Linearity of sevoflurane peak area versus the volume of the sample pre-concentrated in Tenax GR adsorption tube.*

From the figures above, it can be seen that sevoflurane has a good linearity both in terms of response of mass spectrometry detector (R^2 = 0.999) and breakthrough volume on Tenax GR adsorption tube (R^2 = 0.997) in the range considered.

4.3.3 Time stability of sevoflurane concentration in the Nalophan bag

A gaseous sample of sevoflurane was used to evaluate the stability of the concentration of this gas in the Nalophan bag. A volume (5 µL) of liquid sevoflurane was injected in the flow of pure air during the filling of a 2 L Nalophan bag. The sevoflurane concentration in the bag was 477 ppmv.

To simplify the experimental procedure, triplicate direct injections of 50 µL of bag sample into the GC-MS were performed soon after filling (Time 0) and after 0.5, 2.5, 5 and 24 hours.

Figure 4.12 shows the sevoflurane average peak area (normalized with respect to the peak area at time zero) as a function of the storage time in the bag.

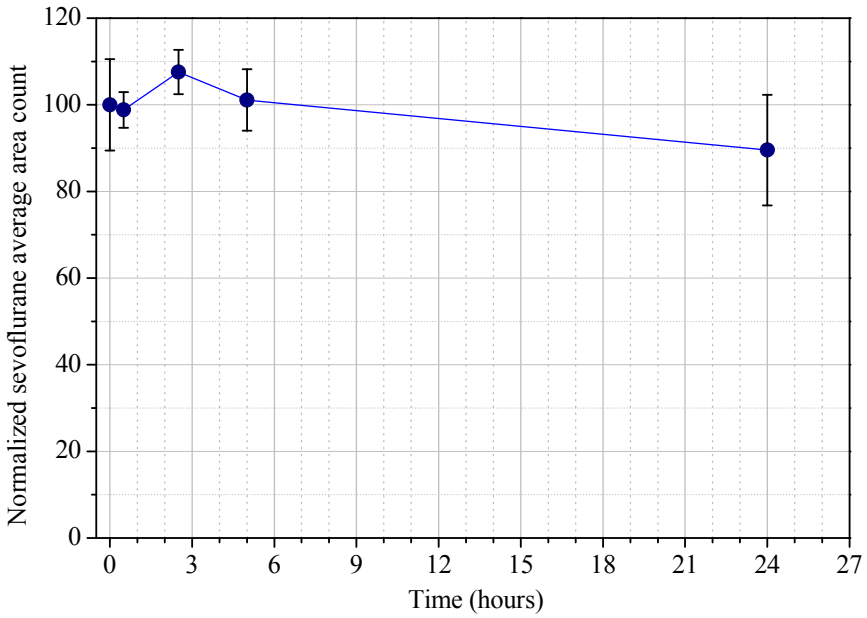

Figure 4.12*Time stability of sevoflurane sample in the Nalophan bag.*

The sevoflurane concentration in the Nalophan bag was stable within 6 hours and had a 10 % decrease within 24 hours.

4.4 Method validation for the analysis of spent dialysate samples

4.4.1 Calibration curves

Standard working solutions of uric acid, creatinine and β_2-microglobulin were used to calibrate the HPLC system in the concentration range of 2-50, 0.6-60 and 2-25 µg/mL respectively. Such ranges include the concentration ranges observed in dialysate samples, which are 2-33, 0.8-47 and 0.5-7.3 µg/mL for uric acid, creatinine and β_2-microglobulin respectively. The UV

absorbances of the uric acid, creatinine and β_2-microglobulin solutions were measured in triplicate at 292, 235 and 280 nm respectively, whereas the fluorescence emission of the β_2-microglobulin solution was measured at 340 nm (excitation wavelength 220 nm).

The detector signal (i.e. peak area) obtained by flow-injection was then plotted against the corresponding concentration value (Figures 4.13 – 4.15).

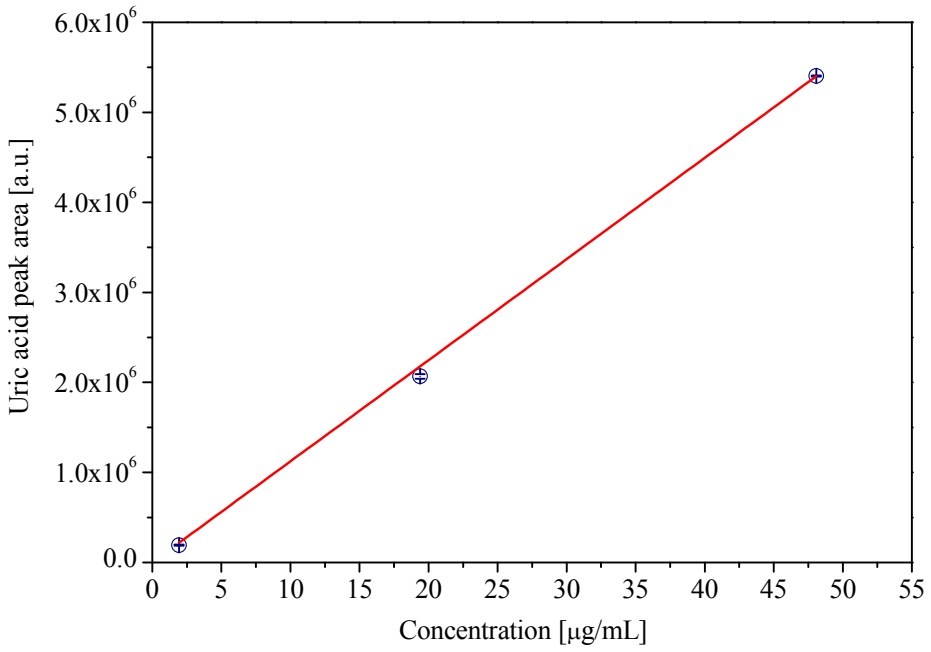

Figure 4.13*Calibration curve of uric acid at 292 nm.*

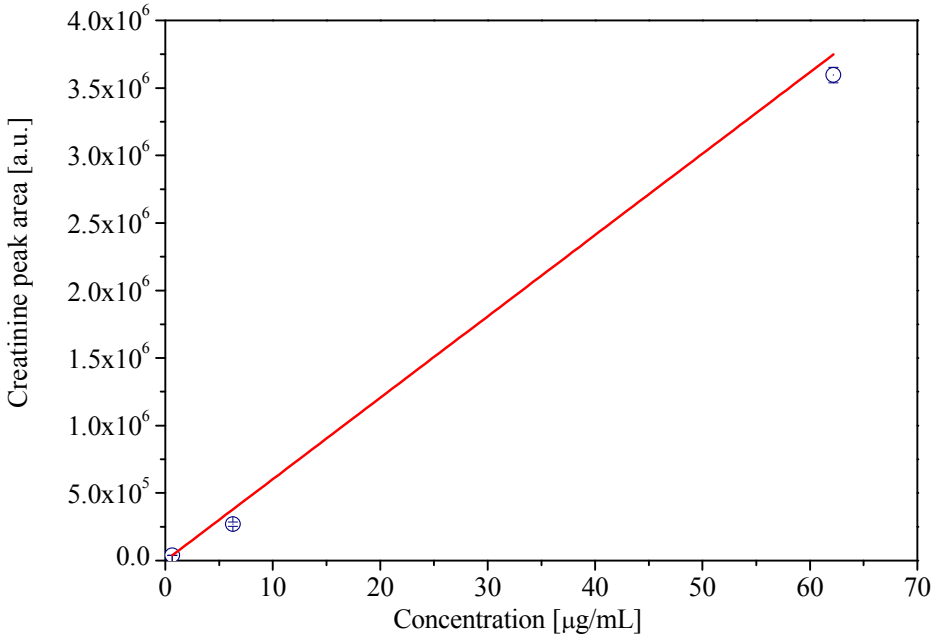

Figure 4.14 *Calibration curve of creatinine at 235 nm.*

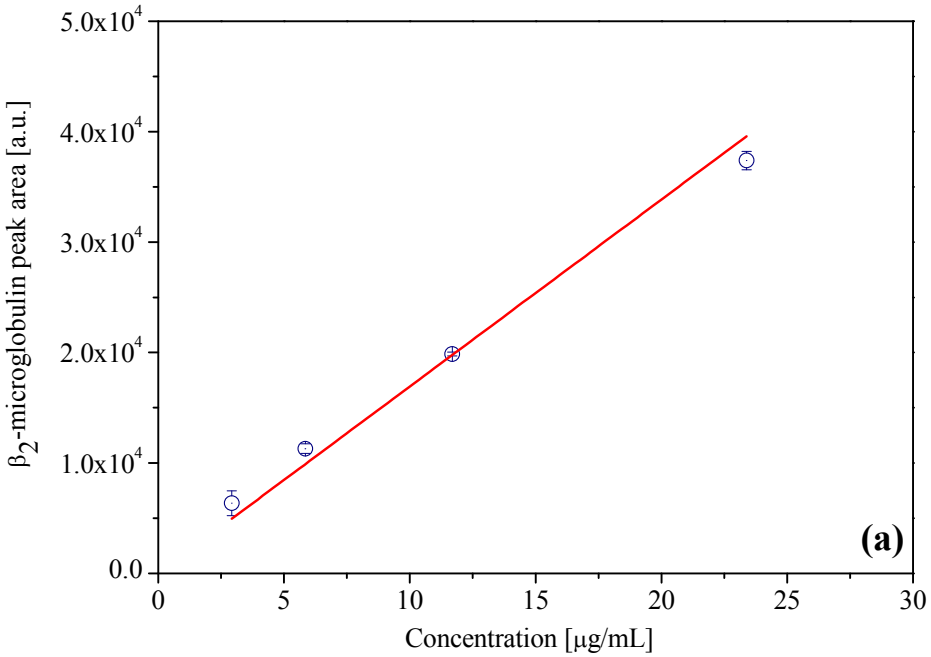

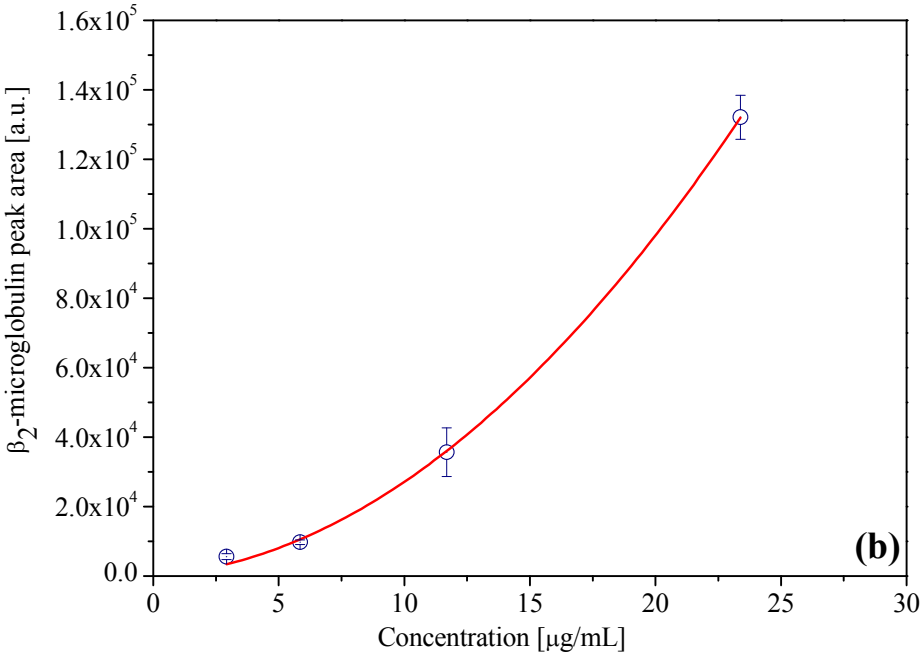

Figure 4.15 *Calibration curve of ß2-microglobulin at 280 nm* (a) *and 220-340 nm* (b).

The uric acid peak area linearly increased with concentration in the range 2 – 50 µg/mL. According to a linear regression analysis, the best fit model was: y = (112000 ± 400) x, R^2 = 0.999. The creatinine peak area linearly increased with concentration in the range 0.6 – 60 µg/mL. According to a linear regression analysis, the best fit model was: y = (60000 ± 2000) x, R^2 = 0.997. The β_2-microglobulin peak area increased with concentration in the range 2 – 25 µg/mL. According to a linear regression analysis, the best fit model for UV was: y = (1690 ± 10) x, R^2 = 0.998, whereas according to a polynomial regression analysis, the best fit model for fluorescence was y = (220 ± 10) x^2 + (500 ± 200) x, R^2 = 0.999.

Due to the relevance of its contribution to UV absorbance (Table 5.5), a particular attention was paid to the uric acid.

The HPLC system was also calibrated by spiking a pooled dialysate sample (obtained by pooling aliquots (100 µL) of each patient sample collected 240 minutes after the beginning of the dialysis

treatment) with standard working solutions. The slopes of the two calibration curves (i.e. in standard working solutions and in dialysate samples) were compared to exclude the presence of possible matrix effect. The second curve was then used to measure the concentration of uric acid in samples collected from eight patients 10 and 240 minutes after the hemodialysis beginning. These results were compared to the result obtained by biochemical methods (Table 4.12).

The calibration curve in spent dialysate was obtained by adding 50 µL of standard working solutions with uric acid concentrations of 50, 100, 150 and 300 µg/mL respectively to 450 µL aliquots of the pooled dialysate reference sample.

The chromatographic separation was carried out in isocratic conditions by a XTerra MS-C18 column thermostated at 25 °C. The mobile phase consisted of 98% of a 1% formic acid solution in water and 2% acetonitrile. The flow rate and the injection volume were 1 mL/min and 25 µL respectively. All HPLC measurements were carried out by setting the spectrophotometric detector at an absorption wavelength of 292 nm.

Figure 4.16 shows chromatographic peaks relevant to uric acid in the spent dialysate reference sample (A) (retention time = 4.18 min).

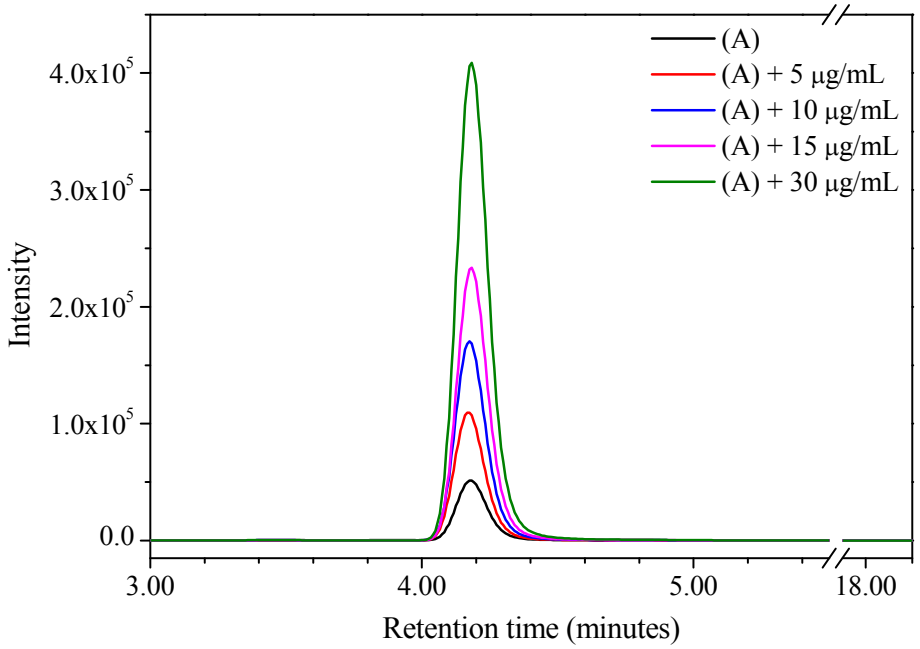

Figure 4.16 *Chromatographic peaks of uric acid in the spent dialysate reference sample as it is (black line) and after addition of different amounts of uric acid: 5 (red line), 10 (blue line), 15 (magenta line) and 30 (green line) µg/mL.*

According to a linear regression analysis, the best fit model for uric acid in the reference dialysate sample was: y = (86300 ± 700) x + (440000 ± 12000), R^2 = 0.999. The slope of the curve was compared to the one obtained in standard working solutions (87700 ± 300) by testing the null hypothesis and their difference resulted not significant (P = 0.80, two-tailed).

Obtaining the same shape and position of the uric acid peaks in standard working solutions and spiked reference sample, and the same slope of the calibration curve too, made us exclude the presence of any notable matrix effect.

The equation of calibration curve in spent dialysate was used to calculate the uric acid concentration in the samples collected from eight patients 10 and 240 minutes after the hemodialysis

beginning (Table 4.12). A good agreement was found with values obtained by biochemical methods.

Table 4.12 *Comparison between uric acid concentration measured in spent dialysate samples by biochemical methods (A) and by HPLC (B).*

Samples		**A**	**B**	**Percent error (%)**
t = 10 min	P1	22	23	-2
	P2	22	23	-3
	P3	12	11	-6
	P4	4	4	3
	P5	15	14	-6
	P6	23	23	-1
	P7	19	19	-3
	P8	7	7	2
t = 240 min	P1	6	6	7
	P2	11	11	-1
	P3	5	5	7
	P4	2	2	-9
	P5	6	6	5
	P6	7	7	7
	P7	4	4	-8
	P8	3	3	0.2

The maximum percentage deviation for all the samples was less than 10 % and one-way analysis of variance calculated a probability higher than 98% for the two datasets not to be significantly different. Such agreement proved that the HPLC system was correctly calibrated and indirectly confirmed the accuracy of the estimates of the average percentage contribution of uric acid to the overall signal (paragraph 5.4).

CHAPTER 5

Clinical applications: results and discussion

5.1 Monitoring of warfarin therapy

The study on oral anticoagulants was approved by the Ethics Committee of the Azienda Ospedaliero Universitaria Pisana (AOUP) with the deliberation n° 2592. The analytical methodology described in chapter 3 and 4 was used for a clinical study involving 50 patients undergoing oral anticoagulant therapy with Coumadin®, whose active principle is Warfarin sodium, and ten nominally healthy subjects, for non invasive monitoring of the warfarin in oral fluid.

All patients and nominally healthy volunteers were accepted in the study after receiving oral and written information and signing a written informed consent. The enrolment and sampling were carried out at a local anticoagulation clinic (Surveillance centre for oral anticoagulant therapy-AOUP). Both activities were performed while patients were waiting for the periodic check of the degree of anticoagulation of their blood. The collection of oral fluid samples was carried out in the morning (from 8:30 to 10:00 or so) to avoid any effect due to possible circadian variations.

Fifty adults (27 males, 23 females) patients on warfarin therapy were recruited. Patients with hepatic or kidney pathologies were excluded from the study. The enrolled subjects were treated for atrial fibrillation (AF, 62%), deep vein thrombosis (DVT, 12%),

pulmonary embolism (PE, 10%), as mechanical or biological heart valve bearers (MHV, 10%) or for other reasons (6%). Their mean age was 74 ± 9 years (range, 42 – 88 years) and they were on an average warfarin dose of 27 ± 13 mg/week (range, 5 – 57.5 mg/week). INR values varied from 1.2 to 3.8, with an average value of 2.3 ± 0.6. Approximately three fifths of the patients (31) had INR values within the recommended range for anticoagulation (2.0 - 3.0). The distributions of warfarin doses and INR values among the patients are reported in Figures 5.1 and 5.2 respectively.

The values of INR and the weekly dose of Coumadin assigned to each patient were provided by the laboratory of the clinic (Clinical chemical laboratory of the Azienda Ospedaliero Universitaria Pisana, AOUP).

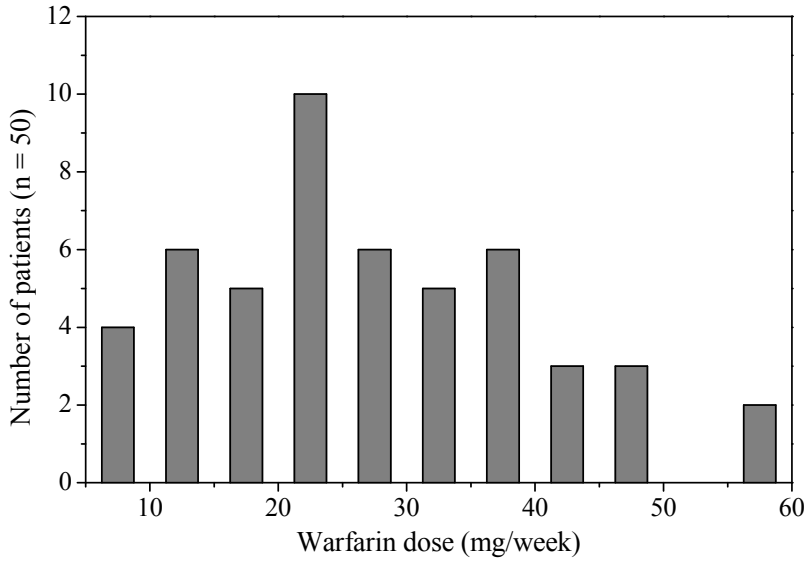

Figure 5.1 *Distribution of the warfarin doses in the patients undergoing oral anticoagulant therapy.*

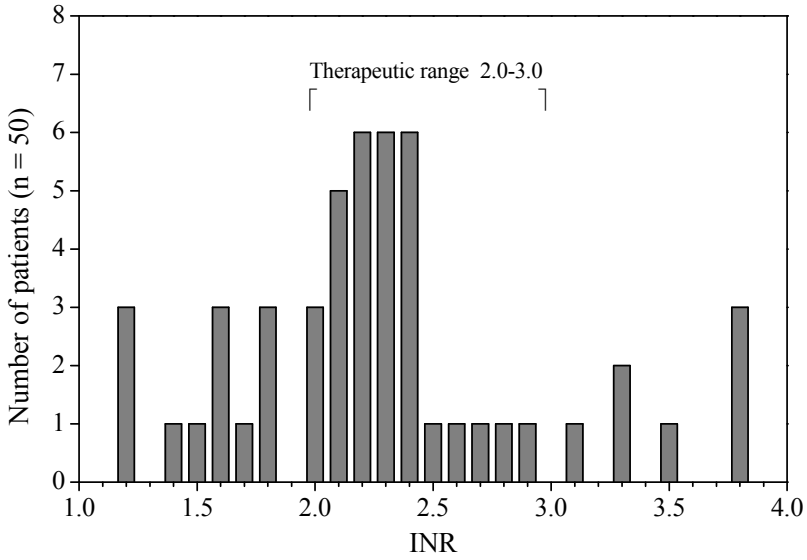

Figure 5.2 *Distribution of the INR values in the patients undergoing oral anticoagulant therapy.*

The Mann-Witney test did not highlight statistically significant gender differences ($p < 0.05$) for any of the above parameters.

Ten nominally healthy subjects who were not taking any drug also contributed to the study by providing control samples.

The concentration of warfarin in the oral fluid samples of patients enrolled in this study was determined using the calibration curve shown in Figure 4.7 (chapter 4).

The average concentration of warfarin in the oral fluid samples was 2.5 ± 1.6 ng/mL, with values ranging from 0.8 to 7.6 ng/mL, whereas the pH of the oral fluid was 6.7 ± 0.4 in the range 6.0 - 7.5 (Figure 5.3).

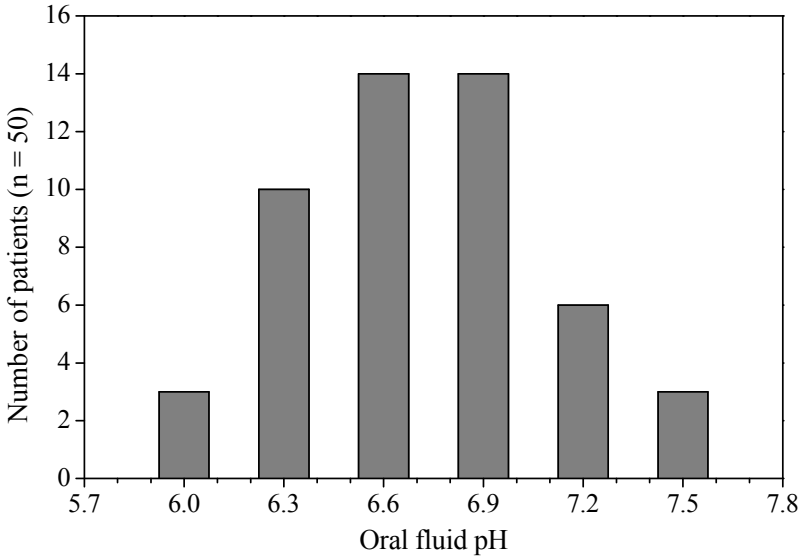

Figure 5.3 *Distributions of the oral fluid pH values in patients undergoing oral anticoagulant therapy.*

Principal component analysis, PCA [256, 257], was used to obtain an overall view of the internal structure of the data. The principal component analysis produces two plots in which similar items are located close to one another: the score plot (Figure 5.4 (a)) shows the relationships between the objects, and the loadings plot (Figure 5.4 (b)) shows the correlation between the variables.

If the two plots are superimposed, the objects characterized by a high value of a variable will be located close to this variable.

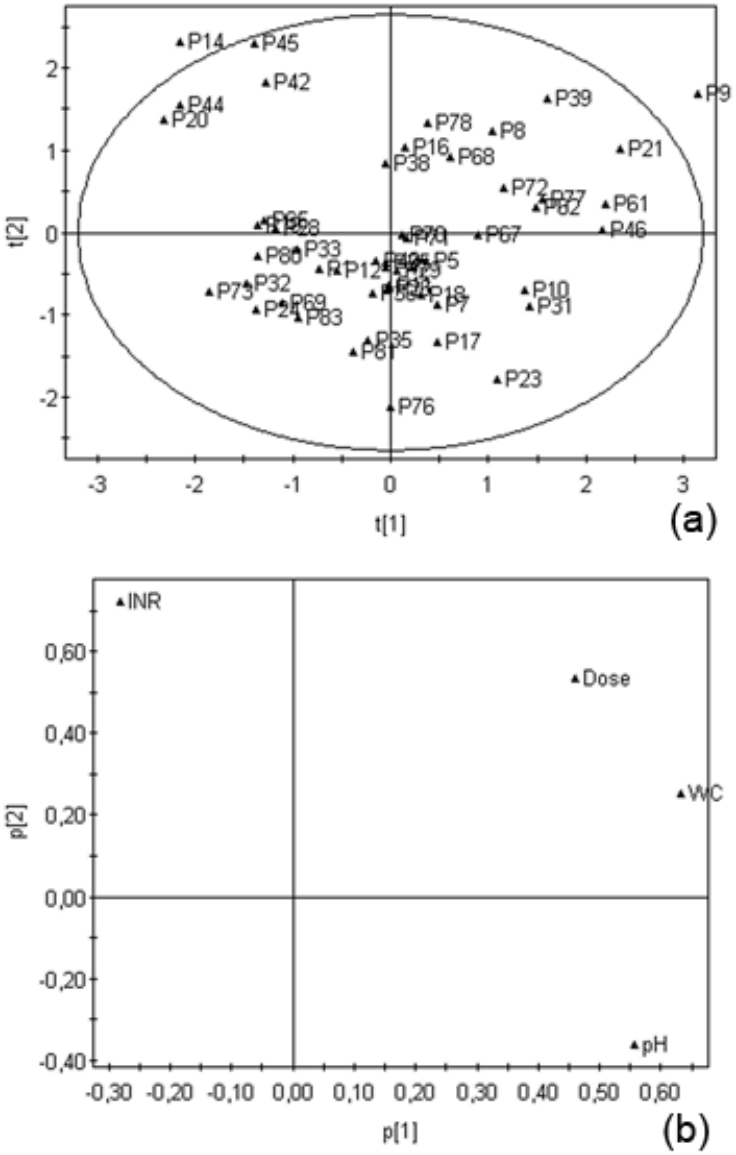

Figure 5.4 *Principal component analysis of patient data: score plot* (a) *and loadings plot* (b). *Legend: pH of the oral fluid (pH), warfarin concentration in the oral fluid (WC), warfarin dose (Dose), INR.*

The score plot shows that the majority of patients with INR values above the recommended range for anticoagulation form a separate group in the upper left corner. The positions of the variables in the loadings plot suggest that most patients with high INR values are taking doses of warfarin and have similar concentrations of warfarin in the oral fluid to patients with INR in the recommended therapeutic range. The main exception is patient P9, who falls in

the upper right corner for taking high doses of warfarin and shows very high concentrations of the drug in the oral fluid. The loadings plot also suggests the existence of a positive correlation between dose and warfarin concentration in the oral fluid as well as a negative correlation between INR and pH values.

Figure 5.5 reports INR (a) and warfarin concentration values in oral fluid (b) versus weekly dose.

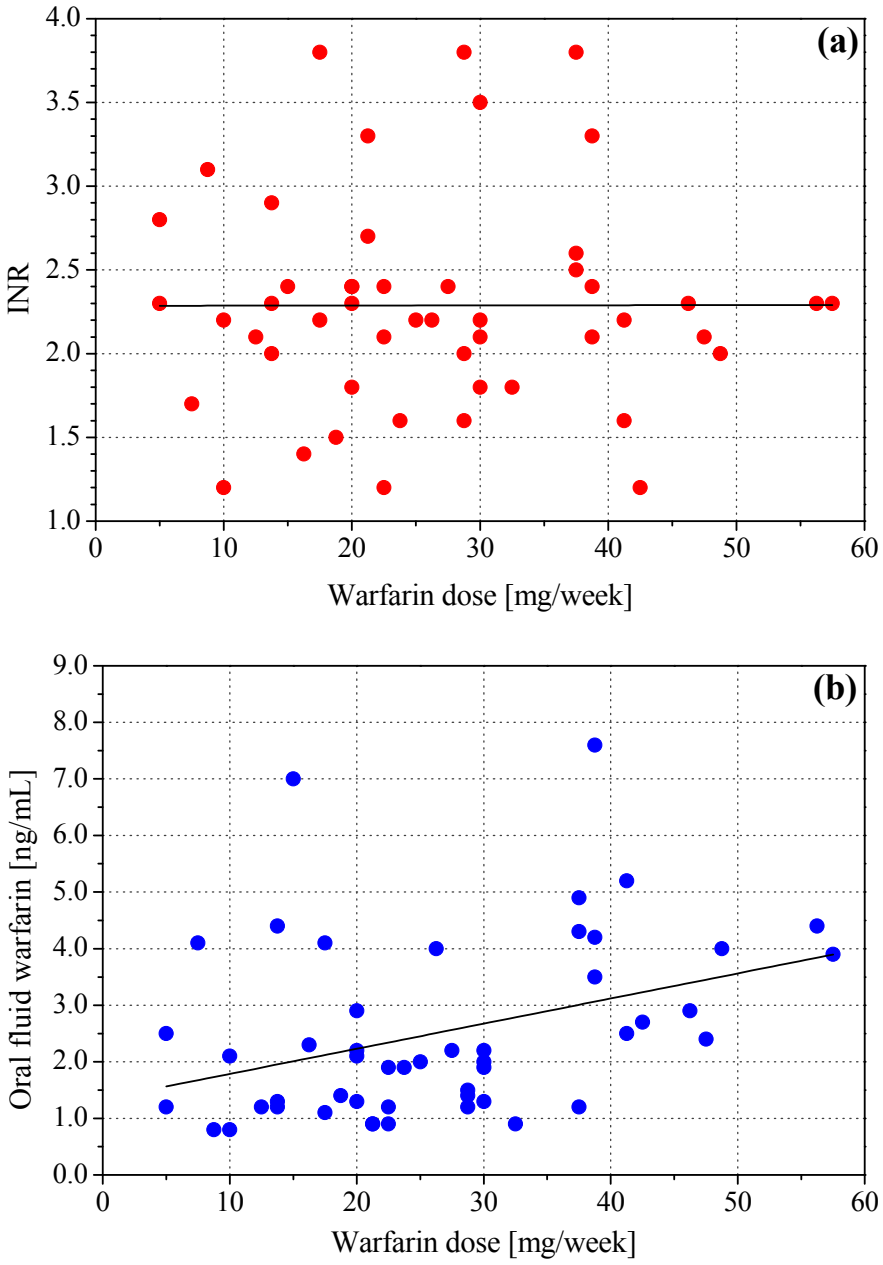

Figure 5.5 *INR* (a) *and warfarin concentration in oral fluid* (b) *versus dose.*

No correlation was found between INR values and dose ($r = -0.03$, $p = 0.85$), whereas there was a clear positive correlation between warfarin concentration in the oral fluid and dose ($r = 0.39$, $p = 0.006$).

The first result reflects the wide variability of patient responses to the drug observed in over fifty years of clinical use. This variability has been ascribed to factors such as gastrointestinal absorption, age, renal and hepatic function, lifestyle (in particular diet, alcohol consumption, smoking etc.) [258, 259]. The concomitant assumption of other drugs can change the fraction of warfarin bound to plasma proteins and influence its pharmacokinetics and pharmacodynamics. Genetic variability in the cytochrome P450 (for specific CYP isoforms) has also been identified as a further key factor [260, 261, 262].

The correlation between warfarin concentration in oral fluid and dosage is also not surprising. Warfarin concentration in oral fluid is expected to mirror (if the pH level in the oral fluid is not much lower than plasma pH) the concentration of free warfarin in plasma, and to be highly correlated to the total warfarin concentration in plasma. The ratio between the concentrations of bound and unbound warfarin in plasma, in fact, is reported to be generally subject to only minor variations (between 0.01 and 0.03), with the exception of the concomitant assumption of other drugs capable of displacing bound warfarin from albumin [263]. Obviously, the degree of correlation between warfarin concentration in oral fluid and dosage cannot be higher than the correlation existing between warfarin concentration in plasma and dosage. A correlation coefficient of $r = 0.55$ was found by Lombardi et al. [264] between total warfarin concentration in plasma and weekly dosage, whereas Huang et al. [265] found a correlation coefficient of 0.378 between the concentration of free warfarin in

plasma and weekly dosage. Our value is compatible with these results.

A correlation was found between the concentration of warfarin in the oral fluid and the pH value (r = 0.37, p = 0.009) (Figure 5.6).

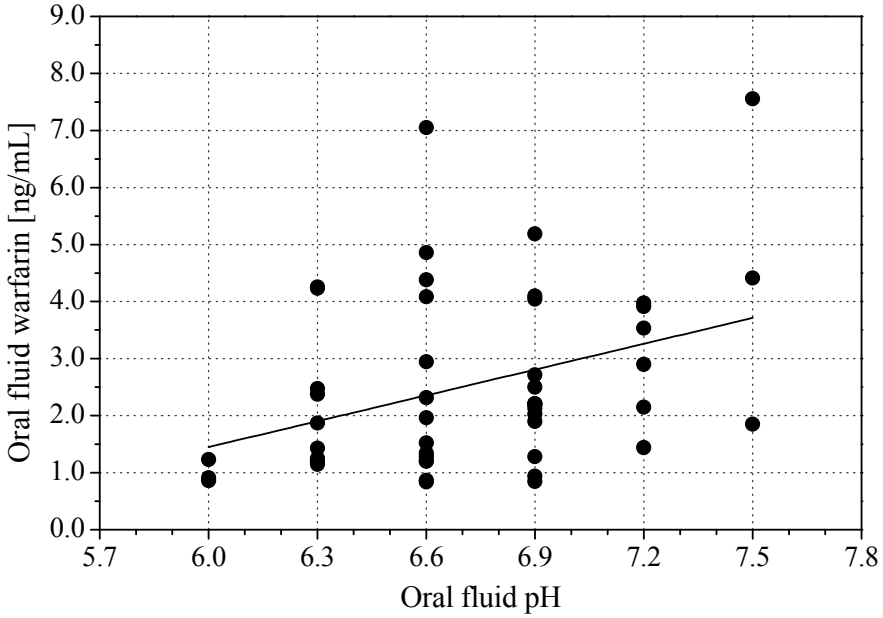

Figure 5.6 *Correlation between concentration of warfarin and pH in oral fluid.*

We believe that this correlation may be due to a hindered warfarin transfer from plasma when pH values of the oral fluid approach the pKa of warfarin (5.19). In fact the lowest warfarin concentration levels in oral fluid were observed in the most acidic samples. Two patients, with pH values of oral fluid lower than 6, had to be excluded from the study because the warfarin concentration in the oral fluid was below the quantification limit.

Figure 5.7 (a) reports the warfarin concentration in oral fluid versus INR. No correlation was found between these two parameters if all samples were included (r = -0.11, p = 0.43). However, if only the samples with pH values equal or higher than

7.2 were considered, a correlation between these two parameters was observed (r = 0.84, p = 0.004, Figure 5.7 (b)).

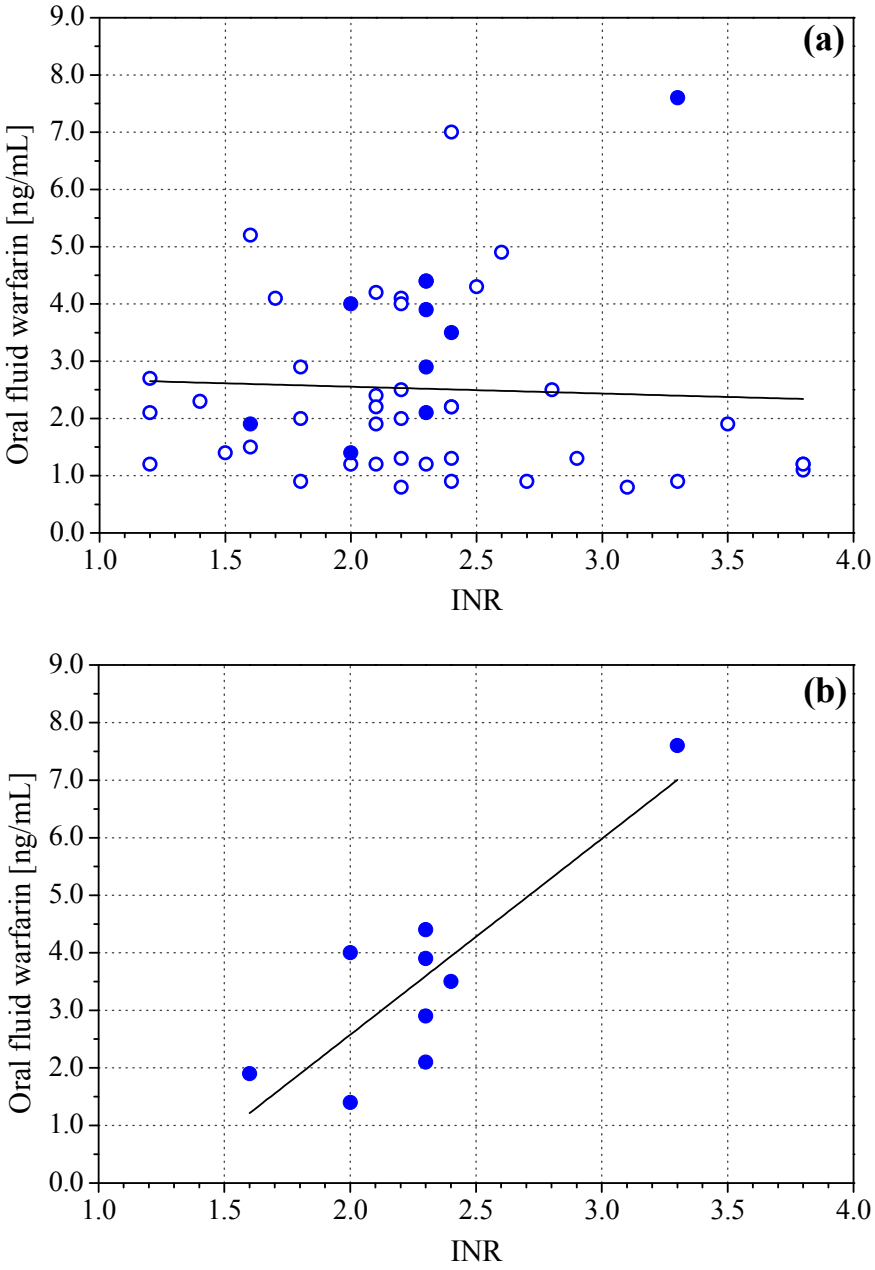

Figure 5.7 *Warfarin concentration in oral fluid versus INR: all the samples* (a) *(samples with a pH level ≥ 7.2 are indicated by full dots) and detail of samples with a pH level ≥ 7.2* (b).

Although the limited number of patients does not enable a firm conclusion to be drawn on this point, the result is compatible with the hypothesis that there is a good correlation between the free

warfarin concentration in plasma and INR, which is only mirrored in the oral fluid when its pH value enables the drug to be transferred from the blood.

Huang et al. [265] found a modest but significant correlation between free warfarin in plasma and INR ($r = 0.207$, $p = 0.03$), as did Lombardi et al. [264] who found a similar correlation between total warfarin in plasma and INR ($r = 0.25$, $p = 0.079$).

In comparison with these studies, our set of patients showed a lower correlation between warfarin concentration in oral fluid and INR when the pH of oral fluid was lower than plasma pH, however they showed a higher correlation when these pH values were in the same range. This suggests that when pH conditions lead to an optimal diffusion from blood, the warfarin assayed in the oral fluid may reflect the pharmacodynamics more precisely, thus maybe overcoming the effect of an unknown confounding factor connected to the complex chemical nature of blood. To confirm this second hypothesis, we used measured oral fluid pH values to calculate the theoretical warfarin concentration values in plasma (c_p) by the Rasmussen equation [266]. This was possible taking into account that the free fraction of oral fluid (f_{of}) is considered practically equal to 1, the free fraction in plasma is assumed equal to 1 % (f_p = 1 % of total) and the plasmatic pH is buffered to the value of 7.40 (7.40 ± 0.05).

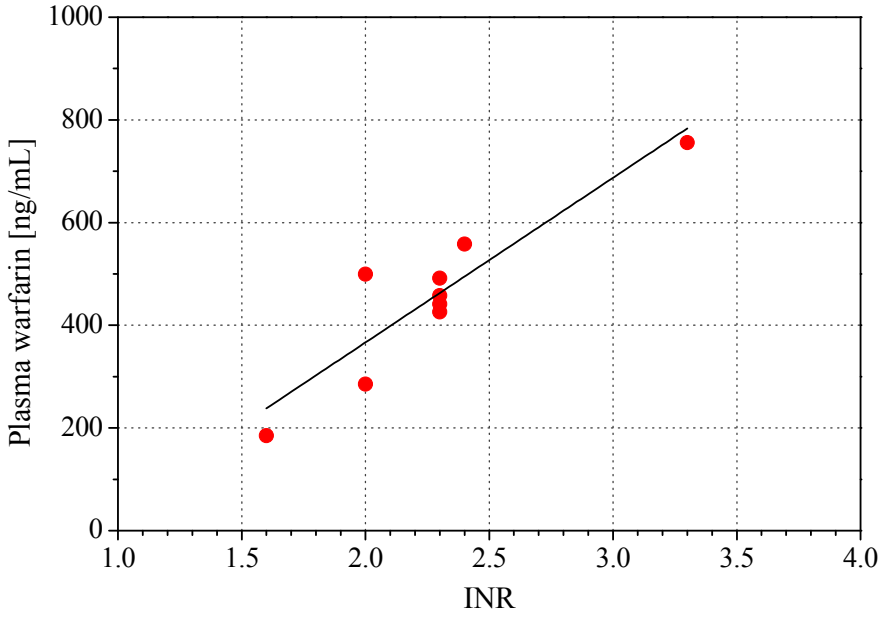

Figure 5.8 *Correlation between calculated concentration of warfarin in plasma and INR for patients with an oral fluid pH ≥ 7.2.*

The use of the pH information resulted in an increased correlation ($r = 0.91$, $p = 0.0006$, Figure 5.8).

These results suggest for the first time the existence of a pH-dependent correlation between oral fluid concentrations of warfarin and INR. If confirmed in a larger number of cases, this result could represent a first step towards the development of non invasive "point of care" systems for monitoring patients on anticoagulation therapy. Such devices, easily managed by the patients themselves, would allow a frequent self-control of the coagulation level. Such control would prevent bleeding events in the time span between two INR checks, reduce the number of checks at the clinics and help the patient in the management of his diet, thus improving the quality of life and reducing costs for national health systems.

5.2 Monitoring of volatile compounds in human breath during oral glucose tolerance test

The possibility of diagnosing diabetes mellitus by volatile compounds in exhaled breath is actively investigated by many researchers. Several breath metabolites, for example acetone [267, 268, 269], isoprene [270], ethanol [271] and methyl nitrate [272, 273], have been investigated for this purpose, however inconsistent data have been reported.

A protocol was defined to test the hypothesis of different breath compositions between healthy and diabetics subjects during oral glucose tolerance tests (OGTTs).

Ubiquitous contamination by isopropanol is a major problem for breath analysis in hospital environment, as this compound is largely used in skin disinfectants. Furthermore, an enzymatic equilibrium exists in blood between this compound and acetone (Figure 5.9) [274], which is linked to lipolysis and is regulated by the concentration ratio of oxidized NAD (NAD^+) and reduced NAD (NADH).

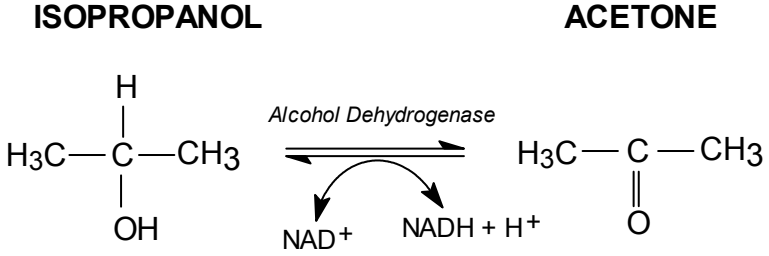

Figure 5.9 *Enzymatic equilibrium between acetone and isopropanol.*

A remarkable isopropanol contamination was identified in an early series of measurements by measuring the concentration levels of this compound in ambient air (Figure 5.10). Such contamination

was directly altering the concentration levels in breath and could also indirectly affect breath acetone levels by enzymatic conversion.

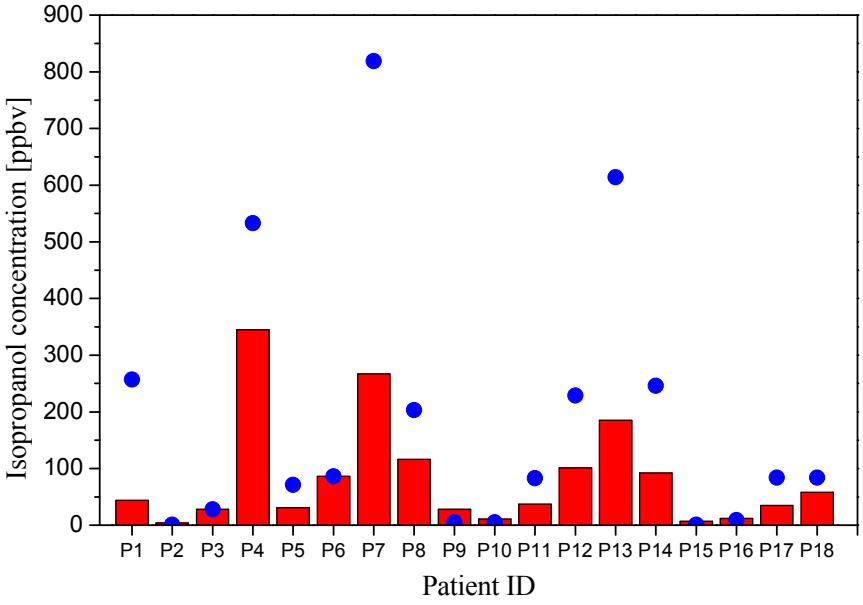

Figure 5.10 *Isopropanol: breath (bars) and ambient air (circles) concentrations.*

Breath sampling was carried out in a dedicated isopropanol free room during OGT tests and room air was analyzed periodically to confirm contamination free status.

Room air samples were collected by a gas-tight cylindrical glass vessel containing a Nalophan bag. A first connector through the vessel lid allowed to connect the bag to the outside, whereas a second connection allowed to connect a pump sucking the air between bag and vessel wall. The decrease of pressure caused by the pump allowed to inflate the bag with room air. After collection, room air samples were transferred from the bag into the adsorption tube and analyzed with the same procedure of breath samples.

Sixteen subjects undergoing OGTT, 6 males and 10 females aged between 35 and 76 years, were enrolled at the Institute of Clinical Physiology (CNR, Pisa, Italy).

Mixed expired breath samples were collected by asking the subjects to blow up a Nalophan bag. Collections were carried out in the morning after a 12 hours fasting, just before glucose administration (Time 0) and then every 30 minutes, in correspondence to the blood drawings for the measurement of glycemia.

Breath and room air samples were treated as described into paragraph 4.1.4 and analyzed according to the methods reported in Table 3.2.

Acetone breath and blood glycaemia concentration values over time measured in pathological and healthy subjects are reported in Figure 5.11.

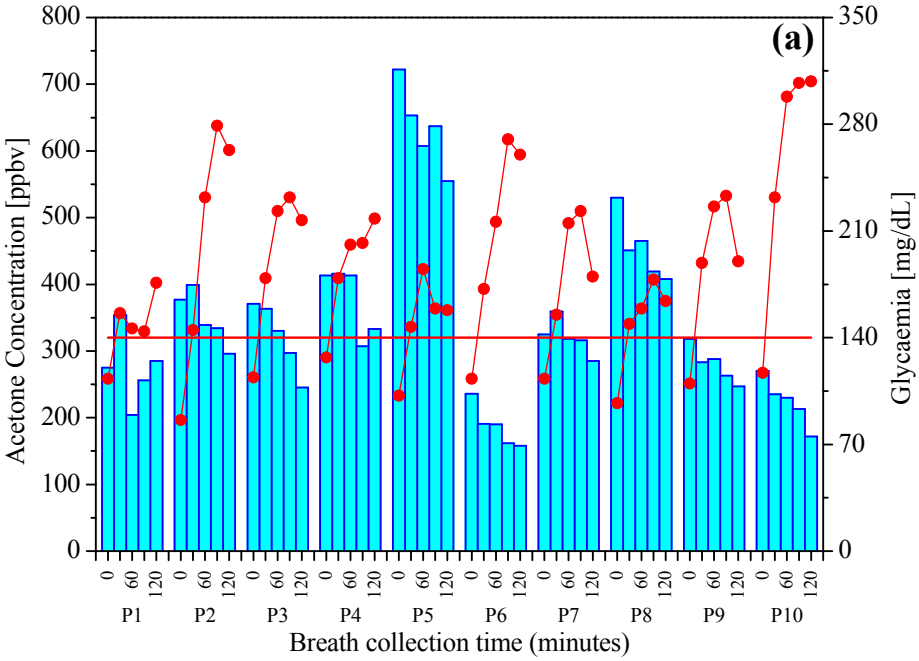

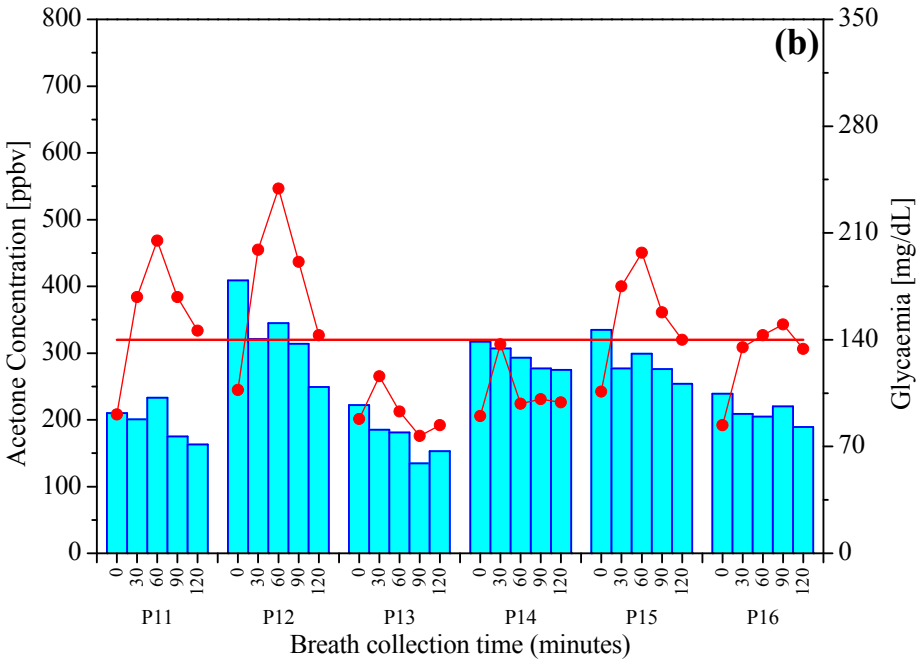

Figure 5.11 *Breath acetone concentrations (bars) and blood glycemia (dots) during OGTT: pathological subjects* (a) *and healthy subjects* (b).

A steady decrease of acetone concentration following the administration of glucose was observed in all subjects. Such decrease is likely the effect of glucose assumption, which shifts metabolism from lipolysis to glycolysis. Lipolysis, i.e. the breakdown of lipids, involves the hydrolysis of triglycerides into free fatty acids followed by further degradation into acetyl units by beta oxidation. This process produces ketones, so the initial high level of acetone is due to the fasting state before test. As glucose is delivered, the acetone production is slowed down and the amount lost in breath is not replaced, giving rise to a decrease in concentration.

No correlation was found between acetone and glycemia trend during OGTT, but the results have shown the capacity of the procedure to appreciate small variation in breath composition, in consequence of the glucose administration.

Analyzing exhaled breath composition during OGT test, we noted the presence of two compounds, namely 3-hydroxy butan-2-one (acetoin) and butane-2,3-dione (diacetyl), that are absent or at very low concentration during fasting state and increase following the glucose administration.

Figures 5.12 and 5.13 show illustrative examples of 3-hydroxy butan-2-one and butane-2,3-dione breath concentration values (of six subjects) during OGT test.

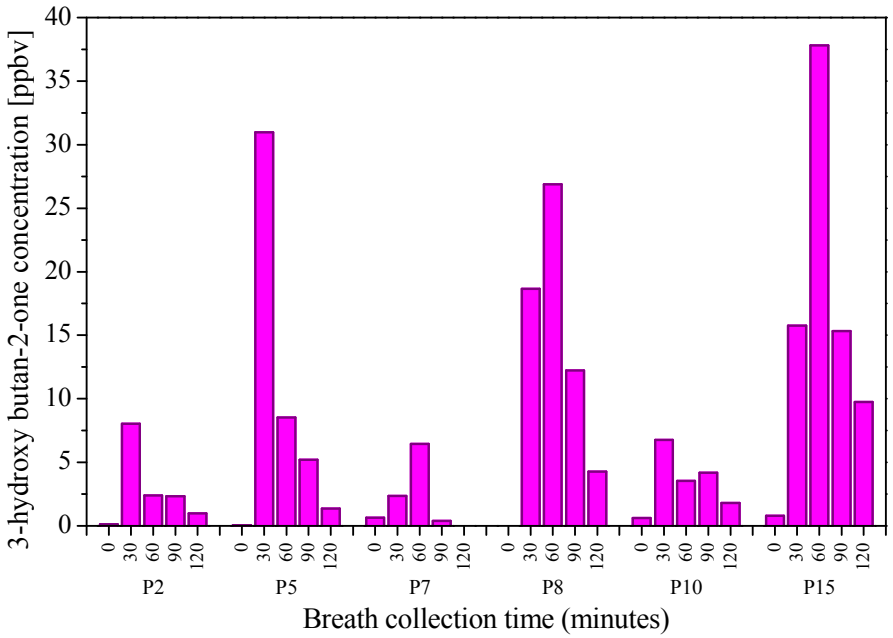

Figure 5.12*Breath 3-hydroxy butan-2-one concentrations during OGT test.*

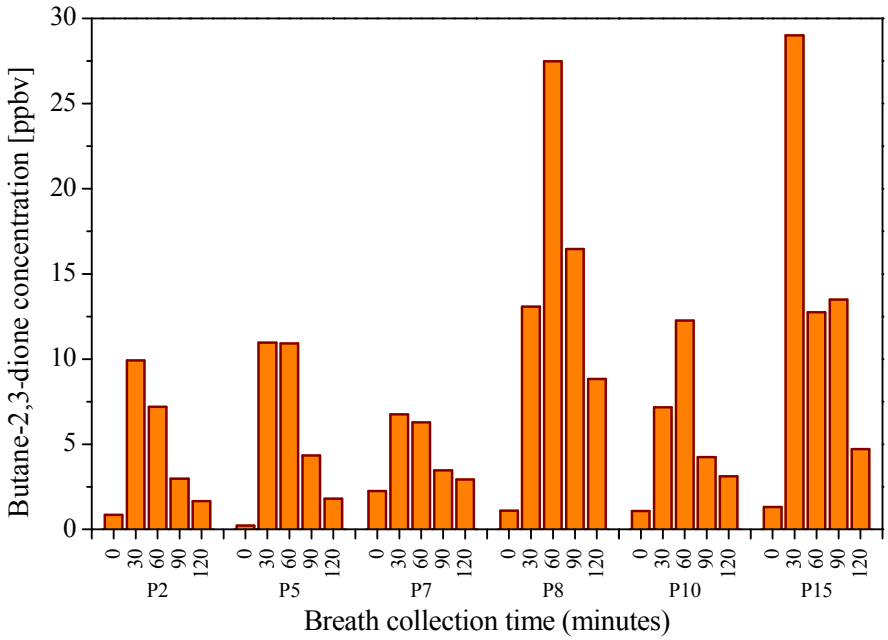

Figure 5.13 *Breath butane-2,3-dione concentrations during OGT test.*

These two compounds are not present in metabolism of humans but shown in glucose metabolic pathways of bacteria [275, 276].
Figure 5.14 shows a schematic detail of the butanoate metabolic pathway, where acetoin and diacetyl are involved: in the case of humans, the path stops at the EC 1.2.4.1 (pyruvate dehydrogenase) enzyme while in the case of bacteria continues with EC 2.2.1.6 (acetolactate synthase), EC 4.1.1.5 (acetolactate decarboxylase) and EC 1.1.1.303 (dyacetyl reductase) enzymes.

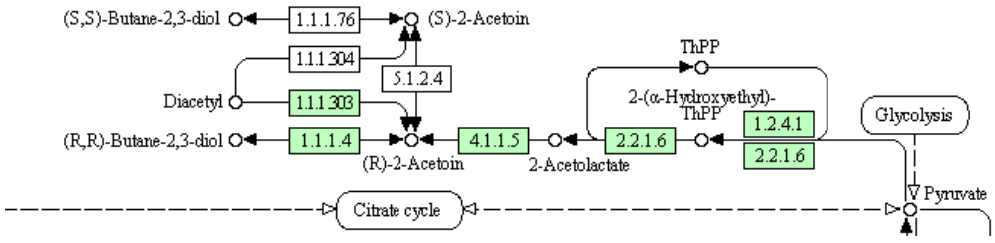

Figure 5.14 *Schematic butanoate metabolism.*

We can thus hypothesized a possible origin of these two compounds due to a catabolism of glucose performed by bacteria

present inside mouth or gut of the subjects and activated during the test.

5.3 Kinetic post-operative elimination of sevoflurane anaesthetic and hexafluoroisopropanol metabolite as measured in exhaled breath

This study was approved by Ethical Committee of Pisa University Hospital. Aim of the study was the development of pharmacokinetic models relevant to the elimination kinetics of sevoflurane and its metabolite hexafluoroisopropanol (HFIP) in the exhaled breath of patients undergoing various surgeries. Since sevoflurane conversion to HFIP happens in the liver, this would be a first step towards investigating the possibility of a non-invasive monitoring of the liver function in case of liver transplants.

Six patients with a supposedly healthy liver undergoing a variety of surgeries were recruited at Pisa hospital (Operative Unit of Medicine and Surgery, Azienda Ospedaliero Universitaria Pisana). Table 5.1 provides a summary of personal and clinical information for these patients, including gender, age, height, body weight, body mass index, type of surgery, duration of surgery, and total dose of anaesthetic.

The total dose of anaesthetic delivered to the patients was estimated by recording the ventilation data and sevoflurane input/output concentration values in the endotracheal tube. No HFIP measurements could be carried out during surgery.

Table 5.1 *Summary of personal and clinical information concerning the patients.*

Personal data					
ID	**Genger**	**Age**	**Height (m)**	**Body weight (Kg)**	**Body Mass Index (Kg/m²)**
1	M	73	1.68	80	28
2	F	67	1.63	53	20
3	F	69	1.65	77	28
4	F	72	1.64	75	28
5	M	73	1.70	80	28
6	M	74	1.77	92	29
Clinical data					
ID	**Type of surgery**	**Duration of surgery (h)**	**Estimated dose of anaesthetic (g)**		
1	Descending colectomy	3	18.9		
2	Distal pancreatectomy	2.7	19		
3	Adrenalectomy and splenectomy	4.1	10.8		
4	Bowel resection with colostomy	6.3	41.1		
5	Gastrectomy	4.4	34.1		
6	Lower anterior resection	8.7	78.4		

Post-operative breath samples were collected for up to 6 days by asking the subjects to inflate Nalophan bags. Collection times were the patient's awakening, the morning and afternoon of the two days following surgery, and mornings from the third day on. Sample analysis was performed as soon as possible, in any case within two hours from sampling. Breath samples were treated as described into paragraph 4.1.4 and then thermally desorbed and analyzed according to the methods reported in Table 3.2.

Post-operative breath concentrations of sevoflurane and HFIP are reported in Figures 5.15 and 5.16 respectively.

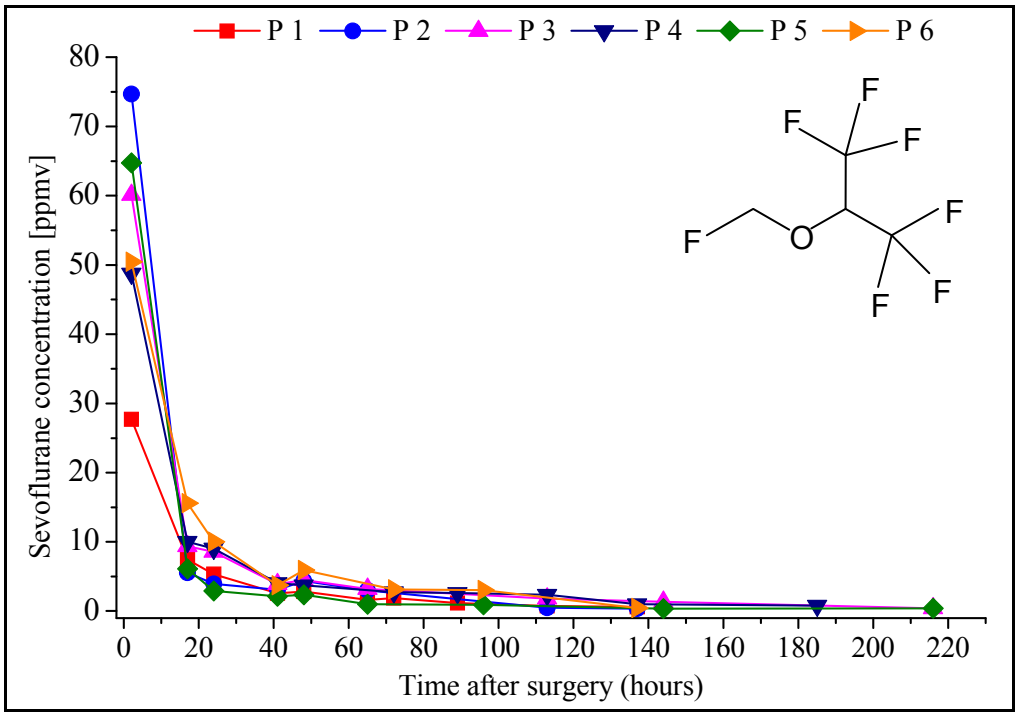

Figure 5.15 *Post-operative sevoflurane concentrations in the exhaled breath of patients after various surgeries.*

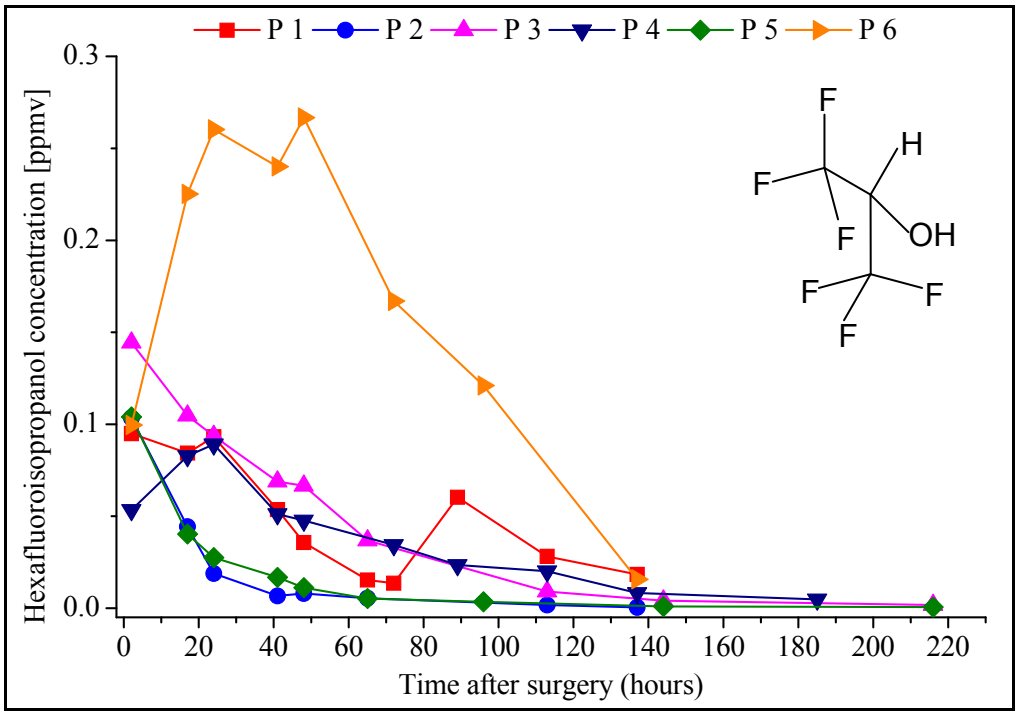

Figure 5.16 *Post-operative HFIP concentrations in the exhaled breath of patients after various surgeries.*

A rapid wash-out of sevoflurane within 24 hours was observed in all the patients, whereas the post-operative HFIP concentration profiles in breath were more varied. Such variability may be associated to the possible genetic heterogeneity of hepatic metabolic pathways (uridine diphosphate glucuronosylltransferase (UDPGT), cytochrome CYP 2E1) and/or to different dose of anaesthetic (higher doses could simply take longer to be eliminated). A fast pulmonary clearance of the anaesthetic is mirrored by a slightly slower wash-out of the metabolite.

A generic classical pharmacokinetic model based on the approximated breath data was developed thanks to the collaboration with prof. Pleil of the University of North Carolina. The method is based on work previously developed by Pleil et al. [277] for assessing the environmental exposure to methyl tertiary butyl ether (MTBE) and the elimination of the primary metabolite tertiary butyl alcohol (TBA).

The first data set comprised values from Kharasch et al. [278]. These subjects were nominally healthy non-smokers, with normal indexes for liver and renal function, who underwent elective surgeries and were under sevoflurane anaesthesia for 3 hours. Empirical data of blood measurements were estimated from graphs and discussions in the available literature [278, 279]. They are presented in Table 5.2 both in the original units of μM in plasma and in converted units of expected concentrations in exhaled breath.

Table 5.2 *Literature values and unit conversion for sevoflurane uptake and sevoflurane and HFIP elimination produced from Kharasch et al. [278] and Bourdeaux et al. [279].*

Time (hrs)	Sevoflurane blood (µM)	HFIP total blood (µM)	(Estimated) HFIP free blood (µM)	(Approx.) Sevoflurane breath (ppmv)	(Approx.) HFIP breath (ppmv)
0	0	0	0	0	0
0.1	400			14892	
1	650	14	2.1	24200	56
2	700	21	3.15	26062	85
3	700	29	4.35	26062	117
4	190	26	3.9	7074	105
5	120	45	6.75	4468	182
6	70	33	4.95	2606	133
7	60	42	6.3	2234	169
9	43	33	4.95	1601	133
11	33	34	5.1	1229	137
12		33	4.95		133
24		23	3.45		93
36		17	2.55		69
48		12	1.8		48
60		7	1.05		28
72		5	0.75		20

For sevoflurane, we used the accepted value 0.65 for blood/breath partition coefficient [279] and the near body temperature approximation of 24.2 liters/mole of an ideal gas. For HFIP, we first converted the total HFIP measurements into the expected free HFIP partition (see column 3) that is available for pulmonary elimination as discussed by Bourdeaux et al. [279]. The blood/breath ratio for HFIP is not available in the literature. We estimated a value of 6.0 based on ratios of sevoflurane/HFIP in plasma from Kharasch compared to sevoflurane/HFIP ratios in

breath observed by us. The resultant calculated breath concentrations, expressed as ppmv in air, are given in columns 5 and 6. We note that these approximations serve only as scaling factors and so do not affect the shape of the graphs or the subsequent models.

A second set of empirical data of blood measurements are estimated from graphs and discussions from Yasuda et al. [280] and are presented in Table 5.3. These data do not include values for the metabolite HFIP and so are only useful for validating the uptake and elimination kinetics of sevoflurane itself. In these experiments, the researchers used seven healthy male volunteers (age 23 ± 3 yrs) and administered 1% sevoflurane gas for 30 minutes. Data are expressed as a ratio of end tidal exhalation and administered concentrations; for consistency with Table 5.2, we have converted the data into ppmv in the last column of Table 5.3.

Table 5.3 *Literature values and unit conversion for sevoflurane uptake and elimination from Yasuda et al. [280].*

Time (hrs)	Sevoflurane Fa/Fi	Sevoflurane Fa/Fa0	Sevoflurane (ppmv)
0.000	0		0
0.013	0.46		4600
0.017	0.55		5500
0.025	0.64		6400
0.033	0.68		6800
0.050	0.72		7200
0.083	0.75		7500
0.125	0.78		7800
0.167	0.79		7900
0.208	0.8		8000
0.250	0.81		8100
0.333	0.82		8200
0.417	0.835		8350
0.483	0.84		8400
0.517		0.4	3360
0.625		0.1	840
0.833		0.06	504
1.167		0.032	269
1.500		0.02	168
2.000		0.012	101
2.500		0.01	84
24.000		0.007	59

The model is developed for sevoflurane using three empirical compartments: a first “central” compartment (blood), a second compartment (HPT - highly perfused tissues), and a third compartment (PPT - poorly perfused tissues) (Figure 5.17). The metabolite is tracked using one or two compartments as the empirical data dictate; the rate constant Ko is in units of

mass/time, the rate constants labelled as K_i's) are in units of 1/time, C1 and C2 are in units of 1/time and represent all unrecovered losses including those via exhaled breath. Furthermore, the concentrations in the various compartments automatically reflect their respective hypothetical volumes of distribution because we have access to experimental concentration data. We note that blood concentrations are considered directly proportional to breath concentrations under the assumptions of linear kinetics for both sevoflurane and HFIP, respectively. The conceptual diagram is shown in Figure 5.17.

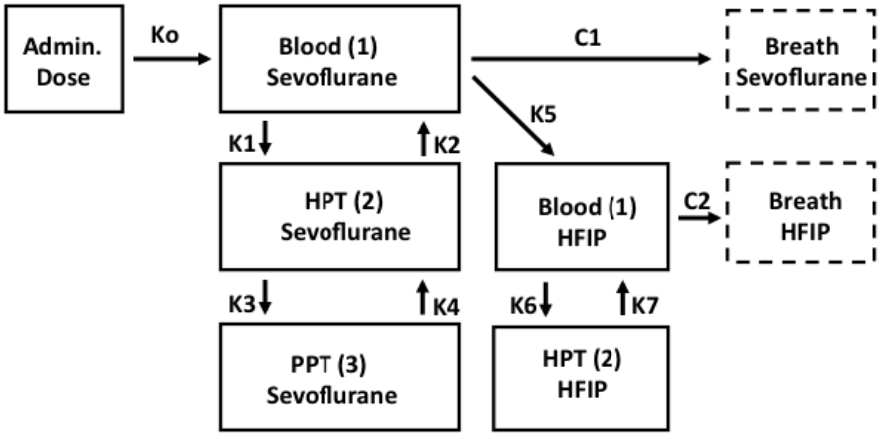

Figure 5.17 *Conceptual model for sevoflurane absorption (administration), distribution, metabolism and elimination (ADME). Model assumes linear kinetics (rates independent of concentration) and proportional elimination via breath. Annotated arrows represent rate constants and the boxes represent concentrations of the respective compounds. Note that C1 and C2 represent losses to breath plus other unknown loss pathways.*

Calculational model

Based on the concepts of linear kinetics and the diagram in Figure 5.17, we write difference equations to calculate the concentrations in each of the compartments as an incremental function of time:

$$C_{Blood\ Sev}(t+\Delta t) = C_{Blood\ Sev}(t) + \Delta t\cdot(C_a\cdot K_o) - \Delta t\cdot[(C1+K1+K5)\cdot C_{Blood\ Sev}(t)] + \Delta t\cdot[K2\cdot C_{HPT\ Sev}(t)] \quad (5.1)$$

$$C_{HPT\ Sev}(t+\Delta t) = C_{HPT\ Sev}(t) + \Delta t\cdot[K1\cdot C_{Blood\ Sev}(t) + K4\cdot C_{PPT\ Sev}(t)] - \Delta t\cdot[(K3+K2)\cdot C_{HPT\ Sev}(t)] \quad (5.2)$$

$$C_{PPT\ Sev}(t+\Delta t) = C_{PPT\ Sev}(t) + \Delta t\cdot[K3\cdot C_{HPT\ Sev}(t) - K4\cdot C_{PPT\ Sev}(t)] \quad (5.3)$$

$$C_{Blood\ HFIP}(t+\Delta t) = C_{Blood\ HFIP}(t) + \Delta t\cdot[K5\cdot C_{Blood\ Sev}(t) + K7\cdot C_{HPT\ HFIP}(t)] - \Delta t\cdot[(K6+C2)\cdot C_{Blood\ HFIP}(t)] \quad (5.4)$$

$$C_{HPT\ HFIP}(t+\Delta t) = C_{HPT\ HFIP}(t) + \Delta t\cdot[K6\cdot C_{Blood\ HFIP}(t) - K7\cdot C_{HPT\ HFIP}(t)] \quad (5.5)$$

Subsequently, under the assumptions that the breath concentrations are proportional (via blood/breath partition coefficients) to the blood concentrations, we calculate:

$$C_{Breath\ Sev}(t) = 0.65\cdot C_{Blood\ Sev}(t) \quad (5.6)$$

and

$$C_{Breath\ HFIP}(t) = 6.0\cdot C_{Blood\ HFIP}(t) \quad (5.7)$$

where the C(t)'s denote concentrations, the subscripts identify the compartments and the compounds, and the K_i's and C_i's denote time constants as described in the previous section. The equations can be quickly implemented using spreadsheet software such as Excel (Microsoft, Seattle, WA). The partition estimates are linear functions and so any uncertainty is adjusted during the model fine-tuning procedure through the adjustment of a single scaling parameter.

Methods for estimating initial parameters

The incremental equations are quantified using reasonable estimates for rate parameters that are then adjusted to fit over the

empirical data. Typically, the first step is to estimate the initial uptake rate parameter (Ca · Ko) using Eq. 5.1 above. The initial conditions are that concentrations throughout the body are zero at time = 0 and we rearrange the equation setting $C_{bloodSev}(t)$ and $C_{HPTSev}(t)$ to be very close to zero, and solve for an estimate of the initial slope:

$$C_a \cdot K_o \approx [C_{Blood\ Sev}(t+\Delta t) - C_{Blood\ Sev}(t)]/\Delta t \quad (5.8)$$

which can be empirically evaluated using the earliest (uptake) data points available. Given this initial estimate for the uptake parameter and an empirical estimate for the steady state concentration from data observation, we can estimate the initial half-life in the first compartment using a re-arrangement of equation 1 from above and the understanding that the slope of the curve is zero:

$$[C_{Blood\ Sev}(t+\Delta t) - C_{Blood\ Sev}(t)]/\Delta t = 0 = (C_a \cdot K_o) - [C1+K1+K5] \cdot C_{Blood\ Sev}(t) + [K2 \cdot C_{HPT\ Sev}(t)] \quad (5.9)$$

And therefore:

$$(C_a \cdot K_o) = [C1+K1+K5] \cdot C_{Blood\ Sev}(t) - [K2 \cdot C_{HPT\ Sev}(t)] \quad (5.10)$$

This is further reduced with the assumption that $[K1 \cdot C_{bloodSev}(t)] \approx [K2 \cdot C_{HPTSev}(t)]$ at steady state conditions leaving the approximation:

$$(C_1 + K5) \approx (C_a \cdot K_o)/C_{Blood\ Sev}(t=ss) \quad (5.11)$$

where $C_{bloodSev}(t=ss)$ is the steady state concentration and (Ca · Ko) has been estimated in Eq. 5.8.

Starting with these basic estimates from empirical data, we can construct the initial model that can then be further empirically refined with trial and error for the second and third compartments as well as the metabolite parameters.

Initial model construction

The ppmv estimated data from Kharasch et al. (Table 5.2) was used to develop the sevoflurane and HFIP incremental models using the approach presented in the methods section. The initial estimate for sevoflurane uptake (Ca + Ko) was 2482 ppm/min, the steady state concentration estimate in exhaled breath is 26,062 ppmv, and the initial elimination rate estimate (C1 + K5) is 0.0952 using methods explained above. Subsequently, higher compartments were empirically fitted and initial estimates modified to account for approximations; Figure 5.18 (a) shows data overlaid onto the model. The two-compartment HFIP data were subsequently modelled by trial and error, and the data vs. model comparison is shown in Figure 5.18 (b).

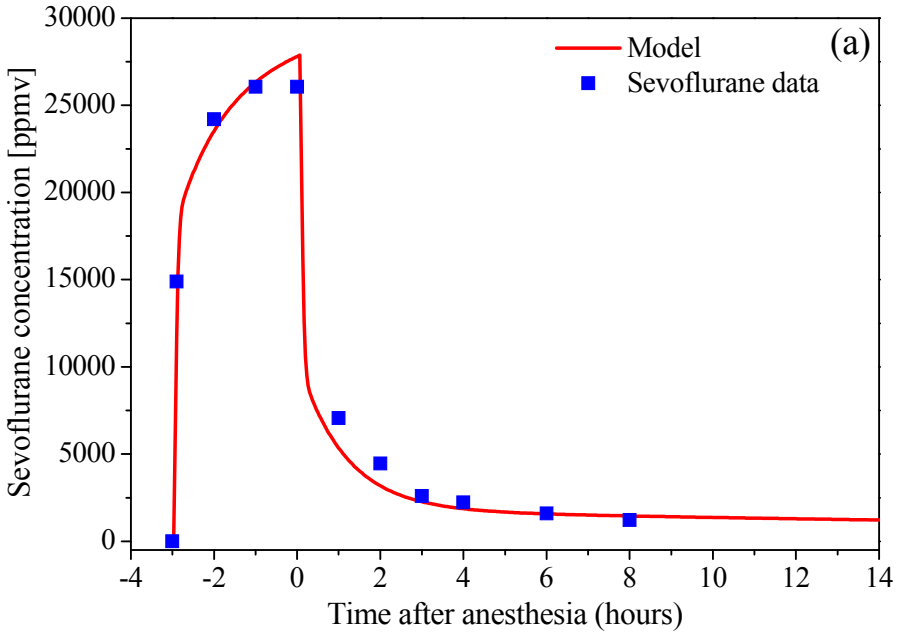

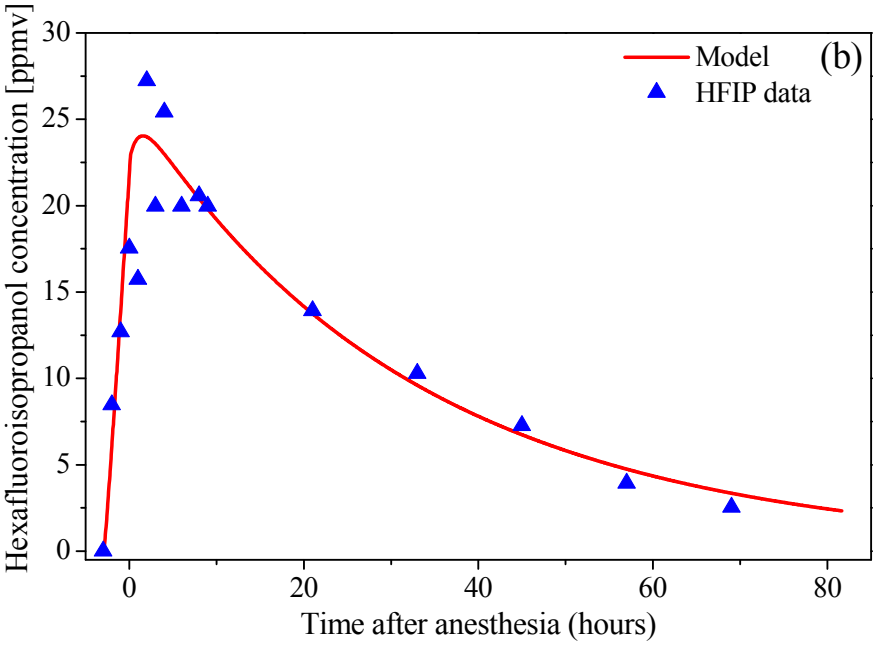

Figure 5.18 *Empirical breath data from Table 5.2* [278]. *3 hours anesthesia of 6 subjects overlaid onto fitted incremental models; sevoflurane* (a) *and HFIP metabolite* (b) *concentration in exhaled breath. Time scales (x-axes) are set to accommodate available data.*

We see that both models represent the respective data sets well over a long time frame. We note that there is a great deal of variability in the HFIP measurements early in the post-anaesthesia period and so the model was fitted among these points and may not necessarily represent any specific individual.

Model application: Yasuda data

To test the assumption that the sevoflurane model (and by inference, the HFIP model) are both subject to linear kinetics, we apply the existing model from above to the completely independent data from Yasuda et al. [280] as shown in Figure 5.19. The only adjustment is for the different administered sevoflurane concentration (10,000 ppmv) and shorter administration time (30 min). Here we see that the model slightly under-predicts speed of uptake, and also under-predicts speed of elimination, but overall shape and levels are consistent with other data. We attribute this

apparent higher pulmonary efficiency to the pre-selection of healthy young subjects (mean age 23 yrs) and the fact that they did not undergo invasive surgery. In contrast, the patients from Table 5.2 upon which the model was constructed, all had invasive, albeit elective surgery and ranged up to 80 yrs. in age.

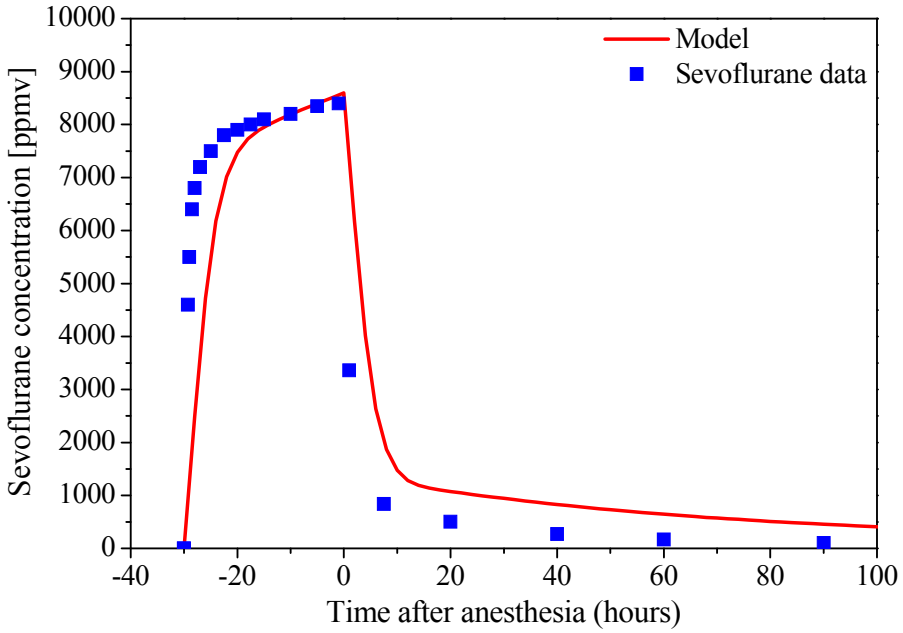

Figure 5.19 *Original model based on Table 5.2 data applied to sevoflurane data from Table 5.3.*

These models were used to fit our data (Figures 5.20 and 5.21).

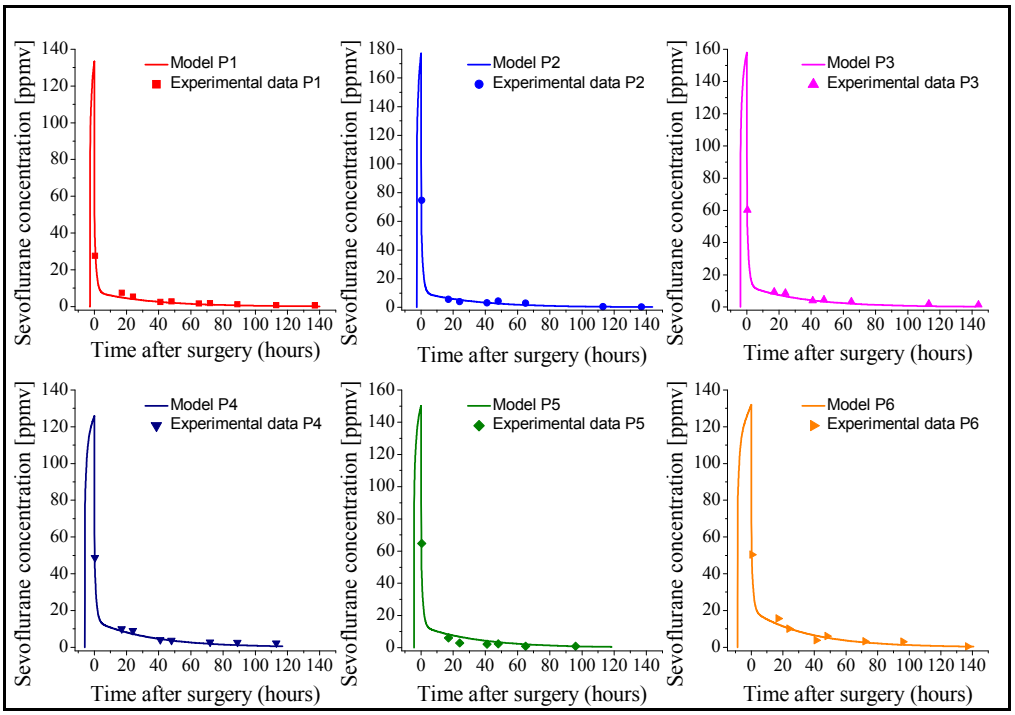

Figure 5.20 *Sevoflurane model and experimental breath data of 6 subjects undergoing different surgeries.*

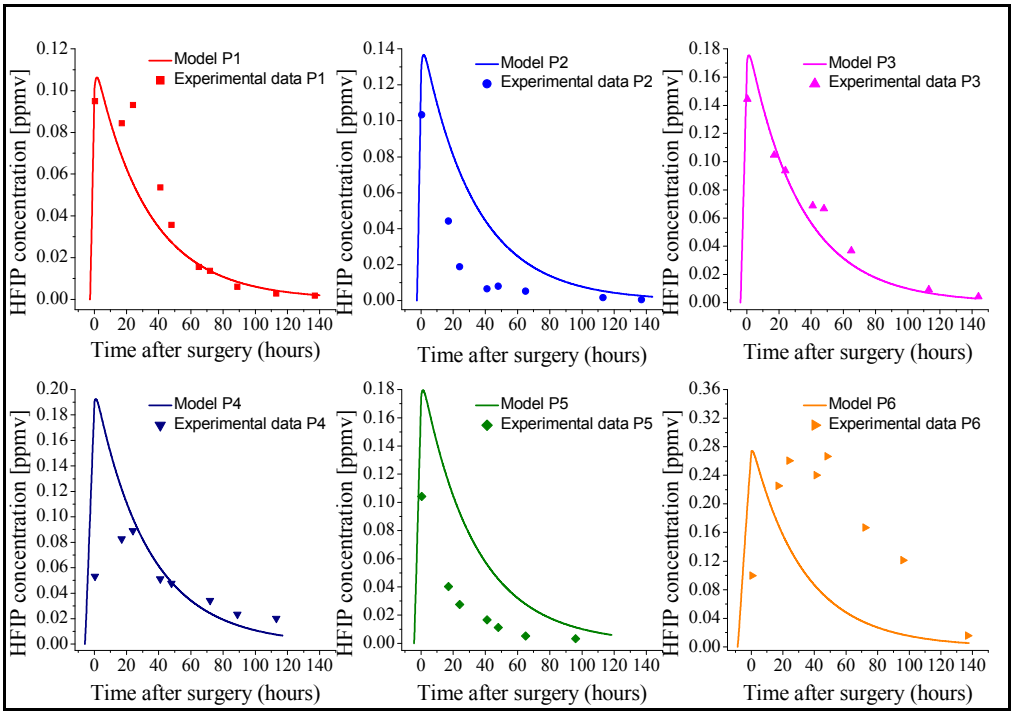

Figure 5.21 *Hexafluoroisopropanol model and experimental breath data of 6 subjects undergoing different surgeries.*

The sevoflurane elimination kinetics after surgery were consistent in all subjects, whereas the production and elimination of HFIP varied to some extent. We developed subject specific parameters for HFIP metabolism and interpreted the differences in the context of timing and dose of anaesthesia, type of surgery, and specific host factors including gender, age and physical parameters.
Subsequent studies will allow us to evaluate if such differences correlate with the clinical state, and in particular with the recovery of the liver function in case of liver transplants.

5.4 Monitoring of uremic toxins in spent dialysate

According to experts, filtration in dialysis is a mature technology which is not expecting large breakthroughs in the next 10-15 years. Despite of this, patient monitoring during the dialysis and the assessment of the dialysis dose are still at their infancy, notwithstanding the potential advantages in terms of quality of life and extension of the survival duration that tailored treatments could achieve. For this reason, the idea of a non-invasive real time monitoring of the efficiency of hemodialysis from the analysis of spent dialysate is very attractive. Many uremic toxins absorb in the UV region and the monitoring of UV absorbance was proposed as a possible tool for a non invasive evaluation of the dialysis dose [281, 282, 283, 284]. However, the relative contribution of the main uremic toxins to UV absorption is still not clear. Moreover, fluorimetric measurements on spent dialysate samples have never been reported in literature.

Aim of this study was to assess contributions of the main uremic toxins to UV absorbance and fluorimetric emission of spent dialysate, to estimate correlations among UV absorbance at specific

wavelengths and uremic toxin concentrations in dialysate and plasma, and to evaluate the possibility to build a model capable of predicting concentration values of these toxins in blood using spectrophotometric and/or spectrofluorimetric data.

Twenty-three patients, 16 males and 7 females aged between 41 and 88 years, were enrolled in this study after signing written informed consent. They were treated three times a week by standard bicarbonate hemodialyses (duration 210, 240 or 270 minutes) at the Operative Unit of Nephrology of the Azienda Ospedaliero Universitaria Pisana. Twelve patients were treated by a low-flux polysulfone membrane (F8, Fresenius, Homburg, K_{UF} = 1.8 mL/h/mmHg, Surface = 1.8 m^2), height patients were treated by a high-flux triacetate membrane (N190FH, Nipro, Japan, K_{UF} = 84.74 mL/h/mmHg, Surface = 1.9 m^2), and three patients were treated by a high-flux acrylonitrile and sodium methallyl sulfonate copolymer membrane (NEPH500, Gambro, Lund, K_{UF} = 65 mL/h/mmHg, Surface = 2.15 m^2).

Spent dialysate samples were collected 10, 30, 60, 120, 180 and 240 minutes after the beginning of the hemodialysis treatments. Blood samples were also collected before connecting the patient to the dialysis machine and 60, 120 and 240 min after the beginning of the dialysis session.

Aliquots of each spent dialysate sample were analyzed both by flow-injection and HPLC according to the experimental conditions reported in 3.6. Aliquots of each spent dialysate and blood samples were also analyzed in the laboratory of the clinic (Clinical chemical laboratory of the Azienda Ospedaliero Universitaria Pisana, AOUP) to determine the concentration of urea, uric acid, creatinine and β_2-microglobulin by standard methods.

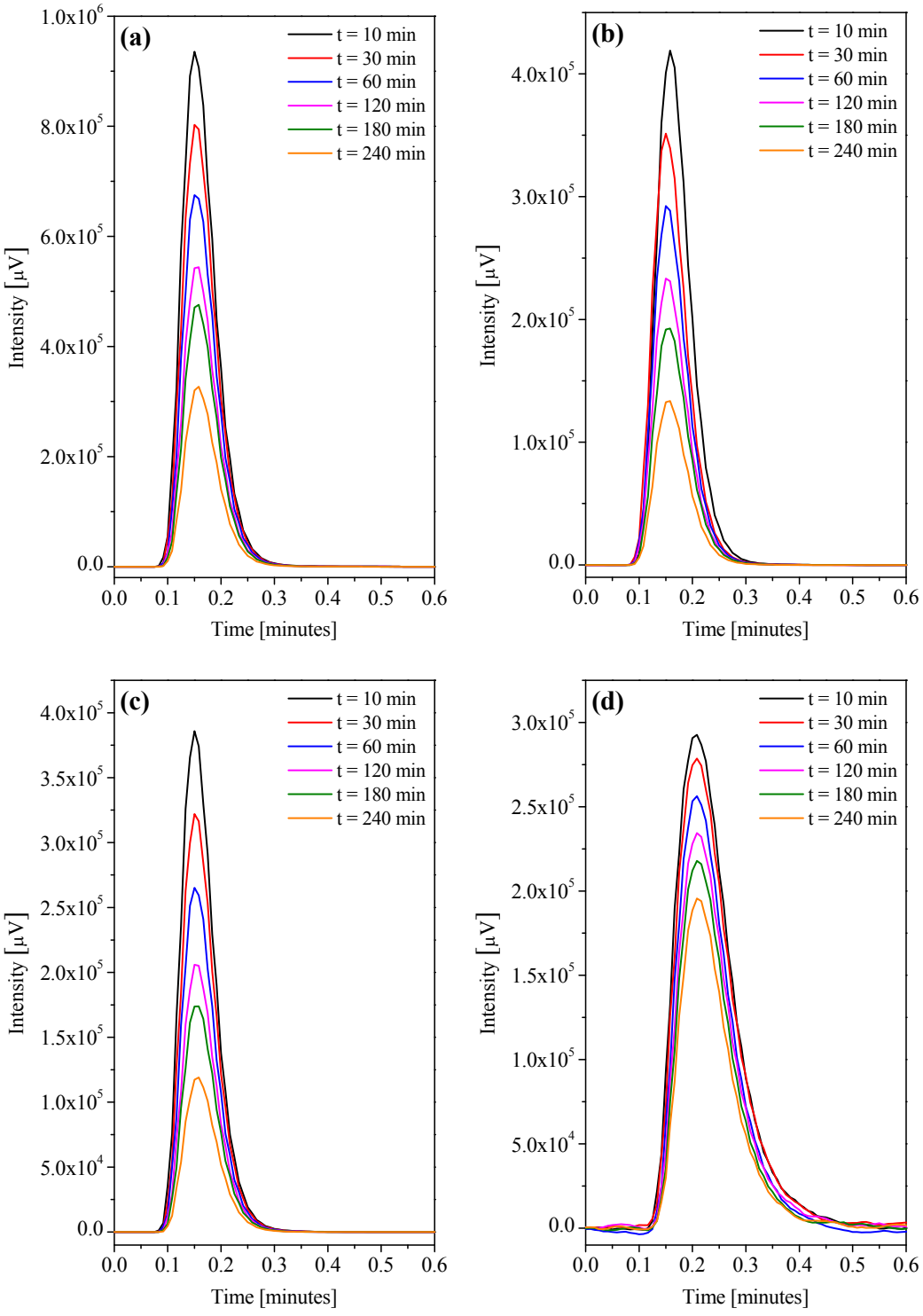

Figure 5.22 *Typical UV signals at λ_{abs} = 235 nm* (a), *λ_{abs} = 280 nm* (b), *λ_{abs} = 292 nm* (c) *and fluorescence signals at λ_{Exc} = 220 nm and λ_{Em} = 340 nm* (d) *obtained in spent dialysate at various sampling times.*

Figure 5.22 shows illustrative examples of UV and fluorescence signals at various sampling times. As expected, a monotonic decrease was observed in all signal intensities as dialysis went on due to the corresponding decrease of toxin concentrations in spent dialysate. The integration of the flow-injection signals relevant to spent dialysate samples collected at various times allowed to monitor the decay of signal intensity during treatment (Figure 5.23).

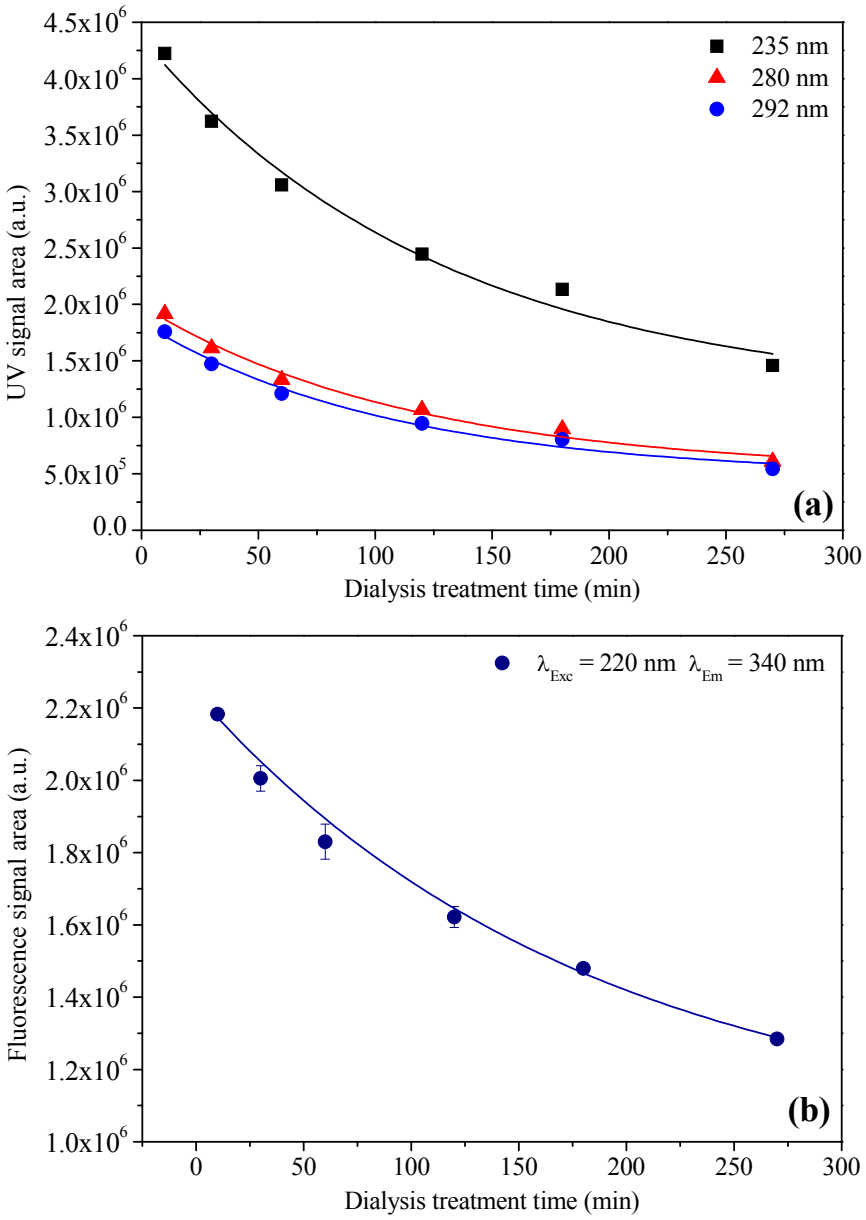

Figure 5.23 *UV absorption at λ_{abs} = 235, 280, 292 nm* (a) *and fluorescence emission at λ_{Exc} = 220 nm and λ_{Em} = 340 nm* (b) *of samples collected at different times during a dialysis session.*

Table 5.4 shows the correlations existing among data obtained with high-flux membranes. Similar values were obtained for all pairs of variables with low-flux membranes (with the exception of β_2-microglobulin, which cannot diffuse through these membranes).

Table 5.4 *Correlation coefficients among the variables relevant to high-flux membranes. UV absorption (λ_{abs} = 235, 280 and 292 nm) and fluorescence emission (λ_{Exc} = 220 nm, λ_{Em} = 340 nm) were measured by flow-injection analysis.*

Correlation coefficient (r)	**UV λ=235**	**UV λ=280**	**UV λ=292**	**Fluo λ=340**	**C_{SD} Urea**	**C_{SD} Uric acid**	**C_{SD} Crea**	**C_{SD} β2M**
UV λ=235	1	0.95	0.96	0.72	0.76	0.85	0.82	0.50
UV λ=280		1	0.93	0.75	0.75	0.84	0.77	0.51
UV λ=292			1	0.63	0.65	0.90	0.78	0.43
Fluo λ=340				1	0.73	0.64	0.74	0.67
C_{SD} Urea					1	0.67	0.86	0.47
C_{SD} Uric acid						1	0.85	0.62
C_{SD} Crea							1	0.64
C_{SD} β2M								1

The UV absorption data obtained at the three different wavelengths are highly correlated (correlation coefficients ≥ 0.93). Good correlations were also found among fluorescence emission and UV absorption data. In this case, the highest value was found between fluorescence emission and UV absorption at λ_{abs} = 280 nm (r = 0.75). This result confirms the hypothesis that the fluorescence signal is mainly due to amino acids (tryptophan, tyrosine,

phenylalanine), peptides and proteins, which have absorption bands at 280 nm.

Our findings also suggest that no additional information is obtained when more than one absorption wavelength is considered. Good correlations (correlation coefficients ≥ 0.67) also existed among the concentrations of the small molecules, i.e. urea, uric acid and creatinine, and among these variables and UV absorption at different wavelengths (correlation coefficients ≥ 0.65). The concentration of β_2-microglobulin, a small protein, showed its highest correlation coefficient (r = 0.67) with fluorescence emission. The correlation coefficients depict a scenario in which photometric and fluorimetric signals are likely due to the cumulative contribution of many different chemicals, which are all removed according to the same kinetics.

This is particularly true for small molecules. Figure 3.4 demonstrates that urea has no appreciable absorption in the range 200 – 600 nm, nevertheless its concentration values had good correlation with UV absorption data (correlation coefficients ≥ 0.65). β_2-microglobulin showed a slightly different behaviour when compared to the other molecules, but this can be easily explained with its different size. Correlations suggested that spectrofluorimetric data could be slightly more informative than UV absorption regarding its concentration values.

From the observations above, it appears that photometric and fluorimetric measurements of spent dialysate supply complementary information and have the potential for non-invasive real time monitoring of the efficiency of hemodialysis treatment.

The highest correlation coefficient (r = 0.90) reported in table 5.4 was found between the concentration of uric acid and UV absorption at λ_{abs} = 292 nm. Figure 5.24 shows the complete set of these data (23 dialysis sessions, 6 samples per session). Data

relevant to patients treated by a low-flux membrane are reported as red circles, whereas data of patients treated by a high-flux membrane are reported as blue circles. No remarkable differences can be observed among patients treated by a low or high-flux membranes.

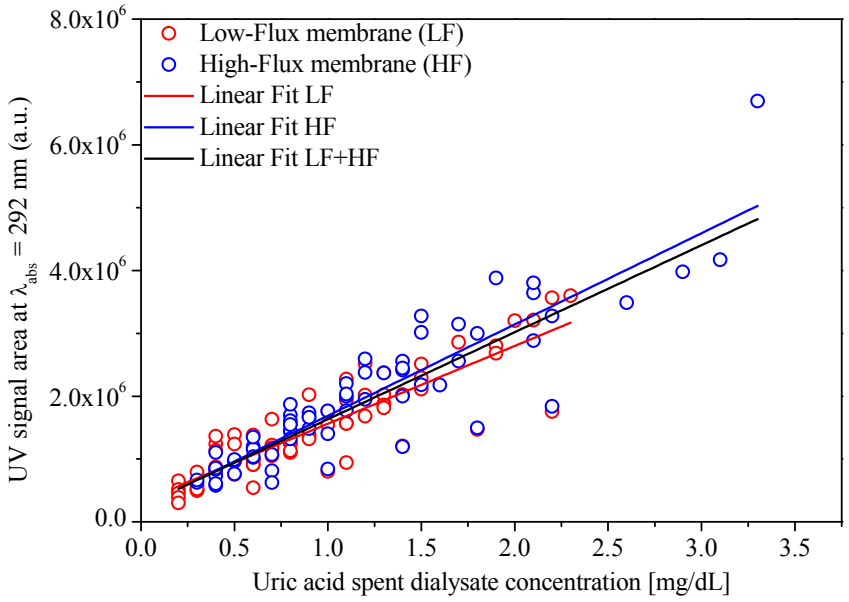

Figure 5.24 *UV absorption (λ_{abs} = 292 nm, flow-injection analysis) versus uric acid concentration in spent dialysate samples.*

The high value of this correlation coefficient suggests that uric acid may be responsible for an important fraction of UV absorption at 292 nm. To verify this hypothesis, the percentage contribution of each uremic toxin to the overall UV or fluorescence signal was estimated according to the following relation:

$$C_i\% = \frac{A_i}{A_{sample}}\% \qquad (5.12)$$

where A_i is the area of the peak of the *i^{th}-compound* calculated from its concentration value in spent dialysate sample and from its calibration curve (Figures 4.13 – 4.15), whereas A_{sample} is the area of the peak of the spent dialysate sample analyzed by flow-injection (which includes the contributions from all the components).

The average (among all patients) percentage contributions to the UV signal at different wavelengths of urea, creatinine, uric acid and β_2-microglobulin are reported in Table 5.5 together with the corresponding standard deviations. β_2-microglobulin was only present in samples collected from patients treated by high-flux membranes. Urea, creatinine, uric acid did not contribute to the overall fluorescence signal, whereas β_2-microglobulin's contribution was 0.2 % ± 0.1.

Table 5.5 *Average percentage contribution (C_i%) of selected uremic toxins to the overall UV absorption of spent dialysate samples at different wavelengths and corresponding standard deviation (±SD).*

	Percentage contribution (C_i %) ± SD		
Uremic toxin	**UV λ=235 nm**	**UV λ=280 nm**	**UV λ=292 nm**
Urea	0 %	0 %	0 %
Creatinine	20 % ± 10	3 % ± 2	3 % ± 2
Uric acid	30 % ± 10	60 % ± 30	80 % ± 20
β_2-microglobulin	0.3 % ± 0.2	0.2 % ± 0.1	0.2 % ± 0.1

Table 5.5 demonstrates that uric acid provides the most important contribution to the UV signal at 292 nm. Such high percentage suggests that this compound should be preferred to urea as marker of the efficiency of dialysis for small molecules. Since this conclusion conflicts with common belief of urea being responsible for UV absorption, further tests were carried out on uric acid and UV absorption at λ = 292 nm.

The concentrations of uric acid in samples collected from eight patients 10 and 240 minutes after the hemodialysis beginning were determined in our laboratory by calibrating the HPLC system and by spiking spent dialysate samples with standard working solutions (Paragraph 4.4.1).

These results were then compared to values obtained at the clinical chemical laboratory by biochemical methods (Table 4.13), obtaining a good agreement.

The maximum percentage deviation for all the samples was less than 10 % and one-way analysis of variance calculated a probability higher than 98% for the three datasets not to be significantly different. Such agreement proved that the HPLC system was correctly calibrated and indirectly confirmed the accuracy of the estimates of the average percentage contribution of uric acid to the overall signal. The spiking of uric acid to the spent dialysate samples allowed to confirm the identification of its peak within the chromatogram. Furthermore, the linearity of the calibration curve in dialysate samples and the coincidence of the slope value with the corresponding value of the calibration curve in standard working solutions allowed to exclude the existence of any notable matrix effect.

Table 5.6 shows the correlation coefficients between urea, creatinine, uric acid and β_2-microglobulin concentrations in spent dialysate samples (C_{SD}) and in plasma samples (C_{PI}) of all patients[1].

Table 5.6 *Correlation coefficients between spent dialysate and plasma concentrations data.*

Correlation coefficient (r)	**C_{PI} Urea**	**C_{PI} Creatinine**	**C_{PI} Uric acid**	**C_{PI} β2M**
C_{SD} Urea	**0.93**	0.76	0.68	0.27
C_{SD} Creatinine	0.63	**0.92**	0.64	0.44
C_{SD} Uric acid	0.62	0.70	**0.92**	0.50
C_{SD} β2M	0.25	0.51	0.43	**0.74**

[1] 23 dialysis sessions, 3 samples per session. β2-microglobulin was only evaluated in the 11 dialysis sessions with high-flux membranes. Its correlation coefficients with other variables only refer to such sessions.

Strict correlations between plasma and spent dialysate concentration data were observed for all toxins but not for β_2-microglobulin, whose correlation coefficient was remarkably lower than the other (but still quite high).
Good correlations also existed between plasma and dialysate concentrations of different toxins, with the usual exception of β_2-microglobulin.
These results once again indicated that all chemicals were removed according to the same kinetics, with β_2-microglobulin showing a slightly different behaviour.

The good agreement between plasma and dialysate data suggested us to compare the pre- to post-dialysis reduction ratio of urea in plasma (URR %) to uric acid reduction ratios estimated by flow-injection and biochemical analysis in spent dialysate and by biochemical analysis in plasma. The URR% is an important parameter widely used to quantify the effectiveness of the dialysis treatment.
The uric acid reduction ratio (UARR %) was calculated according to:

$$UARR\% = \frac{UA_{pre} - UA_{post}}{UA_{pre}}\% \qquad (5.13)$$

where UA_{pre} and UA_{post} are the pre- and post-dialysis uric acid concentration levels respectively. The existence of a transient phase at the dialysis beginning, due to the time needed to establish the proper fluxes of dialysis fluids as well as the physical equilibrium across the membrane, suggested us to consider, for spent dialysate datasets, the uric acid concentration in the samples collected at t = 10 minutes as UA_{pre}.

The good agreement found among urea and uric acid reduction ratios (Table 5.7) proofs that this molecule and spectrophotometric methods can be used to assess the effectiveness of treatment.

Table 5.7 *Uric acid reduction ratios in spent dialysate determined by flow- injection analysis (A) and by biochemical method (B). Uric acid reduction ratios (C) and urea reduction ratios (D) in plasma. Comparison between A and B, C, D.*

	Reduction Ratio (RR %)						
ID	**A**	**B**	**C**	**D**	**Percentage deviation A-B (%)**	**Percentage deviation A-C (%)**	**Percentage deviation A-D (%)**
P1	69	73	73	70	5	5	1
P2	49	50	71	67	2	31	27
P3	51	58	57	61	13	11	17
P4	58	50	67	75	-17	12	22
P5	53	60	63	56	11	16	5
P6	66	70	74	74	5	11	10
P7	85	79	72	63	-8	-19	-35
P9	74	77	78	81	4	6	10
P10	74	79	79	78	6	6	5
P11	73	76	76	74	4	4	1
P12	56	63	72	71	11	22	21
P13	72	73	77	79	2	7	9
P14	77	86	88	82	10	11	6
P15	74	79	80	78	6	8	5
P16	66	68	68	62	2	2	-8
P17	84	88	79	75	5	-6	-12
P18	73	77	77	76	5	5	3
P19	69	76	72	66	9	3	-5
P20	73	76	76	69	5	5	-6
P21	78	81	64	72	4	-20	-8
P22	73	75	78	82	3	6	12
P23	71	77	76	69	7	6	-3

In summary, excellent correlations were obtained between UV absorption at λ_{abs} = 292 nm and uric acid concentration in spent dialysate (r = 0.90, Table 5.4), and between uric acid concentration in spent dialysate and in plasma (r = 0.92, Table 5.6). Furthermore, we showed that uric acid provides the most important contribution to the UV absorption at λ_{abs} = 292 nm in spent dialysate (C_{UA} % = 75 %, Table 5.5). For this reasons, we used the complete set of data to build a linear model (Figure 5.25) estimating the uric acid concentration in plasma from the UV absorption data at λ_{abs} = 292 nm:

$$UA_{Pl}\ [mg/dL] = 1.57 \cdot 10^{-6}\ UV_{abs}\ [A.U.] + 0.75$$

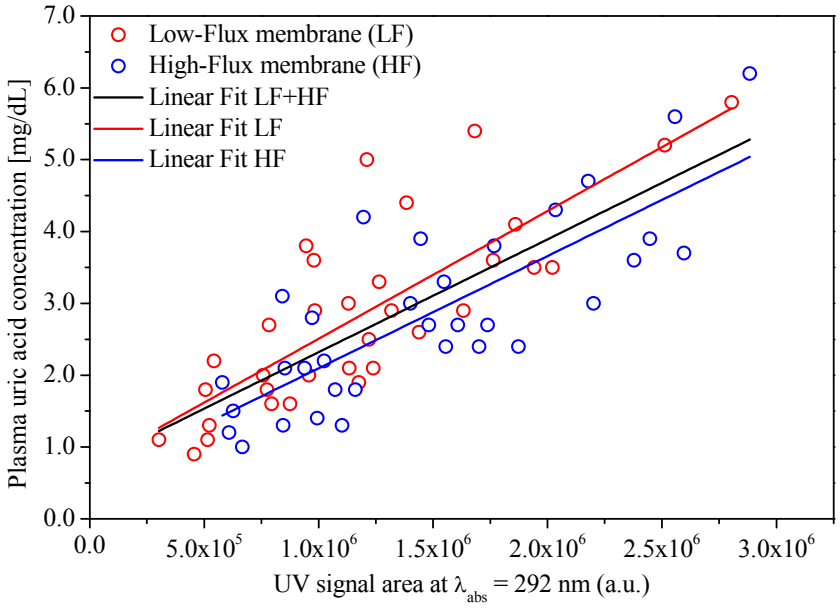

Figure 5.25 *Uric acid concentrations in plasma versus UV absorption at λ_{abs} = 292 nm. Data relevant to patients treated by low- and high-flux membrane are reported as red and blue circles respectively.*

The accuracy of prediction was estimated by "leave-one-out" cross-validation [285, 286, 287]. As the name suggests, leave-one-out cross-validation (LOOCV) involves using a single observation from the original sample as the validation data, and the remaining observations as the training data. This is repeated such that each

observation in the sample is used once as the validation data. This is the same as a K-fold cross-validation with K being equal to the number of observations in the original sample. Leave-one-out cross-validation is usually very expensive from a computational point of view because of the large number of times the training process is repeated.

Data from 22 dialysis sessions (3 data per session) were used to build the model (calibration set), then the uric acid concentrations predicted by the model from UV absorption data were compared to the actual data relevant to the remaining session (validation set). Such procedure was repeated for each session and an average percentage error in prediction of 26 % was calculated.

This result allows to be optimistic about the possibility of a real time non invasive monitoring of dialysis by spectrophotometric measurements in spent dialysate. More accurate predictions could likely be obtained by models built from single patient's data. Such models could represent a valid tool for clinicians to assess removal of uremic toxins and deliver personalized hemodialysis treatments.

CONCLUSIONS

Non traditional human fluids have been confirmed as useful sources of chemical information when making a diagnosis or monitoring a therapy, provided that reliable analytical methods are available.

A clinical study was performed, which involved 50 patients under oral anticoagulant therapy with warfarin. Warfarin concentration was determined in oral fluid samples using an optimized method based on HPLC with fluorimetric detection. The results demonstrated the existence of a pH-dependent correlation between oral fluid concentrations of warfarin and INR. If confirmed in a larger sample of cases, this result could represent a first step towards the development of non-invasive "point of care" systems for monitoring patients on anticoagulation therapy. Such an outcome would improve a patient's quality of life and increase the safety of anticoagulation therapies.

Chemical analysis of exhaled breath samples, which was performed using an optimized method based on thermal desorption gas chromatography and mass spectrometry was applied to the non-invasive monitoring of both endogenous volatile compounds during a oral glucose tolerance test, and sevoflurane and its metabolite (HFIP) after surgery. For the latter, a three-compartment pharmacokinetic model was developed and fitted to the post-operative sevoflurane and HFIP breath data. The results suggest that the elimination kinetics of sevoflurane and HFIP could potentially provide useful information on liver function in a non-invasive way for use in monitoring patients who have had liver transplants .

Spent dialysate samples collected at different times during the hemodialysis treatment of 23 patients were analyzed by spectrophotometric and spectrofluorimetric measurements at various wavelengths. A linear model was developed capable of predicting uric acid concentrations in blood from the absorbance of spent dialysate at 292 nm. This very promising result shows that the real time non-invasive monitoring of toxins removal is feasible, which would represent a valid tool for clinicians to deliver personalized hemodialysis treatments.

References

[1] Mandel ID. The role of saliva in maintaining oral homeostasis. *J Am Dent Assoc* 1989;119:298–304.

[2] Sreebny L. Saliva: its role in health and disease. *Int Dent J* 1992;42:291–304.

[3] Van Nieuw Amerongen AV, Veerman ECI. Saliva — the defender of the oral cavity. *Oral Dis* 2002;8:12–22.

[4] Van Nieuw Amerongen AV, Bolscher JG, Veerman ECI. Salivary proteins: protective and diagnostic value in cariology? *Caries Res* 2004;38:247–53.

[5] Lawrence HP. Salivary markers of systemic disease: non-invasive diagnosis of disease and monitoring of general health. *J Can Dent Assoc* 2002;68:170–4.

[6] Rindi G, Manni E. Fisiologia Umana, vol. 2, UTET, 2001.

[7] Carranza M, Ferraris ME, Galizzi M. Structural and morphometrical study in glandular parenchyma from alcoholic sialosis. *J Oral Pathol & Med* 2005;34:374–9.

[8] Hu S, Denny P, Denny P, et al. Differentially expressed protein markers in human submandibular and sublingual secretions. *Int J Oncol* 2004;25:1423–30.

[9] Ritschel WA, Tompson GA. Methods Find. Exp. Clin. Pharmacol. 1983;5:511–25.

[10] Chicharro JL, Lucia A, Perez M, Vaquero AF, Urena R. Saliva composition and exercise. *Sports Med* 1998;26:17–27.

[11] Lentner C. (Editor), Geigy Scientific Tables, 8th ed., Vol. 1, Ciba-Geigy, West Caldwell, NJ, 1981, pp. 114–22.

[12] Aps JKM, Martens LC. Review: the physiology of saliva and transfer of drugs into saliva. *Forensic Sci Int* 2005;150:119–31.

[13] Nagler RM, Hershkovich O, Lischinsky S, Diamond E, Reznick AZ. Saliva analysis in the clinical setting: revisiting an underused diagnostic tool. *J Investig Med* 2002;50:214–25.

[14] Yamaguchi M, Takada R, Kambe S, et al. Evaluation of time-course changes in gingival crevicular fluid glucose levels in diabetics. *Biomed Microdevices* 2005;7:53–8.

[15] Thaysen JH, Thorn NA, Schwartz IL. Excretion of sodium, potassium, chloride and carbon dioxide in human parotid saliva. *American Journal of Physiology* 1954;178:155-9.

[16] Booth RE, Johnson JP, Stockand JD. Aldosterone. *Adv Physiol Educ* 2002;26:8–20.

[17] Jensdottir T, Nauntofte B, Buchwald C, Bardow A. Effects of sucking acidic candy on whole-mouth saliva composition. *Caries Res* 2005;39:468–74.

[18] Walsh NP, Laing SJ, Oliver SJ, Montague JC, Walters R, Bilzon JLJ. Saliva parameters as potential indices of hydration status during acute dehydration. *Med Sci Sports Exerc* 2004;36:1535–42.

[19] Sato K, Kang WH, Saga K, Sato KT. Biology of sweat glands and their disorders. I. Normal sweat gland function. *J Am Academy of Dermatol* 1989;20:537-66.

[20] Jusko WJ, Milsap RL. Pharmacokinetic principles of drug distribution in saliva. *Annals New York Academy of Science* 1993;694:36-47.

[21] Marini A, Cabassi E. La saliva: approccio complementare nella diagnostica clinica e nella ricerca biologica. *Ann Fac Med Vet Parma* 2002;22:295–311.

[22] Haeckel R. Saliva, an alternative specimen in clinical chemistry. *J Int Fed Clin Chem* 1990;2:208-17.

[23] Haeckel R, Hänecke P. Application of saliva for drug monitoring. An in vivo model for transmembrane transport. *Eur J Clin Chem Clin Biochem* 1996;34:171-91.

[24] Meyer H. Arch Exp Pathol Pharmakol 1899;42:109.

[25] Meyer W, Hemmi H. Biochem Z 1935;272:39.

[26] Hansch C, Dunn WJ. Linear relationships between lipophilic character and biological activity of drugs. *J Pharmaceutical Sci* 1972;61:l-19.

[27] Mucklow JC, Bending MR, Kahn GC, Dollery CT. Drug concentration in saliva. *Clinical Pharmacology and Therapeutics* 1978;24:563-70.

[28] Matin SB, Wan SH, Karam JH. Pharmacokinetics of tolbutamide: prediction by concentration in saliva. *Clinical Pharmacology and Therapeutics* 1974;16:1052-8.

[29] Rasmussen F. Salivary excretion of sulphonamides and barbiturates by cows and goats. *Acta Pharmacologica et Toxicologica*. 1964;21:11-9.

[30] Kidwell DA, Holland JC, Athanaselis S. Testing for drugs of abuse in saliva and sweat. *Journal of Chromatography B* 1998;713:111-35.

[31] Sandin B, Chorot P. Changes in skin, salivary, and urinary pH as indicator of anxiety level in humans. *Psychophysiology* 1985;22:226-30.

[32] Navazesh M. Methods for collecting saliva. *Annals of the New York Academy of Sciences* 1993;694:72–7.

[33] Samyn N, Laloup M, De Boeck G. Bioanalytical procedures for determination of drugs of abuse in oral fluid. *Anal Bioanal Chem* 2007;388:1437–53.

[34] Gröschl M, Köhler H, Topf HG, Rupprecht T, Rauh M. Evaluation of saliva collection devices for the analysis of steroids, peptide and therapeutic drugs. *J Pharmaceut Biomed* 2008;47:478-86.

[35] Gallardo E, Queiroz JA. The role of alternative specimens in toxicological analysis. *Biomed Chromatogr* 2008;22:795-821.

[36] Langel K, Engblom C, Pehrsson A, Gunnar T, Ariniemi K, Lillsunde P. Drug Testing in Oral Fluid-Evaluation of Sample Collection Devices. *Journal of Analytical Toxicology* 2008;32:393- 401.

[37] Kintz P and Samyn N. Unconventional samples and alternative matrices. In *Handbook of Analytical Separations*, Vol. 2, Bogusz MJ (ed.). Elsevier Science: Amsterdam, 2000;459–88.

[38] Sunshine I, Sutliff JP, in Wong SHY and Sunshine I (Editors), Handbook of Analytical Therapeutic Drug Monitoring and Toxicology, CRC Press, Boca Raton, FL, 1997;253–64.

[39] Barnes AJ, Kim I, Schepers R, Moolchan ET, Wilson L, Cooper G, Reid C, Hand C and Huestis MA. Sensitivity, specificity, and efficiency in detecting opiates in oral fluid with the Cozart Opiate Microplate EIA and

GC-MS following controlled codeine administration. *Journal of Analytical Toxicology* 2003;27:402–7.

[40] Thieme D, Anielski P, Grosse J, Sachs H, Mueller RK. Identification of Anabolic Steroids in Serum, Urine, Sweat and Hair. Comparison of Metabolic Patterns. *Analytica Chimica Acta* 2003;483:299–306.

[41] Cooper G, Wilson L, Reid C, Baldwin D, Hand C, Spiehler V. Comparison of GC-MS and EIA results for the analysis of methadone in oral fluid. *Journal of Forensic Science* 2005b;50:928–32.

[42] Campora P, Bermejo AM, Tabernero MJ, Fernandez P. Use of gas chromatography/mass spectrometry with positive chemical ionization for the determination of opiates in human oral fluid. *Rapid Communications in Mass Spectrometry* 2006;20:1288–92.

[43] Quintela O, Andrenyak DM, Hoggan AM, Crouch DJ. A validated method for the detection of Delta 9-tetrahydrocannabinol and 11-nor-9-carboxy-Delta 9-tetrahydrocannabinol in oral fluid samples by liquid chromatography coupled with quadrupole time-of-flight mass spectrometry. *Journal of Analytical Toxicology* 2007;31:157–64.

[44] Pujadas M, Pichini S, Civit E, Santamarina E, Perez K, de la Torre R. A simple and reliable procedure for the determination of psychoactive drugs in oral fluid by gas chromatography–mass spectrometry. *Journal of Pharmaceutical and Biomedical Analysis* 2007;44:594–601.

[45] Mortier KA, Maudens KE, Lambert WE, Clauwaert KM, Van Bocxlaer JF, Deforce DL, Van Peteghem CH, De Leenheer AP. Simultaneous, quantitative determination of opiates, amphetamines, cocaine and benzoylecgonine in oral fluid by liquid chromatography quadrupole-time-of-flight mass spectrometry. *Journal of Chromatography B* 2002;779:321–30.

[46] Jones J, Tomlinson K, Moore C. The simultaneous determination of codeine, morphine, hydrocodone, hydromorphone, 6-acetylmorphine, and oxycodone in hair and oral fluid. *Journal of Analytical Toxicology* 2002;26:171–5.

[47] Wood M, Laloup M, Ramirez Fernandez MM, Jenkins KM, Young MS, Ramaekers JG, De Boeck G, Samyn N. Quantitative analysis of multiple illicit drugs in preserved oral fluid by solid-phase extraction and liquid

chromatography–tandem mass spectrometry. *Forensic Science International* 2005;150:227–38.

[48] Ngwa G, Frich D, Blum K, Newland G. Simultaneous analysis of 14 benzodiazepines in oral fluid by solid-phase extraction and LC-MS-MS. *Journal of Analytical Toxicology* 2007;31:369–76.

[49] Brunet BR, Barnes AJ, Scheidweiler KB, Mura P, Huestis MA. Development and validation of a solid-phase extraction gas chromatography-mass spectrometry method for the simultaneous quantification of methadone, heroin, cocaine and metabolites in sweat. *Anal Bioanal Chem* 2008;392:115–27.

[50] Concheiro M, Shakleya DM, Huestis MA. Simultaneous analysis of buprenorphine, methadone, cocaine, opiates and nicotine metabolites in sweat by liquid chromatography tandem mass spectrometry. *Anal Bioanal Chem* 2011;400:69–78.

[51] Follador MJD, Yonamine M, Silva RL. Detection of cocaine and cocaethylene in sweat by solid-phase microextraction and gas chromatography/mass spectrometry. *Journal of Chromatography B* 2004;811:37–40.

[52] Pragst F. Application of solid-phase microextraction in analytical toxicology. *Analytical and Bioanalytical Chemistry* 2007;388:1393–414.

[53] Boron WF, Boulpaep EL.. *Medical physiology*, Elsevier, 2005;598 pp.

[54] Paiva M. Gas transport in the human lung. *J Appl Physiol* 1973; 35:401-10.

[55] Schubert JK, Spittler KH, Braun G, Geiger K, Guttmann J. CO_2-controlled sampling of alveolar gas in mechanically ventilated patients. *Journal of Applied Physiology* February 2001;90:486-92.

[56] Cope KA, Watson MT, Forster A, Sehrnert SS, Risby TH. Effect of ventilation on the collection of exhaled breath humans. *J Appl Physiol* 2004;96:1371-9.

[57] Risby TH, Solga SF. Current status of clinical breath analysis. *Appl Phys B* 2006;85:421–6.

[58] Phillips M. Method for the collection and assay of volatile organic compounds in breath. *Anal Biochem* 1997;247:272–8.

[59] Schubert JK, Miekisch W, Birken T, Geiger K, Noeldge-Schomburg GFE. Impact of inspired substance concentrations on the results of breath analyses in mechanically ventilated patients. *Biomarkers* 2005;10:138-52.

[60] Basanta M, Koimtzis T, Singh D, Wilson I, Thomas CLP. An adaptive breath sampler for use with human subjects with an impaired respiratory function. *Analyst* 2007;132:153-63.

[61] Risby TH, Sehnert SS. Clinical application of breath biomarkers of oxidative stress status. *Free Radic Biol Med* 1999;27:1182–92.

[62] Plebani C, Tranfo G, Salerno A, Panebianco A, Marcelloni AM. An optimized sampling and GC-MS analysis method for benzene in exhaled breath as a biomarker for occupational exposure. *Talanta* 1999;50:409–12.

[63] Dyne D, Cocker J, Wilson H K. A novel device for capturing breath samples for solvent analysis. *Sci Total Environ* 1997;199:83–9.

[64] Hyšpler R, Crhov`a S, Gasparic J, Zadak J, Czkova Z, Balasova M. Determination of isoprene in human expired breath using solid phase microextraction and gas chromatography-mass spectrometry. *J Chromatogr B* 2000;739:183–90.

[65] Pleil JD, Lindstrom AB. Collection of a single alveolar exhaled breath for volatile organic compounds analysis. *Am J Ind Med* 1995a;28:109–21.

[66] Pleil JD, Lindstrom AB. Measurement of volatile organic compounds in exhaled breath as collected in evacuated electropolished canisters. *J Chromatogr B* 1995b;665:271–9.

[67] Pleil JD, Lindstrom AB. Sampling and analysis of exhaled human breath as an exposure assessment tool. *Proc Healthy Buildings* 1995;pp 507–11.

[68] Oliver KD, Pleil JD, McClenny WA. Sample integrity of trace level volatile organic compounds in ambient air stored in SUMMA polished canisters. *Atmospheric Environment* 1986;20:1403-11.

[69] McClenny WA, Pleil JD, Evans GF, Oliver KD, Holdren MW, Winberry WT. Canister-based method for monitoring toxic VOCs in ambient air. *Journal of the Air and Waste Management Association* 1991;41:1308-18.

[70] Lindstrom AB, Pleil JD. A review of the USEPA's single breath canister (SBC) method for exhaled volatile organic biomarkers. *Biomarkers* 2002;7:189-208.

[71] Deng C, Zhang J, Yu X, Zhang W, Zhang X. Determination of acetone in human breath by gas chromatography–mass spectrometry and solid-phase microextraction with on-fiber derivatization. *J Chromatog B* 2004;810:269–75.

[72] Steeghs MML, Cristescu SM, Munnik P, Zanen P, Harren FJM. An off-line breath sampling and analysis method suitable for large screening studies. *Physiol Meas* 2007;28:503–14.

[73] Mochalski P, Wzorek B, Sliwka I, Amann A. Suitability of different polymer bags for storage of volatile sulphur compounds relevant to breath analysis. *J Chromatog B* 2009;877:189-96.

[74] Gordon SM, Wallace LA, Pellizzari ED, O'Neill HJ. Human breath measurements in a clear-air chamber to determine half-lives for volatile organic compounds. *Atmos Environ* 1988;22:2165–70.

[75] Knutson MD, Lim AK, Viteri FE. A practical and reliable method for measuring ethane and pentane in expired air from humans *Free Radical Biol Med* 1999;27:560–71.

[76] Birken T, Schubert J, Miekisch W, Noeldge-Schomburg G. A novel visually CO2 controlled alveolar breath sampling technique *Technol Health Care* 2006;14:499–506.

[77] Di Francesco F, Loccioni C, Fioravanti M, Russo A, Pioggia G, Ferro M, Roehrer I, Tabucchi S, Onor M. Implementation of Fowler's method for end-tidal air sampling. *J Breath Res* 2008;2:1-10.

[78] Cao W, Duan Y. Current Status of Methods and Techniques for Breath Analysis. *Critical Reviews in Analytical Chemistry* 2007;37:3-13.

[79] Ligor T. Analytical Methods for Breath Investigation. *Critical Reviews in Analytical Chemistry* 2009;39:2-12.

[80] Phillips M, Herrera J, Krishnan S, Zain M, Greenberg J, Cataneo RN. Variation in volatile organic compounds in the breath of normal humans. *J Chromatog B* 1999;729:75–88.

[81] Miekisch W, Schubert JK. From highly sophisticated analytical techniques to life-saving diagnostics: technical developments in breath analysis. *TrAC* 2006;25:665-73.

[82] Phillips M. Breath test in medicine. *Sci Am* 1992;267:74-9.

[83] Gawlowski J, Gierczak T, Jeÿzo A, Niedzielski J. Adsorption of water vapour in the solid sorbents used for the sampling of volatile organic compounds. *Analyst* 1999;124:1553-8.

[84] Lord H, Yu Y, Segal A, Pawliszyn J. Breath Analysis and Monitoring by Membrane Extraction with Sorbent Interface. *Analytical Chemistry* 2002;74:5650-7.

[85] Sanchez JM, Sacks RD. On-line multi-bed sorption trap for VOC analysis of large-volume vapour sample: injection plug width, effects of water vapour and sample decomposition. *J Sep Sci* 2005;28:22-30.

[86] Belardi RP, Pawliszyn J. The application of chemically modified fused silica fibers in the extraction of organics from water matrix samples and their rapid transfer to capillary columns. *Water Poll Res J Canada* 1989;24:179-91.

[87] Vas G, Vekey K. SPME: a powerful sample preparation tool prior to mass spectrometric analysis. *J Mass Spectrom* 2004;39:233-54.

[88] Grote C, Pawliszyn J. Solid-phase microextraction for the analysis of human breath. *Anal Chem* 1997;69:587-96.

[89] Matisova E, Medved'ova M, Vraniakova J, Simon P. Optimisation of solid-phase microextraction of volatiles. *J Chromatog A* 2002;960:159–64.

[90] Prosen H, Zupančič-Kralj L. Solid-phase microextraction. *TrAC* 1999;18:272-82.

[91] Namiesnik J, Zygmunt B, Jastrzębska A. Application of solid-phase microextraction for determination of organic vapours in gaseous matrices. *J Chromatog A* 2000;885:405-18.

[92] Matisova E, Skrabakova S. Carbon sorbents and their utilization for the preconcentration of organic pollutants in environmental samples. *J Chromatog A* 1995;707:145-79.

[93] http://www.markes.com Thermal Desorption Technical Support, Note 21, *Analytical Thermal Desorption: Developing and Optimising Methods.* 2002;3 pp.

[94] Dettmer K, Engewald W. Adsorbent materials commonly used in air analysis for adsorptive enrichement and thermal desorption of volatile organic compounds. *Anal Bioanal Chem* 2002;373:490-500.

[95] Dettmer K, Knobloch Th, Engewald W. Stability of reactive low boiling hydrocarbons on carbon based adsorbents typically used for adsorptive enrichment and thermal desorption. *Fresenius J Anal Chem* 2000;366:70-8.

[96] Baltussen E, Cramers CA, Sandra PJF. Sorptive sample preparation-a review. *Anal Bioanal Chem* 2002;373:3-22.

[97] Spänel P, Smith D. Selected ion flow tube: a technique for quantitative trace gas analysis of air and breath. *Medical and Biological Engineering and Computing* 1996;34:409–19.

[98] Spänel P, Cocker J, Rajan B, Smith D. Validation of the sift technique for trace gas analysis of breath using the syringe injection technique. *Ann Occup Hyg* 1997;41:373-82.

[99] Smith D, Spänel P. Selected ion flow tube mass spectrometry (SIFT-MS) for online trace gas analysis. *Mass Spectrometry Reviews* 2005;24:661–700.

[100] Diskin AM, Spänel P, Smith D. Time variation of ammonia, acetone, isoprene, and ethanol in breath: a quantitative SIFT MS study over 30 days. *Physiol Measur* 2003;24:107-20.

[101] Wilson PF, Freeman CG, McEwan MJ, Milligan DB, Allardyce RA, Shaw GM. Alcohol in breath and blood: a selected ion flow tube mass spectrometric study. *Rapid Commun Mass Spectrom* 2001;15:413-17.

[102] Smith D, Wang T, and Spänel P. On-line, simultaneous quantification of ethanol, some metabolites and water vapour in breath following the ingestion of alcohol. *Physiol Measur* 2002;23:477-89.

[103] Diskin AM, Spänel P, Smith D. Increase of acetone and ammonia in urine headspace and breath during ovulation quantified using selected ion flow tube mass spectrometry. *Physiol Measur* 2003;24:191-99.

[104] Abbot SM, Elder JB, Spänel P, Smith D. Quantification of acetonitrile in exhaled breath and urinary headspace using selected ion flow tube mass spectrometry. *Int J Mass Spectrom* 2003;228:655-65.

[105] Wilson PF, Freeman CG, McEwan MJ, Milligan DB, Allardyce RA, Shaw GM. *In situ* analysis of solvents on breath and blood: a selected ion flow tube mass spectrometric study. *Rapid Commun Mass Spectrom* 2002;16:427-32.

[106] Lindinger W, Hansel A, Jordan A. Proton-transfer-reaction mass spectrometry (PTR-MS): on-line monitoring of volatile organic compounds at pptv levels. *Chem Soc Rev* 1998;27:347–54.

[107] Hansel A, Jordan A, Holzinger R, Prazeller P, Vogel W, Lindinger W. Proton-transfer-reaction mass spectrometry: on-line trace gas analysis at the ppb level. *Int J Mass Spectrom Ion Proc* 1995;150:609-19.

[108] Moser B, Bodrogi F, Eibl G, Lechner M, Rieder J, Lirk P. Mass spectrometric profile of exhaled breath. Field study by PTR-MS. *Respir Physiol Neurol* 2005;145:295-300.

[109] Harrison GR, Critchley AD, Mayhew CA, Thompson JM. Real-time breath monitoring of propofol and its volatile metabolites during surgery using a novel mass spectrometric technique: a feasibility study. *Brit J Anaesth* 2003;91:797-99.

[110] Lirk P, Bodrogi F, Raifer H, Greiner K, Ulmer H, Rieder J. Elective haemodialysis increases exhaled isoprene. *Nephrol Dial Transplant* 2003;18:937-941.

[111] Jordan A, Hansel A, Holzinger R, Lindinger W. Acetonitrile and benzene in the breath of smokers and nonsmokers investigated by proton-transfer reaction mass spectrometry (PTR-MS). *International Journal of Mass Spectrometry and Ion Processes* 1995;148:L1–L3.

[112] Baumbach JI, Vautz W, Ruzsanyi V. Metabolites in human breath: ion mobility spectrometers as diagnostic tools for lung diseases. In Amann A, Smith D. (Eds.) *Breath Analysis for Clinical Diagnosis and Therapeutic Monitoring* Part A, 2005;53-66.

[113] Sankaran S, Loyola B, Zhao W, Morgan JT, Molina M, Schivo M, Kenyon NJ, Davis CE. Micromachined differential mobility spectrometers for breath analysis. *Sensors, IEEE* 2007;1:16-9.

[114] Frank M, Farquar G, Adams C, Bogan M, Martin A, Benner H, Spadaccini C, Steele P, Sankaran S, Loyola B, Morgan J, Davis CE.

Modular sampling and analysis techniques for real-time analysis of human breath. *Sensors, IEEE* 2007;1:10-3.
[115] Baumbach JI, Westhoff M. Ion mobility spectrometry to detect lung cancer and airway infections. *Spectrosc Eur* 2006;18:22-7.
[116] Ruzsanyi V, Baumbach JI, Sielemann S, Litterst P, Westhoff M, Freitag L. Detection of human metabolites using multi-capillary columns coupled to ion mobility spectrometers. *J Chromatog A* 2005;1084:145-51.
[117] Murtz M. Breath diagnostics using laser spectroscopy, *Opt Photon News* 2005;16:30-5.
[118] McCurdy M, Bakhirkin Y, Wysocki G, Lewicki R, Tittel F. Recent advances of laser spectroscopy based techniques for applications in breath analysis. *J Breath Res* 2007;1:12 pp.
[119] Wang C, Sahay P. Breath Analysis Using Laser Spectroscopic Techniques: Breath Biomarkers, Spectral Fingerprints, and Detection Limits. *Sensors* 2009;9:8230-62.
[120] Roller C, Kosterov A, Tittel F, Uehara K, Gmachl C, Sivco D. Carbonyl sulphide detection with thermoelectrically cooled mid-infrared quantum cascade laser. *Optics Letters* 2003;28:2052-4.
[121] Halmer D, Thelen S, Hering P, Mürtz M. Online monitoring of ethane traces in exhaled breath with a difference frequency generation spectrometer. *Appl Phys B: Lasers Opt* 2006;85:437–43.
[122] Dumitras DC, Dutu DC, Matei C, Magureanu AM, Petrus M, Popa C, Patachia M. Measurements of ethylene concentration by laser photoacoustic techniques with applications at breath analysis. *Rom Rep Phys* 2008;60:593–602.
[123] Halmer D, von Basum G, Hering P, Murtz M. Mid-infrared cavity leak-out spectroscopy for ultrasensitive detection of carbonyl sulfide. *Opt Lett* 2005;30:2314–6.
[124] Fleischer M, Simon E, Rumpel E, Ulmer H, Harbeck M, Wandel M, Fietzek C, Weimar U, Meixner H. Detection of volatile compounds correlated to human diseases through breath analysis with chemical sensors. *Sens Actuat B* 2002;83:245–9.
[125] Di Natale C, Macagnano A, Martinelli E, Paolesse R, D'Arcangelo G, Roscioni C, Finazzi-Agro A, D'Amico A. Lung cancer identification by the

analysis of breath by means of an array of non-selective gas sensors. *Biosens Bioelectron* 2003;18:1209–18.

[126] Yu JB, Byun HG, So MS, Huh JS. Analysis of diabetic patients breath with conducting polymer sensor array. *Sens Actuat B* 2005;108:305–8.

[127] Drukker W. History of Hemodialysis, in *Replacement of the renal function by Dialysis*, edited by Drukker W., Parsons M., Maher J. F., Martinus Nijhoff Publishers Boston, 1983, pp. 3-52.

[128] Hoenich NA, Woffindin C, Ronco C. Haemodialysers and associated devices, in *Replacement of renal function by dialysis*, edited by Jacobs C, Kjellstrand CM, Koch KM, Winchester JF, 4th ed, Dordrecht, Kluwer Academic Publisher, 1996, pp 188-230.

[129] Sargent JA, Gotch FA. Principles and Biophysics of Dialysis *in Replacement of the renal function by Dialysis*, edited by Drukker W, Parsons M, Maher JF, Martinus Nijhoff Publishers Boston, 1983, pp. 53-96.

[130] Levy J, Morgan J, Brown E. Oxford Handbook of Dialysis, Oxford University Press, Oxford, 2001.

[131] Ronco C, Fabris A, Feriani M. Hemodialysis fluid composition, in *Replacement of renal function by dialysis*, edited by Jacobs C, Kjellstrand CM, Koch KM, Winchester JF, 4th ed, Dordrecht, Kluwer Academic Publisher, 1996, pp 256-276.

[132] Baurmeister U, Vienken J, Daum V: High-flux dialysis membranes: endotoxin transfer by backfiltration can be a problem. *Nephrol Dial Transplant* 1989;4:89-93.

[133] Canaud BJ, Mion CM: Water treatment for contemporary haemodialysis, in *Replacement of renal function by dialysis*, edited by Jacobs C, Kjellstrand CM, Koch KM, Winchester JF, 4th ed, Dordrecht, Kluwer Academic Publisher, 1996, pp 231-255.

[134] Vanholder R, De Smet R, Glorieux G, Argiles A, Baurmeister U, Brunet P, Clark W, Cohen G, De Deyn PP, Deppisch R, Descamps-Latscha B, Henle T, Jorres A, Lemke HD, Massy ZA, Passlick-Deetjen J, Rodriguez M, Stegmayr B, Stenvinkel P, Tetta C, Wanner C, Zidek W.

Review on uremic toxins: classification, concentration, and interindividual variability. *Kidney Int* 2003;63:1934-43.

[135] Hirsh J, Dalen J, Anderson DR, Poller L, Bussey H, Ansell J, Deykin D. Oral anticoagulants: mechanism of action, clinical effectiveness, and optimal therapeutic range. *Chest* 2001;119:8S-21S.

[136] Dam H. The antihaemorrhagic vitamin of the chick. *Biochem.J.* 1935;29:1273-85.

[137] MacCorquodale DW, Binkley SB, Thayer SA, Doisy EA. On the constitution of vitamin K1. *J.Am.Chem.Soc.* 1939;61(7):1928-29.

[138] Nelsestu G, Zytkovic T, Howard JB. Mode of action of vitamin-K - Identification of gamma-carboxyglutamic acid as a component of prothrombin. *J.Biol.Chem.* 1974;249(19):6347-50.

[139] Manotti C, Moia M, Palareti G, Pengo V, Ria L, Dettori AG. Effect of computer-aided management on the quality of treatment in anticoagulated patients: a prospective, randomized, multicenter trial of APROAT (Automated PRogram for Oral Anticoagulant Treatment). *Haematologica* 2001;86(10):1060-70.

[140] Ansell J, Hirsh J, Dalen J, Bussey H, Anderson D, Poller L, Jacobson A, Deykin D, Matchar D. Managing oral anticoagulant therapy. *Chest* 2001;119 Suppl(1):22–38.

[141] Marongiu F. La terapia anticoagulante orale oggi. Workshop FCSA - Campobasso, 9 maggio 2009.

[142] Campbell HA, Link KP. Studies on the hemorrhagic sweet clover disease. IV. The isolation and crystallization of the hemorrhagic agent. *J Biol Chem* 1941;138:21-33.

[143] Huebner CF, Link KP. Studies on the hemorrhagic sweet clover disease. VI. The synthesis of the d-diketone derived from the hemorrhagic agent through alkaline degradation. *J Biol Chem* 1941;138:529-34.

[144] Link KP. The discovery of dicumarol and its sequels. *Circulation* 1959;19:97-107.

[145] Kucharski A. Medical management of political patients: the case of Dwight D. Eisenhower. *Perspectives in Biology and Medicine.* 1978;22:115-26.

[146] Wardrop D, Keeling D. The story of the discovery of heparin and warfarin. *Br J Haematol* 2008;141:757-63.

[147] Pharmacy Times, Top 200 Prescription Drugs of 2007, Available at: http://www.pharmacytimes.com/issue/pharmacy/2008/2008-05/2008-05-8520. Accessed June 8, 2011.

[148] Wong YWJ, Davis PJ. Analysis of warfarin and its metabolites by reversed-phase ion-pair liquid chromatography with fluorescence detection. *J Chromatogr A* 1989;469:281-91.

[149] O'Reilly RA, Nelson E, Levy G. Physicochemical and physiologic factors affecting the absorption of warfarin in man. *J Pharm Sci* 1966;55:435-7.

[150] http://sitem.herts.ac.uk/aeru/footprint/en/Reports/681.htm.

[151] Kelly JG, O'Malley K. Clinical pharmacokinetics of oral anticoagulants. *Clin Pharmacokinet* 1979;4:1-15.

[152] Sadowski J, Booth SL, Mann KG, Malhotra OP, Bovill EG. Structure and mechanism of activation of vitamin K antagonists. New York; 1996.

[153] Cannegieter SC, Rosendaal FR, Wintzen AR, Vandermeer FJM, Vandenbroucke JP, Briet E. Optimal oral anticoagulant-therapy in patients with mechanical heart-valves. *N Engl J Med* 1995;333:11-7.

[154] Turpie AGG, Gunstensen J, Hirsh J, Nelson H, Gent M. Randomized comparison of 2 intensities of oral anticoagulant-therapy after tissue heart valve replacement. *Lancet* 1988;1:1242-5.

[155] Matchar DB, Mccrory DC, Barnett HJM, Feussner JR. Medical-treatment for stroke prevention. *Ann Intern Med* 1994;121:41-53.

[156] Hurlen M, Abdelnoor M, Smith P, Erikssen J, Arnesen H. Warfarin, aspirin, or both after myocardial infarction. *N Engl J Med* 2002;347:969-74.

[157] Hirsh J. The optimal duration of anticoagulant therapy for venous thrombosis. *N Engl J Med* 1995;332:1710–1.

[158] Whitlon DS, Sadowski JA, Suttie JW. Mechanisms of coumarin action: significance of vitamin K epoxide reductase inhibition. *Biochemistry* 1978;17:1371-7.

[159] Fasco MJ, Hildebrandt EF, Suttie JW. Evidence that warfarin anticoagulant action involves two distinct reductase activities. *J Biol Chem* 1982;257:11210–2.

[160] Garcia AA, Reitsma PH. Vkorc1 and the vitamin K cycle. *Vitam Horm* 2008;78:23-33.

[161] Shearer MJ. Vitamin-K metabolism and nutriture. *Blood Rev* 1992;6:92-104.

[162] Chan E, McLachlan A, O'Reilly R, Rowland M. Stereochemical aspects of warfarin drug interactions: use of a combined pharmacokinetic-pharmacodynamic model. *Clin Pharmacol Ther* 1994;56:286-94.

[163] Pitsiu M, Parker EM, Aarons L, Holt B, Rowland M, Chan E, Serlin M, Breckenridge A. A comparison of the relative sensitivities of factor VII and prothrombin time measurements in detecting drug interactions with warfarin. Inter-relationship among individual vitamin K-dependent clotting factors at different levels of anticoagulation. *Eur J Clin Pharmacol* 1992;42:645-9.

[164] Price PA. Role of vitamin K–dependent proteins in bone metabolism. *Annu Rev Nutr* 1988;8:565–83.

[165] Pettifor JM, Benson R. Congenital malformations associated with the administration of oral anticoagulants during pregnancy. *J Pediatr* 1975;86:459-62.

[166] Katzung BG. Basic & clinical pharmacology. New York: McGraw Hill; 2000.

[167] Holford NH. Clinical pharmacokinetics and pharmacodynamics of warfarin. Understanding the dose-effect relationship. *Clin Pharmacokinet* 1986;11:483-504.

[168] Yacobi A, Levy G. Protein binding of warfarin enantiomers in serum of humans and rats. *J Pharmacokinet Biopharm* 1977;5:123-31.

[169] Kaminsky LS, Zhang ZY. Human P450 metabolism of warfarin. *Pharmacol Ther* 1997;73:67-74.

[170] Lewis RJ, Trager WF, Robinson AJ, Chan KK. Warfarin metabolites: the anticoagulant activity and pharmacology of warfarin alcohols. *J Lab Clin Med* 1973;81:925-31.

[171] Booth SL, Centurelli MA. Vitamin K: a practical guide to the dietary management of patients on warfarin. *Nutr Rev* 1999;57:288-96.

[172] Sorano GG, Biondi G, Conti M, Mameli G, Licheri D, Marongiu F. Controlled vitamin K content diet for improving the management of poorly controlled anticoagulated patients: a clinical practice proposal. *Haemostasis* 1993;23:77–82.

[173] Wells PS, Holbrook AM, Crowther NR, Hirsh J. Interactions of warfarin with drugs and food. *Ann Intern Med* 1994;121:676–83.

[174] Van der Meer FJ, Rosendaal FR, Vandenbroucke JP, Briët E. Bleeding complications in oral anticoagulant therapy. An analysis of risk factors. *Arch Intern Med* 1993;153:1557-62.

[175] Lindh JD, Holm L, Dahl ML, Alfredsson L, Rane A. Incidence and predictors of severe bleeding during warfarin treatment. *J Thromb Thrombolysis* 2008;25:151-9.

[176] Hirauchi K, Sakano T, Nagaoka T, Morimoto A. Simultaneous determination of vitamin K1, vitamin K1 2,3-epoxide and menaquinone-4 in human plasma by high-performance liquid chromatography with fluorimetric detection. *J Chromatogr* 1988;430:21-9.

[177] Levy RJ, Lian JB. Gamma-carboxyglutamate excretion and warfarin therapy. *Clin Pharmacol Ther* 1979;25:562-70.

[178] Poller L. Thromboplastin and oral anticoagulant control. *Br J Haematol* 1987;67:116-7.

[179] Duxbury BM, Poller L. The oral anticoagulant saga: past, present, and future. *Clin Appl Thromb Hemost* 2001;7:269-75.

[180] Rang HP, Dale MM, Ritter JM, Moore PK. In: Pharmacology - Fifth Edition: Churchill Livingstone; 2003, pp. 319.

[181] Stockley I. Drug interactions. Edn 5 ed. London: The Pharmaceutical Press; 1999, pp. 233.

[182] Holbrook AM, Pereira JA, Labiris R, McDonald H, Douketis JD, Crowther M, Wells PS. Systematic overview of warfarin and its drug and food interactions**.** *Arch Intern Med* 2005;165:1095-106.

[183] Greenblatt DJ, von Moltke LL. Interaction of warfarin with drugs, natural substances, and foods. *J Clin Pharmacol* 2005;45:127-32.

[184] Sellers EM, Koch-Weser J. Displacement of warfarin from human albumin by diazoxide and ethacrynic, mefenamic, and nalidixic acids. *Clin Pharmacol Ther* 1970;11:524-9.

[185] Higashi MK, Veenstra DL, Kondo LML, Wittkowsky AK, Srinouanprachanh SL, Farin FM, et al. Association between CYP2C9 genetic variants and anticoagulation-related outcomes during warfarin therapy. *J Am Med Assoc* 2002;287:1690-8.

[186] Aithal GP, Day CP, Kesteven PJL, Daly AK. Association of polymorphisms in the cytochrome P450 CYP2C9 with warfarin dose requirement and risk of bleeding complications. *Lancet* 1999;353:717-9.

[187] Kirchheiner J, Brockmoller J. Clinical consequences of cytochrome P4502C9 polymorphisms. *Clin Pharmacol Ther* 2005;77:1-16.

[188] Herman D, Peternel P, Stegnar M, Breskvar K, Dolzan V. The influence of sequence variations in factor VII, gamma-glutamyl carboxylase and vitamin K epoxide reductase complex genes on warfarin dose requirement. *Thromb Haemost* 2006;95:782-7.

[189] Rost S, Fregin A, Ivaskevicius V, Conzelmann E, Hortnagel K, Pelz HJ, et al. Mutations in VKORC1 cause warfarin resistance and multiple coagulation factor deficiency type 2. *Nature* 2004;427:537-41.

[190] Geisen C, Watzka M, Sittinger K, Steffens M, Daugela L, Seifried E, et al. VKORC1 haplotypes and their impact on the inter-individual and inter-ethnical variability of oral anticoagulation. *Thromb Haemost* 2005;94:773-9.

[191] Hamberg A, Dahl M, Barban M, Scordo MG, Wadelius M, Pengo V, et al. A PK-PD model for predicting the impact of age, CYP2C9, and VKORC1 genotype on individualization of warfarin therapy. *Clin Pharmacol Ther* 2007;81:529-38.

[192] Sconce E, Khan T, Mason J, Noble F, Wynne H, Kamali F. Patients with unstable control have a poorer dietary intake of vitamin K compared to patients with stable control of anticoagulation. *Thromb Haemost* 2005;93:872-5.

[193] Oreilly RA, Rytand DA. Resistance to Warfarin due to Unrecognized Vitamin-K Supplementation. *N Engl J Med* 1980;303:160-1.

[194] Khan T, Wynne H, Wood P, Torrance A, Hankey C, Avery P, et al. Dietary vitamin K influences intra-individual variability in anticoagulant response to warfarin. *Br J Haematol* 2004;124:348-54.

[195] Loebstein R, Yonath H, Peleg D, Almog S, Rotenberg M, Lubetsky A, et al. Interindividual variability in sensitivity to warfarin - Nature or nurture? *Clin Pharmacol Ther* 2001;70:159-64.

[196] Lurie Y, Loebstein R, Kurnik D, Almog S, Halkin H. Warfarin and vitamin K intake in the era of pharmacogenetics. *Br J Clin Pharmacol* 2010;70:164-70.

[197] Schurgers LJ, Shearer MJ, Hamulyak K, Stocklin E, Vermeer C. Effect of vitamin K intake on the stability of oral anticoagulant treatment: dose-response relationships in healthy subjects. *Blood* 2004;104:2682-9.

[198] Di Nisio M, Middeldorp S, Buller HR. Drug therapy - Direct thrombin inhibitors. *N Engl J Med* 2005;353:1028-40.

[199] Weitz JI, Bates SM. New anticoagulants. *J Thromb Haemost* 2005;3:1843-53.

[200] Ezekowitz MD, Connolly S, Parekh A, Reilly PA, Varrone J, Wang S, et al. Rationale and design of RE-LY: randomized evaluation of long-term anticoagulant therapy, warfarin, compared with dabigatran. *Am Heart J* 2009;157:805-10.

[201] Albers GW, SPORTIF Inv. Stroke prevention in atrial fibrillation: pooled analysis of SPORTIF III and V trials. *Am J Manag Care* 2004;10:S462-9.

[202] Eriksson BI, Dahl OE, Rosencher N, Kurth AA, Van Dijk N, Frostick SP, et al. Oral dabigatran etexilate vs. subcutaneous enoxaparin for the prevention of venous thromboembolism after total knee replacement: the RE-MODEL randomized trial. *J Thromb Haemost* 2007;5:2178-85.

[203] Christensen TD, Larsen TB, Jensen C, Maegaard M, Sørensen B. International normalised ratio (INR) measured on the CoaguChek S and XS compared with the laboratory for determination of precision and accuracy. *Thrombosis and Haemostasis* 2009;101:563–9.

[204] Poller L, Keown M, Ibrahim SA, van der Meer FJ, van den Besselaar AM, Tripodi A, et al. European Concerted Action on Thrombosis. Quality assessment of CoaguChek point-of-care prothrombin time monitors:

comparison of the European community-approved procedure and conventional external quality assessment. *Clinical Chemistry* 2006;52:1843–7.

[205] Sawicki PT. A structured teaching and self-management program for patients receiving oral anticoagulation: a randomized controlled trial. Working Group for the Study of Patient Self-Management of Oral Anticoagulation. *J Am Med Assoc* 1999;281:145–50.

[206] White RH, McCurdy SA, von Marensdorff H, Woodruff DE Jr, Leftgoff L. Home prothrombin time monitoring after the initiation of warfarin therapy. A randomized, prospective study. *Ann Intern Med* 1989;111:730–7.

[207] Anderson DR, Harrison L, Hirsh J. Evaluation of a portable prothrombin time monitor for home use by patients who require long-term oral anticoagulant therapy. *Arch Intern Med* 1993;153:1441–7.

[208] Siebenhofer A, Rakovac I, Kleespies C, Piso B, Didjurgeit U, SPOG 60+ Study Group. Self management of oral anticoagulation reduces major outcomes in the elderly. A randomized controlled trial. *Thromb Haemost* 2008;100:1089-98.

[209] Heneghan C, Alonso-Coello P, Garcia-Alamino JM, Perera R, Meats E, Glasziou P. Self-monitoring of oral anticoagulation: a systematic review and meta-analysis. *Lancet* 2006;367:404-11.

[210] Sheiner LB, Beal SL. Bayesian individualization of pharmacokinetics – simple implementation and comparison with non-Bayesian methods. *J Pharm Sci* 1982;71:1344-8.

[211] Wilson R, James AH. Computer-assisted management of warfarin treatment. *Br Med J* 1984;289:422-4.

[212] Svec JM, Coleman RW, Mungall DR, Ludden TM. Bayesian pharmacokinetic pharmacodynamic forecasting of prothrombin response to warfarin therapy – preliminary evaluation. *Ther Drug Monit* 1985;7:174-80.

[213] Carter BL, Barr W, Rock W, Taylor JW. Warfarin dosage predictions assisted by the analog-computer. *Ther Drug Monit* 1988;10:69-73.

[214] Poller L, Shiach CR, MacCallum PK, Johansen AM, Munster AM, Magalhaes A, et al. Multicentre randomised study of computerised anticoagulant dosage. *Lancet* 1998;352:1505-9.

[215] Poller L, Keown M, Ibrahim S, Lowe G, Moia M, Turpie AG, et al. A multicentre randomised clinical endpoint study of PARMA 5 computer-assisted oral anticoagulant dosage. *Br J Haematol* 2008;143:274-83.

[216] Poller L, Keown M, Ibrahim S, Lowe G, Moia M, Turpie AG, et al. An international multicenter randomized study of computer-assisted oral anticoagulant dosage vs. medical staff dosage. *J Thromb Haemost* 2008;6:935-43.

[217] Ansell J, Hirsh J, Hylek E, Jacobson A, Crowther M, Palareti G. Pharmacology and management of the vitamin K antagonists. *Chest* 2008;133:160S-98S.

[218] Sacks DB, Bruns DE, Goldstein DE, Maclaren NK, McDonald JM, Parrott M. Guidelines and Recommendations for Laboratory Analysis in the Diagnosis and Management of Diabetes Mellitus. *Clinical Chemistry* 2002;48:436–72.

[219] Castano L, Eisenbarth GS. Type-I diabetes. A chronic autoimmune disease of human, mouse, and rat. *Annu Rev Immunol* 1990;8:647–79.

[220] Reaven GM. Role of insulin resistance in human disease. *Diabetes* 1988;37:1595–607.

[221] Sacks DB, McDonald JM. The pathogenesis of type II diabetes mellitus: a polygenic disease. *Am J Clin Pathol* 1996;105:149–56.

[222] Wallin RF, Regan BM, Napoli MD, Stern IJ. Sevoflurane: a new inhalational anesthetic agent. *Anesthesia & Analgesia* 1975;54:758.

[223] Eger EI II. New inhaled anesthetics. *Anesthesiology* 1994;80:906-22.

[224] Jones RM. Desflurane or sevoflurane: inhalation anesthetics for this decade? *British Journal of Anaesthesia* 1990;65:527-36.

[225] Targ A, Yasuda N, Eger EI II. Solubility of I-653, sevoflurane, isoflurane, and halothane in plastics and rubber composing a conventional anesthetic circuit. *Anesthesia & Analgesia* 1989;68:218-25.

[226] Eger EI II, Ionescu P, Gong D. Circuit absorption of halothane, isoflurane, and sevoflurane. *Anesthesia & Analgesia* 1998;86:1070-4.

[227] Patel SS, Goa KL. Sevoflurane: a review of its pharmacodynamic and pharmacokinetic properties and its clinical use in general anaesthesia. *Drugs* 1996;51:658-700.

[228] Quasha AL, Eger EI II, Tinker JH. Determination and application of MAC. *Anesthesiology* 1980;53:315-34.

[229] Scheller MS, SaidmanLJ, Partridge BL. MAC of sevoflurane in humans and the New Zealand white rabbit. *Can J Anaesth* 1988;35:153-6.

[230] Behne M, Wilke HJ, Harder S. Clinical pharmacokinetics of sevoflurane. *Clin Pharmacokinet* 1999;36:13-26.

[231] Yasuda N, Lockhart SH, Eger EI II, Weiskopf RB, Liu J, Laster M, Taheri S, Peterson NA. Comparison of kinetics of sevoflurane and isoflurane in humans. *Anesthesia & Analgesia* 1991;72:316-24.

[232] Shiraishi Y, Ikeda K. Uptake and biotransformation of sevoflurane in humans: a comparative study of sevoflurane with halothane, enflurane, and isoflurane. *J Clin Anesth* 1990;2:381-6.

[233] Kharasch ED, Armstrong AS, Gunn K, Artru A, Cox K, Karol MD. Clinical sevoflurane metabolism and disposition. II. The role of cytochrome P450 2E1 in fluoride and hexafluoroisopropanol formation. *Anesthesiology* 1995;82:1379-88.

[234] De Palma JR, Pittard JD. (2001), Dialysis dose, www.hemodialysis-inc.com

[235] NIH-Publication (1999), no: 99-4556, www.niddk.nih.gov, July 1999.

[236] Canaud B, Bosc JY, Carrol L, Learay-Moragues H, Naviono C, Verzetti G, Thomaseth K. Urea as a marker of adequacy in hemodialysis: Lessons from in vivo urea dynamics monitoring. *Kidney Int* 2000;58:28-40.

[237] Lindsay RM, Sternby J. Future Directions in Dialysis Quantification. *Sem Dial* 2001;14:300-7.

[238] Keshaviah P. Adequacy of dialysis: Comparison of hemodialysis (HD) to CAPD. *Indian Journal of Nephrology* 2002;16:51-5.

[239] Vanholder R, De Smet R, Chen H, Vogeleere P, Ringoir S. Uremic Toxicity: The middle molecule hypothesis revisited. *Seminars in Nephrology*. 1994;14:205-18.

[240] UK Renal Registry Report (2003), UK Renal Registry, Bristol, UK, eds: Ansell D, Feest T.

[241] Gotch FA, Sargent JA. Mechanistic analysis of the National Cooperative Study (NCDS). *Kidney Int* 1985;28:56-534.

[242] Kemp HJ, Parnham A, Tomson CR. Urea kinetic modelling: a measure of dialysis adequacy. *Ann Clin Biochem* 2001;38:20-7.

[243] Shak CG. The role of Urea Kinetic Modelling in Determining Adequacy of Hemodialysis. *Nephrology News & Issues* 1999;13:14-6.

[244] Sternby J. Urea Sensors – A world of Possibilities. *Advances in Renal Replacement Therapy* 1999;6:265-72.

[245] Shinzato T, Nakai S, Fujita Y, Takai I, Morita H, Nakane K, Maeda K. Determination of Kt/V and Protein Catabolic Rate Using Pre- and Postdialysis Blood Urea Nitrogen Concentrations. *Nephron* 1994;67:280-90.

[246] Daugirdas JT, Smye S. Effect of a two compartment distribution on apparent urea distribution volume. *Kidney Int* 1997;51:1270-3.

[247] Fridolin I, Magnusson M, Lindberg LG. Online monitoring of solutes in dialysate using absorption of ultraviolet radiation: technique description. *Int J Artif Organs* 2002;25:748-61.

[248] Olesberg JT, Armitage B, Arnold MA, Flanigan MJ. Online measurement of urea concentration in spent dialysate during hemodialysis. *Proceedings of the SPIE* 2002;4624:95-105.

[249] Hammond KB, Turcias NL, Gibson LE. Clinical evaluation of the macroduct sweat collection system and conductivity analyser in the diagnosis of cystic fibrosis. J Pediatr 1994 ;124:255-60.

[250] Heeley ME, Woolf DA, Heeley AF. Indirect measurements of sweat electrolyte concentration in the laboratory diagnosis of cystic fibrosis. Arch Dis Child 2000;82:420-4.

[251] Ghimenti S., 2007. Sviluppo di nuove metodologie analitiche per lo studio dell'espirato umano. Degree thesis in industrial chemistry. University of Pisa.

[252] Tabucchi S., 2008. Chemical characterization of human breath. PhD thesis in chemical science. University of Pisa.
[253] Wong YWJ, Davis PJ. Analysis of warfarin and its metabolites by reversed-phase ion-pair liquid chromatography with fluorescence detection. J Chromatogr A 1989;469:281-91.
[254] Anderson RK, Kenney WL (1987) Effect of age on heat-activated sweat gland density and flow during exercise in dry heat. J Appl Physiol 63: 1089-1094.
[255] IUPAC. Nomenclature, symbols, units and their usage in spectrochemical analysis–II. Spectrochim Acta Part B At Spectrosc 1978;33:241-5.
[256] Pearson K (1901) On lines and planes of closest fit to systems of points in space. *Philosophical Magazine* 2:559–72.
[257] Jolliffe IT (2002) Principal Component Analysis, 2nd Ed. New York: Springer; 487 pp.
[258] Wells PS, Holbrook AM, Crowther NR, Hirsh J. Interactions of warfarin with drugs and food. *Ann Intern Med* 1994;121:676–83.
[259] Holbrook AM, Pereira JA, Labiris R, McDonald H, Douketis JD, Crowther M, Wells PS. Systematic overview of warfarin and its drug and food interactions. *Arch Intern Med* 2005;165:1095-1106.
[260] Furuya H, Fernandez-Salguero P, Gregory W, Taber H, Steward A, Gonzalez FJ, Idle JR. Genetic polymorphism of CYP2C9 and its effect on warfarin maintenance dose requirements in patients undergoing anticoagulant therapy. *Pharmacogenetics* 1995;5:389–92.
[261] Aithal GP, Day CP, Kesteven PJ, Daly AK. Association of polymorphism in the cytochrome P450 CYP2C9 with warfarin dose requirements and risk of bleeding complications. *Lancet* 1999;353:717–9.
[262] Scordo MG, Pengo V, Spina E, Dahl ML, Gusella M, Padrini R. Influence of CYP2C9 and CYP2C19 genetic polymorphism on warfarin maintenance dose and metabolic clearance. *Clin Pharmacol Ther* 2002;72:702–10.
[263] Sellers EM, Koch-Weser J. Displacement of warfarin from human albumin by diazoxide and ethacrynic, mefenamic, and nalidixic acids. *Clin Pharmacol Ther* 1970;11:524-9.

[264] Lombardi R, Chantarangkul V, Cattaneo M, Tripodi A. Measurement of warfarin in plasma by high performance liquid chromatography (HPLC) and its correlation with the international normalized ratio. *Thromb Res* 2003;111:281–4.

[265] Huang C, Yang J, Du Y, Miao L. Measurement of free concentrations of highly protein-bound warfarin in plasma by ultra performance liquid chromatography–tandem mass spectrometry and its correlation with the international normalized ratio. *Clin Chim Acta* 2008;393:85–9.

[266] Matin SB, Wan SH, Karam JH. Pharmacokinetics of tolbutamide: prediction by concentration in saliva. *Clin Pharmacol Ther* 1974;16:1052-8.

[267] Deng CH, Zhang J, Yu XF, Zhang W, Zhang XM. Determination of acetone in human breath by gas chromatography-mass spectrometry and solid-phase microextraction with on-fiber derivatization. *J Chromatogr B* 2004;810:269–75.

[268] Turner C, Walton C, Hoashi S, Evans M. Breath acetone concentration decreases with blood glucose concentration in type I diabetes mellitus patients during hypoglycaemic clamps. *J Breath Res* 2009;3:6pp.

[269] Wang CJ, Mbi A, Shepherd M. A study on breath acetone in diabetic patients using a cavity ringdown breath analyzer: exploring correlations of breath acetone with blood glucose and glycohemoglobin A1C. *IEEE Sens J* 2010;10:54–63.

[270] Nelson N, Lagesson V, Nosratabadi AR, Ludvigsson J, Tagesson C. Exhaled isoprene and acetone in newborn infants and in children with diabetes mellitus. *Pediatr Res* 1998;44:363–7.

[271] Galassetti PR, Novak B, Nemet D, Rose-Grotton C, Cooper DM, Meinardi S, Newcomb R, Zaldivar F, Blake DR. Breath ethanol and acetone as indicators of serum glucose levels: an initial report. *Diabetes Technol Ther* 2005;7:115–23.

[272] Novak BJ, Blake DR, Meinardi S, Rowland FS, Pontello A, Cooper DM, Galassetti PR. Exhaled methyl nitrate as a noninvasive marker of

hyperglycemia in type 1 diabetes. *Proc Natl Acad Sci, USA* 2007;104:15613–8.

[273] Lee J, Ngo J, Blake DR, Meinardi S, Pontello AM, Newcomb R, Galassetti PR. Improved predictive models for plasma glucose estimation from multi-linear regression analysis of exhaled volatile organic compounds. *J Appl Physiol* 2009;107:155–60.

[274] Kalapos MP. On the mammalian acetone metabolism: from chemistry to clinical implications. *Biochim Biophys Acta* 2003;1621:122–39.

[275] de Graaf AA, Maathuis A, de Waard P, Deutz NEP, Dijkema C, de Vos WM, Venema K. Profiling human gut bacterial metabolism and its kinetics using [U-^{13}C]glucose and NMR. *NMR in Biomedicine* 2010;23:2-12.

[276] Miyoshi A, Rochat T, Gratadoux JJ, Le Loir Y, Oliveira SC, Langella P, Azevedo V. Oxidative stress in *Lactococcus lactis*. *Genetic and Molecular Research* 2003;2:348-59.

[277] Pleil JD, Kim D, Prah JD, Rappaport SM. Exposure reconstruction for reducing uncertainty in risk assessment: example using MTBE biomarkers and a simple pharmacokinetic model. *Biomarkers* 2007;12:331-48.

[278] Kharasch ED, Karol MD, Lanni C, Sawchuk R. Clinical sevoflurane metabolism and disposition. I. Sevoflurane and metabolite pharmacokinetics. *Anesthesiology* 1995;82:1369-78.

[279] Bourdeaux D, Sautou-Miranda V, Montagner A, Perbet S, Constantin JM, Bazin JE, Chopineau J. Simple assay of plasma sevoflurane and its metabolite hexafluoroisopropanol by headspace GC–MS. *Journal of Chromatography B* 2010;878:45–50.

[280] Yasuda N, Lockhart SH, Eger EI II, Weiskopf RB, Liu J, Laster M, Taheri S, Peterson NA. Comparison of kinetics of sevoflurane and isoflurane in humans. *Anesth Analg* 1991;72:316-24.

[281] Uhlin F, Fridolin I, Lindberg LG, Magnusson M. Estimation of delivered dialysis dose by on-line monitoring of the ultraviolet absorbance in the spent dialysate. *Am J Kidney Dis* 2003;41:1026–36.

[282] Uhlin F, Fridolin I, Magnusson M, , Lindberg LG. Dialysis dose (Kt/V) and clearance variation sensitivity using measurement of ultraviolet-absorbance (on-line), blood urea, dialysate urea and ionic dialysance. *Nephrol Dial Transplant* 2006;21:2225–31.

[283] Uhlin F, Pettersson J, Fernstrom A, Lindberg LG. Complementary parameter for dialysis monitoring based on UV absorbance. *Hemodialysis International* 2009;13:492-7.

[284] Daugirdas JT, Tattersall JE. Automated monitoring of hemodialysis adequacy by dialysis machines: potential benefits to patients and cost savings. Kidney International 2010;78:833-5.

[285] Geisser, Seymour (1993). Predictive Inference. New York: Chapman and Hall. ISBN 0412034719.

[286] Kohavi R (1995) A study of cross-validation and bootstrap for accuracy estimation and model selection. *Proceedings of the Fourteenth International Joint Conference on Artificial Intelligence* 2: 1137–43. http://citeseerx.ist.psu.edu/viewdoc/summary?doi=10.1.1.48.529.
(Morgan Kaufmann, San Mateo).

[287] Devijver PA, Kittler J. Pattern Recognition: A Statistical Approach, Prentice-Hall, London, 1982.

Publications

1. S. Ghimenti, T. Lomonaco, M. Onor, L. Murgia, A. Paolicchi, R. Fuoco, L. Ruocco, G. Pellegrini, M. G. Trivella, F. Di Francesco. *Measurement of Warfarin in the Oral Fluid of Patients Undergoing Anticoagulant Oral Therapy*. PLoS ONE, 6(12): e28182. doi:10.1371/journal.pone.0028182.

2. *Breath Analysis: Analytical Methodologies and Clinical Applications* A. Ceccarini, F. Di Francesco, R. Fuoco, S. Ghimenti, M. Onor, S. Tabucchi, and M. G. Trivella in "*Analytical Techniques for Clinical Chemistry: Methods and Applications*" (S. Caroli and Gy. Záray, Eds., J. Wiley & Sons, Publisher), Chapter 23.

3. D. Calia, F. Di Francesco, C. Donadio, R. Fuoco, S. Ghimenti, M. Onor. *Monitoring urea, uric acid, creatinine and β2-microglobulin concentrations in spent dialysate by spectrophotometric and spectrofluorimetric measurements*. Manuscript in preparation.

4. S. Ghimenti, F. Di Francesco, J. D. Pleil, R. Fuoco, M. Onor, C. Comite, N. Catania, M. G. Trivella. *Pharmacokinetic models of post-operative elimination of sevoflurane anaesthetic and hexafluoroisopropanol metabolite as measured in exhaled breath.* Manuscript in preparation.

Papers Presented at Scientific Meeting

1. F. Di Francesco, M. Onor, S. Tabucchi, S. Ghimenti, M. G. Trivella, A. Ceccarini, R. Fuoco. *Sampling bags for breath analysis*, International Scientific Meeting: Breath Analysis in Physiology and Medicine, (4-5 September 2006, Prague, Czech Republic). Oral Presentation.

2. F. Di Francesco, M. Onor, S. Tabucchi, S. Ghimenti, M. G. Trivella, A. Ceccarini, R. Fuoco. *Caratterizzazione chimica dell'espirato umano in pazienti affetti da diabete mediante gascromatografia/spettrometria di massa*, XXII National Congress of the Italian Chemical Society, (10-15 September 2006, Florence, Italy). Poster.

3. F. Di Francesco, S. Ghimenti, M. Onor, S. Tabucchi, R. Fuoco. *Aspetti metodologici del campionamento dell'espirato*, XX Congress of Analytical Chemistry, (16-20 September 2007, University of Tuscia, Viterbo, Italy). Oral Presentation.

4. F. Di Francesco, M. Onor, S. Tabucchi, S. Ghimenti, A. Ceccarini, R. Fuoco. *Development of an analytical procedure for the quantification of volatile compounds in human breath*, XIII Italian-Hungarian Symposium on spectrochemistry: environmental contamination and food safety, (20-24 April 2008, Alma Mater Studiorum University of Bologna, Italy). Oral Presentation.

5. F. Di Francesco, L. Murgia, S. Ghimenti, M. Onor, A. Paolicchi. *Monitoraggio non invasivo di terapie anticoagulanti orali* XXI National Meeting of the Division of Analytical Chemistry of the

Italian Chemical Society, (21-25 September 2008, University of Calabria, Cosenza, Italy). Poster.

6. F. Di Francesco, S. Ghimenti, S. Tabucchi, M. Onor, M. G. Trivella, S. Lenzi, R. Fuoco. *Volatile compounds in human breath during oral glucose tolerance test*, International Conference on Breath and Breath Odor Research "Breath 2009", (26-30 April 2009, Dortmund, Germany). Poster.

7. S. Ghimenti, M. Onor, T. Lomonaco, R. Fuoco, A. Paolicchi, L. Ruocco, G. Pellegrini, M. G. Trivella, F. Di Francesco. *Determinazione del warfarin in campioni di saliva e plasma raccolti da pazienti in terapia anticoagulante*, XXII National Meeting of the Division of Analytical Chemistry of the Italian Chemical Society, (12-16 September 2010, Como, Italy). Oral Presentation.

8. D. Calia, F. Di Francesco, R. Fuoco, S. Ghimenti, A. Kanaki, M. Onor, D. Tognotti, C. Donadio. *Monitoring urea, creatinine and β2-microglobulin concentrations in spent dialysate by spectrophotometric and spectrofluorimetric measurements* World Congress of Nephrology 2011, (8-12 April 2011, Vancouver-CANADA). Poster.

9. S. Ghimenti, J. D. Pleil, M. Onor, C. Comite, N. Catania, M. G. Trivella, R. Fuoco, F. Di Francesco. *Pharmacokinetic models of post-operative elimination of sevoflurane anaesthetic and hexafluoroisopropanol metabolite as measured in exhaled breath* Breath Analysis Summit 2011: International Conference on Breath Research (11-14 September 2011, Parma-Italy). Poster.

10. S. Ghimenti, M. Onor, T. Lomonaco, R. Fuoco, A. Paolicchi, L. Ruocco, G. Pellegrini, M. G. Trivella, F. Di Francesco. *Correlation between salivary concentration of oral anticoagulants*

and anticoagulant effect in thrombotic patients, XXIV National Congress of the Italian Chemical Society, (11-16 September 2011, Lecce, Italy). Oral Presentation.

Schools and Seminars

1. National School on "*Metodologie Analitiche in Spettrometria di Massa*", University of Parma (19-23 May 2008).
2. Ist School on *"Metodi Chemiometrici per il Monitoraggio di Processo"*, University of Modena e Reggio Emilia, Italy (18-20 February 2009).
3. Ist Course on "*Spettrometria di Massa in Ambito Chimico-Clinico*", Meyer Hospital, Florence, Italy (4-8 May 2009).
4. Ist School on "*Microestrazione in fase solida SPME – Applicazioni in campo Alimentare, Ambientale e Tossicologico* ", University of Florence, Italy (1-2 July 2010).
5. Workshop: "*Just Enough Sample Prep with LC-MS/MS Tips & tricks for lower detection limits and increased productivity* " organized by Agilent, University of Florence, Italy (29 September 2011).